Quantifying the Contribution of Tidal Flow Variations to Survival of Juvenile Salmon
Draft Final Report

March 2022

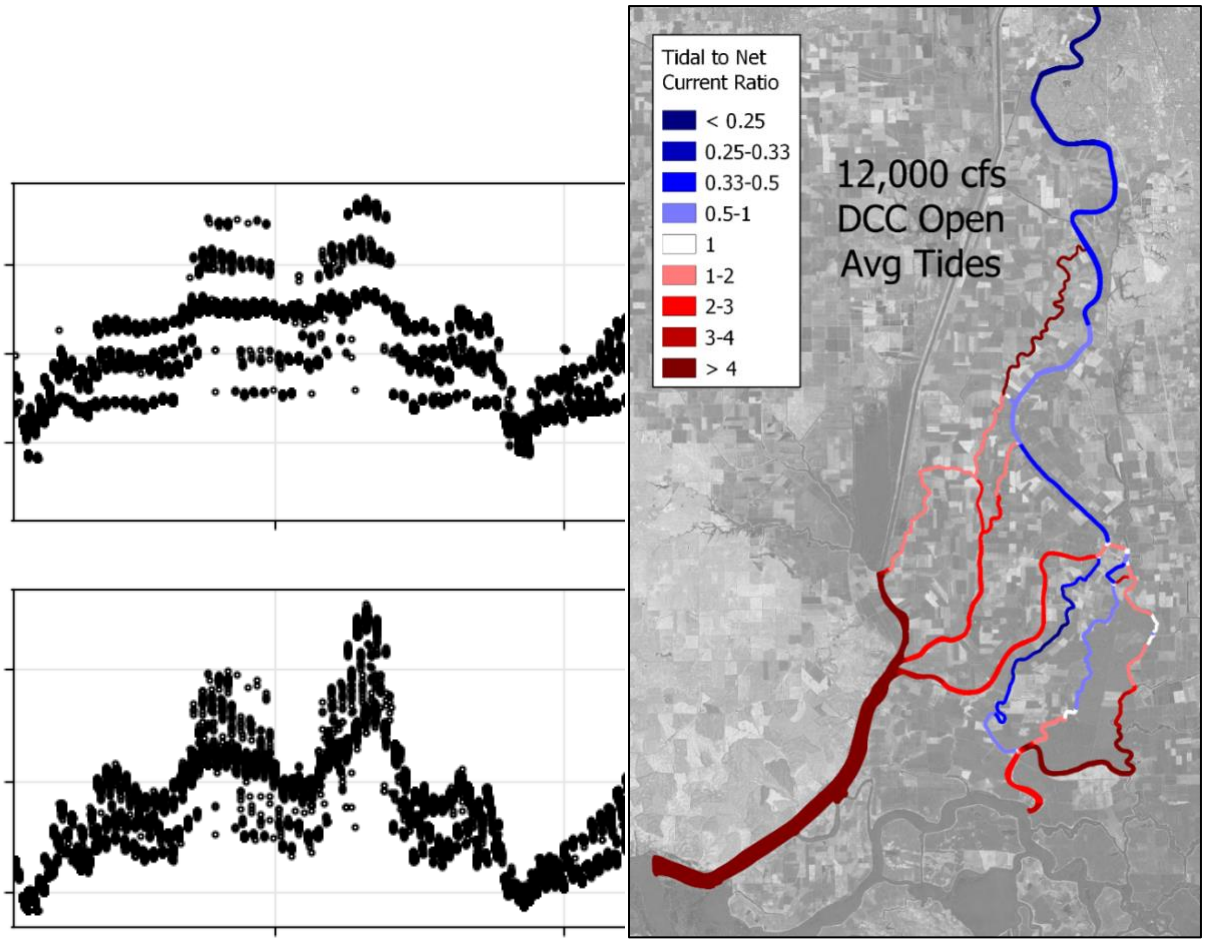

Prepared For:
Delta Stewardship Council
980 Ninth Street, Suite 1500
Sacramento, CA 95814
Contact: Ben Geske
916-204-3002

Prepared By:
Resource Management Associates
1756 Picasso Avenue, Suite G
Davis, CA 95618
Contact: Stephen Andrews
530-564-7043

RMA RESOURCE MANAGEMENT ASSOCIATES
WATER RESOURCES ENGINEERING

Executive Summary

A set of 2D hydrodynamic model simulations were performed in order to examine the experience of passive material transported through the North Delta from a Lagrangian point of view. The North Delta was broken up into a series of reaches, and particle tracking model results were processed to calculate the time spent and distance traveled within each reach and relate it to net flow and tidal conditions (spring-neap phase). The RMA Bay-Delta hydrodynamic and particle tracking models were used for the simulations.

Time and distance metrics were calculated for historical simulations of water years 2007–2011 and input into a Bayesian juvenile salmon survival model to test the hypothesis that reach-specific survival is dependent on time spent and/or distance traveled within that reach. Salmon survival was previously found to be dependent on the magnitude of Sacramento River flow at Freeport (Freeport flow). If survival model results confirm additional dependence on travel times or distances, some proposed physical mechanism for salmon survival can be confirmed or ruled out. And management actions that influence tidal dynamics or redistribute flows through the North Delta can be better evaluated for their impacts on salmon survival. The results of testing with the Bayesian model remain in progress, but are expected in the summer of 2022.

Simulated particle travel times and distances within a reach fell into two main regimes. When net flows were relatively high, reaches became unidirectional (no current reversals on flood tide) and changes in tidal strength or net flow had no impact on travel distance and little impact on travel times. At lower flows when the reach is tidal (having current reversals on flood tide), travel times and distances became highly variable and dependent on the time each particle entered a reach, relative to the start of ebb tide. Particles entering a reach within a few hours of one another may differ in their times spent within the reach by a total of 25 hours (a full tidal day).

A series of steady flow simulations was performed to assess the impact of changes in tidal strength when net flow was held constant. Tidal conditions were found to impact the average particle distance traveled but did not have much effect on travel times. Spring tides caused higher tidal excursions and higher distances traveled, but resulted in similar times spent in the reach as occurred during neap tides. This has implications for large-scale tidal marsh restorations. If a new restoration dampens tides in the North Delta, it can reduce travel distances. But unless that restoration redistributes net flows, it won't impact travel times. If net flows are redistributed, travel times will be reduced in some reaches, but at the expense of

increases in other pathways. This was demonstrated with modeling results of a large-scale restoration scenario.

Any potential impacts to travel times and distances resulting from marsh restorations are flow dependent, and decreases are only important when the reach is in the tidal flow regime (and not unidirectional). This transition between tidal and unidirectional happens at different Freeport flows for different reaches. It may happen over a narrow range of flows, and near the transition point, may alternate back and forth with spring-neap cycling. Net flows during a typical salmon outmigration season may be in the unidirectional range for at least some of the transitional reaches.

A set of simulations with an operable gate at the head of Georgina Slough was modeled. Closure of this gate along with the Delta Cross Channel gates showed significant decreases in travel time and distance traveled (35–50%) versus the open gates condition by increasing net flows through the Sutter, Steamboat, and Sacramento pathways. The gate additionally prevented particles from traveling down Georgian Slough, where modeled results suggested they were half as likely to be transported out of the Delta than particles traveling down other North Delta pathways.

Table of Contents

Table of Figures

List of Tables

Background and Objectives

This is the final report for the Delta Science Program, Delta Stewardship Council (DSC) Agreement No. 18224, supported by funding authorized by the passage of California Proposition 1. It is part of a collaborative effort involving the USGS California Water Science Center (CA WSC) and the USGS Western Fisheries Research Center (WFRC). Funding was provided separately to RMA and the USGS. The USGS DSC agreement number is 18202.

The objective of this project is to quantify the impact of tides and the hydrodynamic environment on the survival of outmigrating juvenile salmon in the northern Sacramento-San Joaquin Delta. The motivation for this study came from field data collected on acoustically-tagged salmon traveling through the system and the Bayesian salmon survival model described in Perry et al. (2018a).

As juvenile salmon migrate from rearing grounds on the upstream Sacramento River towards the San Francisco Bay, they take one of several paths through the network of channels in the North Delta (Figure 1).

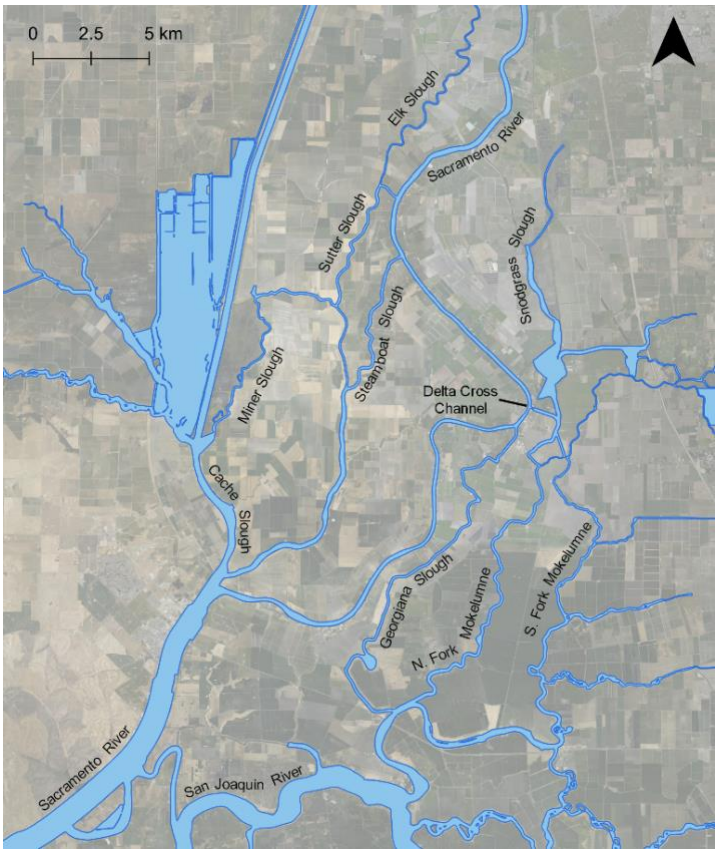

Figure 1 Reaches of the North Delta

Perry et al. (2018a) found salmon survival to be invariant to flow magnitude in reaches that were located either far downstream or far upstream in the system. Except in the case of exceptional droughts or exceptional flood events, these reaches maintain their general hydrodynamic character – tidal/bidirectional flow for the downstream reaches and riverine/unidirectional flow for the upstream reaches. Reaches in-between these two end members were classified as *transitional*. At lower Sacramento River flows they experience bidirectional flow, but at increased flows, the tides are dampened and conditions transition to unidirectional.

Salmon survival through transitional reaches was found to vary significantly with Sacramento River flow magnitude at Freeport ("Freeport flow"). The inflection points in the survival curves roughly corresponded to changes in the hydrodynamic character of the reaches as they shifted from tidal to riverine with increasing flow (Figure 2). Additionally, variability in survival increased at low flows. This also suggested a dependence on tidal dynamics, which interact with the length of a given reach to increase variability in travel time at low flows.

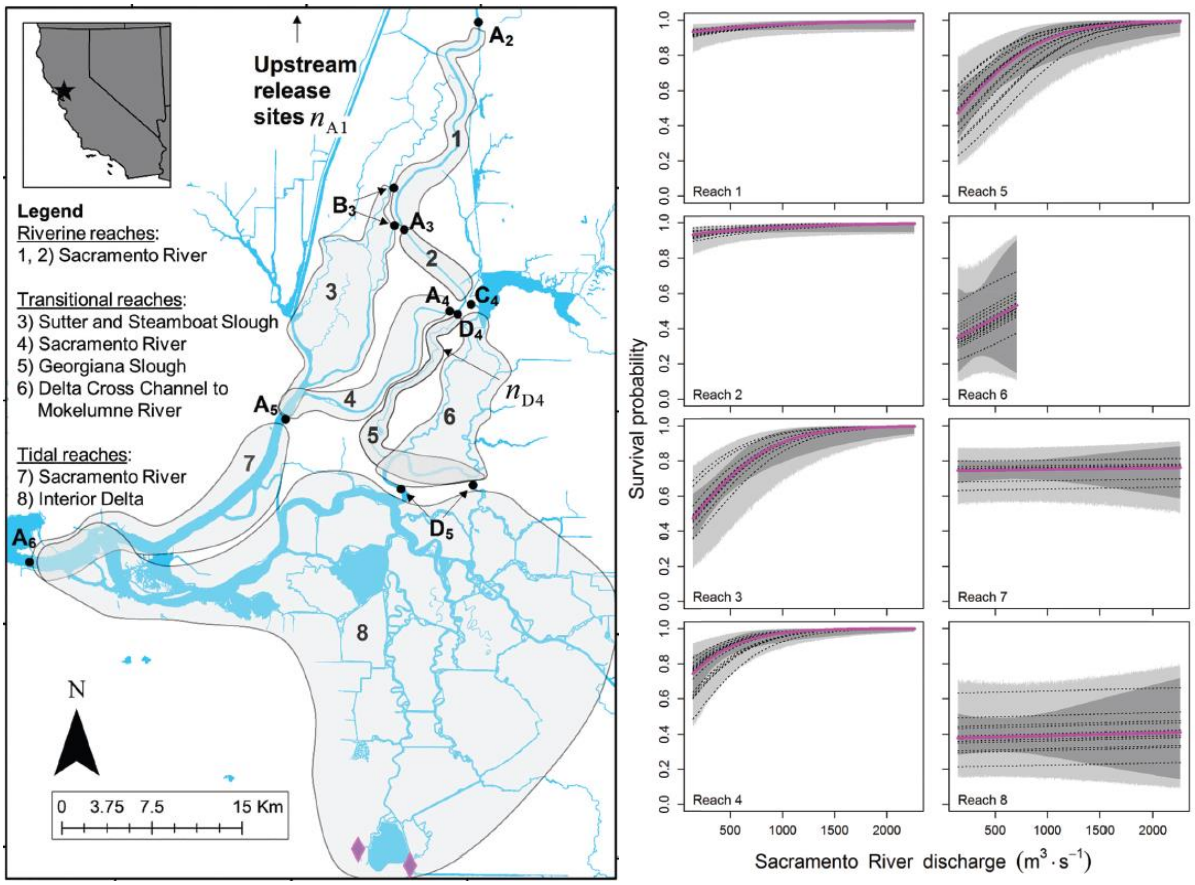

Figure 2 Survival probability of outmigrating juvenile salmon through reaches of the North Delta as a function of Sacramento River discharge. Reach definitions are shown on the right. Figures are from Perry et al. (2018a).

The primary objective of this project is to test the hypothesis that it is the nature of the hydrodynamic environment that directly impacts salmon survival. Although evidence from Perry et al. (2018a) points to this being the case, alternative hypotheses for survival dependence on Freeport flow exist:

- Predator metabolism: higher flows in winter and spring often coincide with colder water temperature than during low flow periods. At low flows, the higher water temperatures may increase the metabolism of predatory fish, leading to more predation on juvenile salmon and lower survival rates.
- Turbidity: higher flows are often associated with increased turbidity, which may decrease salmon mortality by predatory fish (such as striped bass) which rely on sight to hunt.

In order to test the hypothesis that the hydrodynamic character of the transitional reaches is impacting survival, more direct metrics of reach hydrodynamics were calculated and used as covariate inputs to the salmon survival model described by Perry et al. (2018a). These covariates included the total time spent in a given reach and the total distance traveled within that reach. They were calculated based on particle tracking simulations run using a calibrated hydrodynamic model of the upper San Francisco Estuary. If the inclusion of these covariates in the survival model increases the ability of the model to match observed data—above and beyond the Freeport flow covariate—we can better understand the mechanisms responsible for decreased salmon survival at low flows and explore management actions to mitigate them. The current version of the survival model is influenced solely by net flows at Freeport; actions which change tidal patterns throughout the North Delta (e.g., tidal wetland restoration) have no impact on survival model results.

Running the Bayesian survival model in order to test the statistical significance of the new hydrodynamic covariates is the responsibility of the USGS team at the WFRC. At the time of this report, the model setup and simulations are still in progress. A final report detailing their findings is expected in the summer of 2022.

There is also a secondary objective to this project, and it is to describe the hydrodynamic environment of the North Delta and how it responds to flow forcing from the Sacramento River and tidal conditions. The majority of water and sediment and a large portion of nutrients travel into the San Francisco Estuary by passing through the network of channels in the North Delta. The path water takes and how long it takes to get there has implications for nutrient cycling and ecosystems along the way as well as at the downstream end in the San Francisco Bay. In historical year simulations of particles made for this study, only 35% of the particles that traveled through the Delta Cross Chanel ultimately exited the Delta past Chipps Island.

Conversely, about 80% of the particles that traveled down Sutter or Steamboat Slough or the Sacramento River exited. As part of the North Delta Diversion project, water will be exported from locations near Freeport, reducing the flows through the North Delta. This work will help understand the implications for the fate and transport of the remaining water and material at reduced flows.

Work to describe the North Delta hydrodynamics was accomplished in collaboration with the USGS CA WSC team. A primary objective of their part of the project was to quantify the hydrodynamic character of the North Delta using data from their network of fixed-site monitoring stations (an *Eulerian* reference frame). By relating Eulerian reference frame metrics to those calculated from modeled particle tracking results (a *Lagrangian* reference frame) salmon model covariates can be developed for future conditions without reliance on additional particle tracking simulations.

The following section of the report describes the setup and details of the hydrodynamic and particle tracking models, and how the travel time and distance traveled covariates were developed. The results section presents summary graphics for these metrics, along with supporting data describing the tidal characteristics of the North Delta. A final section summarizes the main points and management implications derived from this study.

Modeling Approach

RMA Bay-Delta Model Description

The RMA Bay-Delta model was chosen for this analysis. It is a hydrodynamic and water quality model that predicts flow and water levels and is a well-established tool for analysis of impacts of proposed projects in the Sacramento-San Joaquin Delta. A summary of representative applications of the RMA Bay-Delta Model is given at: https://www.rmanet.com/services/numerical-modeling/rma-bay-delta-model/.

The RMA Bay-Delta Model was chosen based on its ability to provide accurate simulations of Delta-wide hydrodynamics and its calibration to flows through the North Delta as part of previous projects in collaboration with the USGS, Sacramento Regional Sanitation District, and the CA Department of Water Resources (DWR). The RMA Bay-Delta Model utilizes the RMA2 hydrodynamics and RMA11 water quality transport finite element computational engines. The finite element model formulation allows use of an unstructured computation mesh where resolution can be increased locally to represent the details of rapidly varying topography. The RMA2 and RMA11 engines support combining two-dimensional (2D), depth-averaged computational elements and one-dimensional (1D), cross-sectionally averaged elements in a single mesh. In the RMA Bay-Delta Model all large channels, embayments, and tidal marsh

restoration areas are represented in 2D. Additional 2D mesh areas were added around the major junctions in the North Delta for more accurate predictions of junction hydrodynamics and particle entrainment; this was done during a previous study of North Delta particle tracking, in collaboration with the USGS CA WSC.

The RMA Bay-Delta Model does not directly simulate the effects of stratified flow, which would require application of a three-dimensional (3D) model. The effects of stratification are approximately incorporated into the model through calibration exercises where mixing coefficients are adjusted to best represent the observed salinity field for a historic period, or to best represent the simulated salinity field from a 3D model simulation for a proposed condition. For the simulations in this project, we have assumed the transitional reaches are located far enough upstream to not be appreciably impacted by density driven transport. For this reason and to conserve computational effort, the simulations were run without simulation of salinity.

Model Geometry and Bathymetry

RMA's Bay-Delta model grid was developed using an in-house, GIS-based, graphical user interface program (RMA, 2003). The program allows for development of the finite element mesh over layers of bathymetry points and bathymetry grids, GIS shapefiles and aerial images. The grid, shown in Figure 3, extends from Martinez at the west end of Suisun Bay to the Sacramento River above the confluence with the American River, and the San Joaquin River near Vernalis.

Model bathymetry is shown in Figure 4. For all areas of the Delta, the most current, best quality bathymetric data were used to set grid elevations. This includes data collected by a wide array of governmental agencies (DWR, USGS, USACE, and NOAA) and individual companies (e.g., cbec, Wetland and Water Resources, and Environmental Data Solutions). The bathymetry data sets include cross-section measurements, single-beam transects, and multi-beam bathymetry surveys[1]. Most of these datasets have been compiled and documented by DWR and can be downloaded from DWR's Delta Modeling Section site[2]. Other bathymetry data set sources are described in previous RMA Bay-Delta model calibration documents.

Model Boundary Conditions

Figure 3 shows the locations of model boundary conditions. The boundary conditions used in simulations for this project are:

[1] https://gis.water.ca.gov/arcgisimg/rest/services/Bathymetry

[2] https://data.cnra.ca.gov/dataset/san-francisco-bay-and-sacramento-san-joaquin-delta-dem-for-modeling-version-4-2

Tidal boundary at Martinez

Inflows:
Sacramento River above American River
American River near Sacramento
San Joaquin River near Vernalis
Yolo Bypass and Yolo Bypass Toe Drain
Mokelumne River near Thornton
Cosumnes River
Calaveras River

Exports/Diversions:
State Water Project (SWP), Clifton Court Forebay gates
Central Valley Project (CVP), Tracy Pumping Plant
Contra Costa Water District; Old River, Victoria Canal, Rock Slough exports
North Bay Aqueduct, Barker Slough Pumping Plant

Major Control Structures:
Delta Cross Channel gates
Suisun Marsh Salinity Control Gates (SMSCG)

A set of distributed, smaller scale water withdrawals and return flows (Delta Island Consumptive Use, DICU) was prescribed based on estimates from DWR. These are shown in Figure 5. The seasonal South Delta agricultural barriers were typically not installed for the historical periods modeled in this study (November through May).

Water levels at the Martinez boundary were increased +0.2 ft from observed to account for baroclinic forcing effects not accounted for in the uncoupled hydrodynamic model simulations performed for this study.

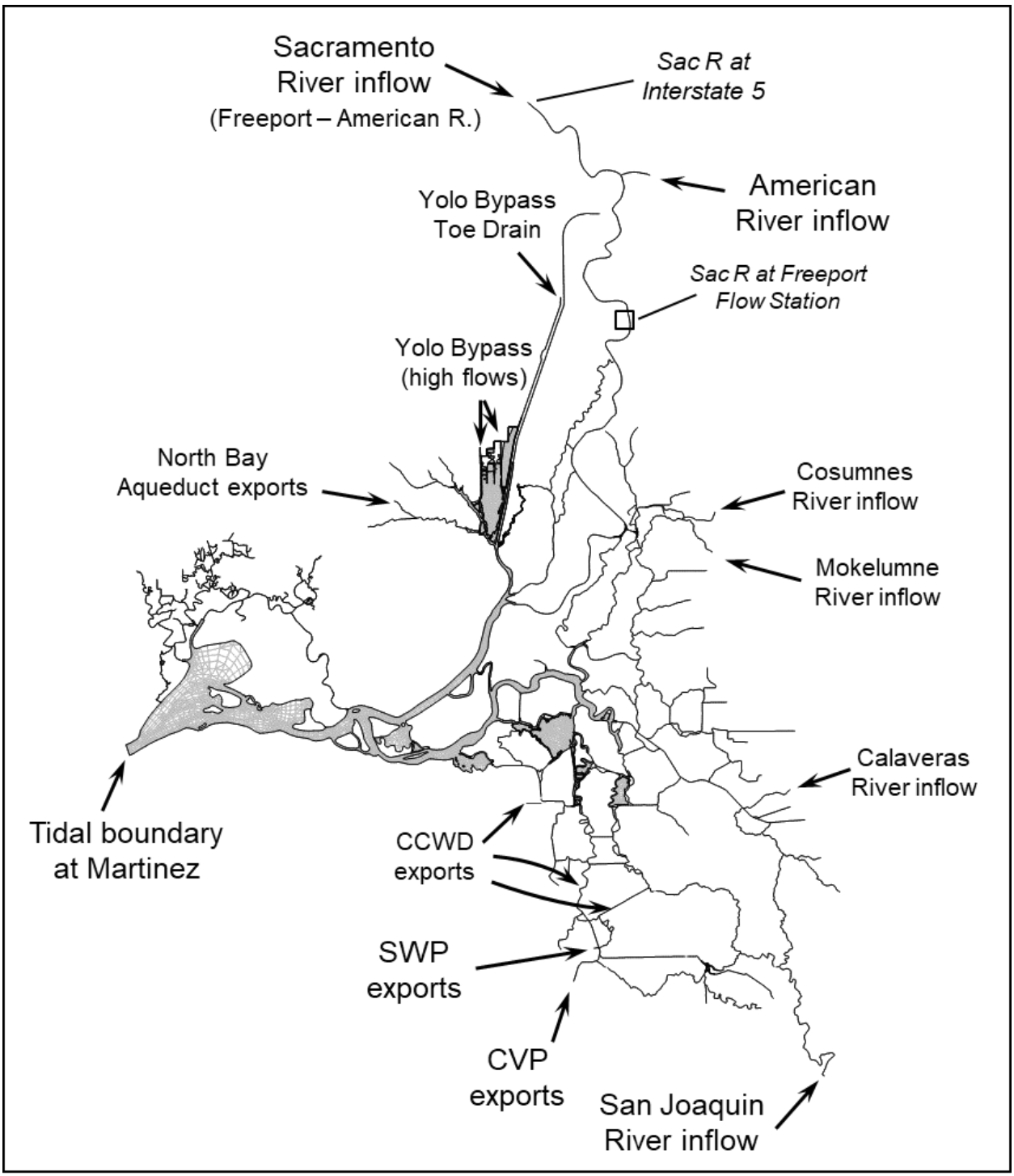

Figure 3 RMA Bay-Delta Model grid extents and locations of boundary conditions

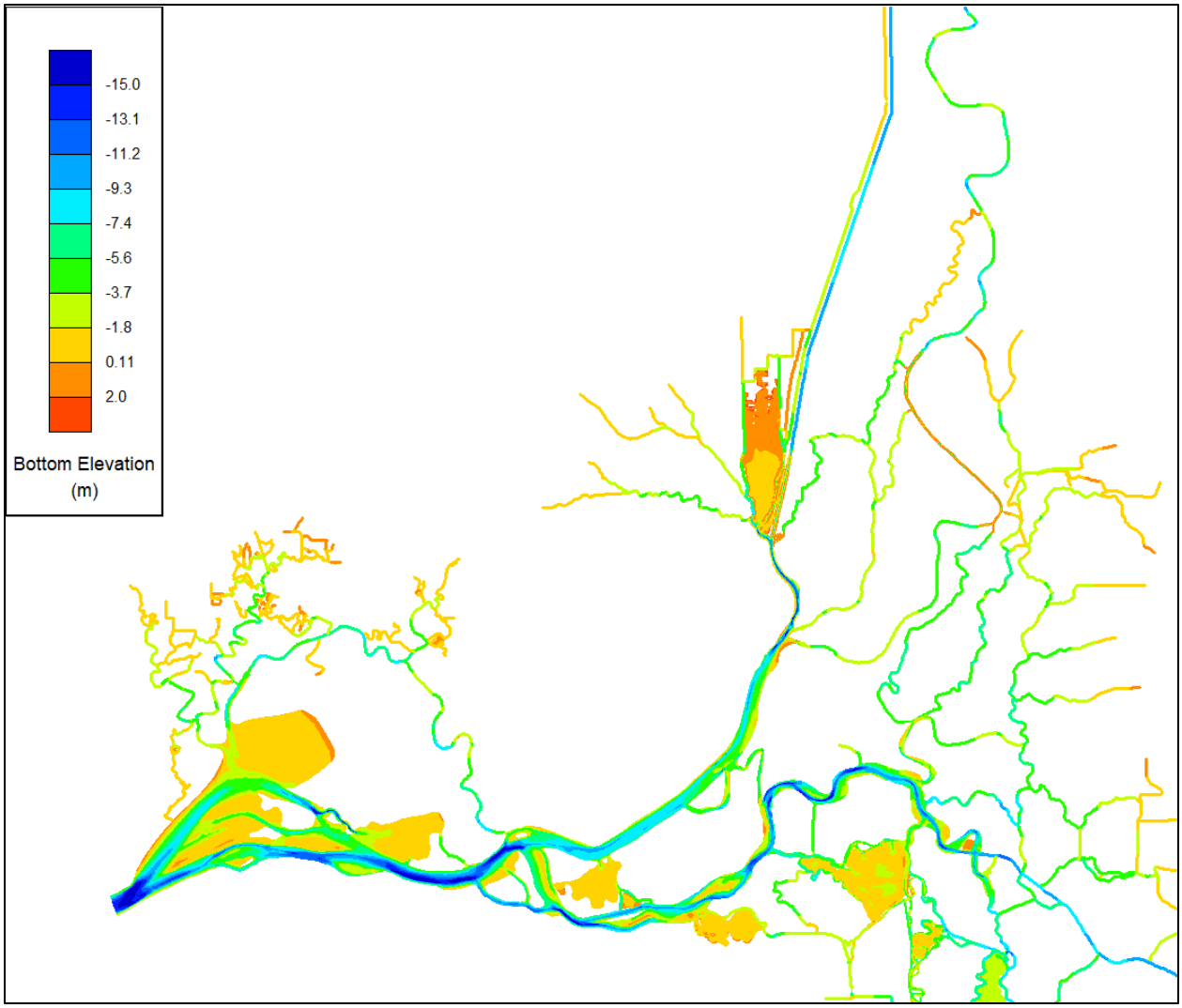

Figure 4 RMA Bay-Delta Model bathymetry

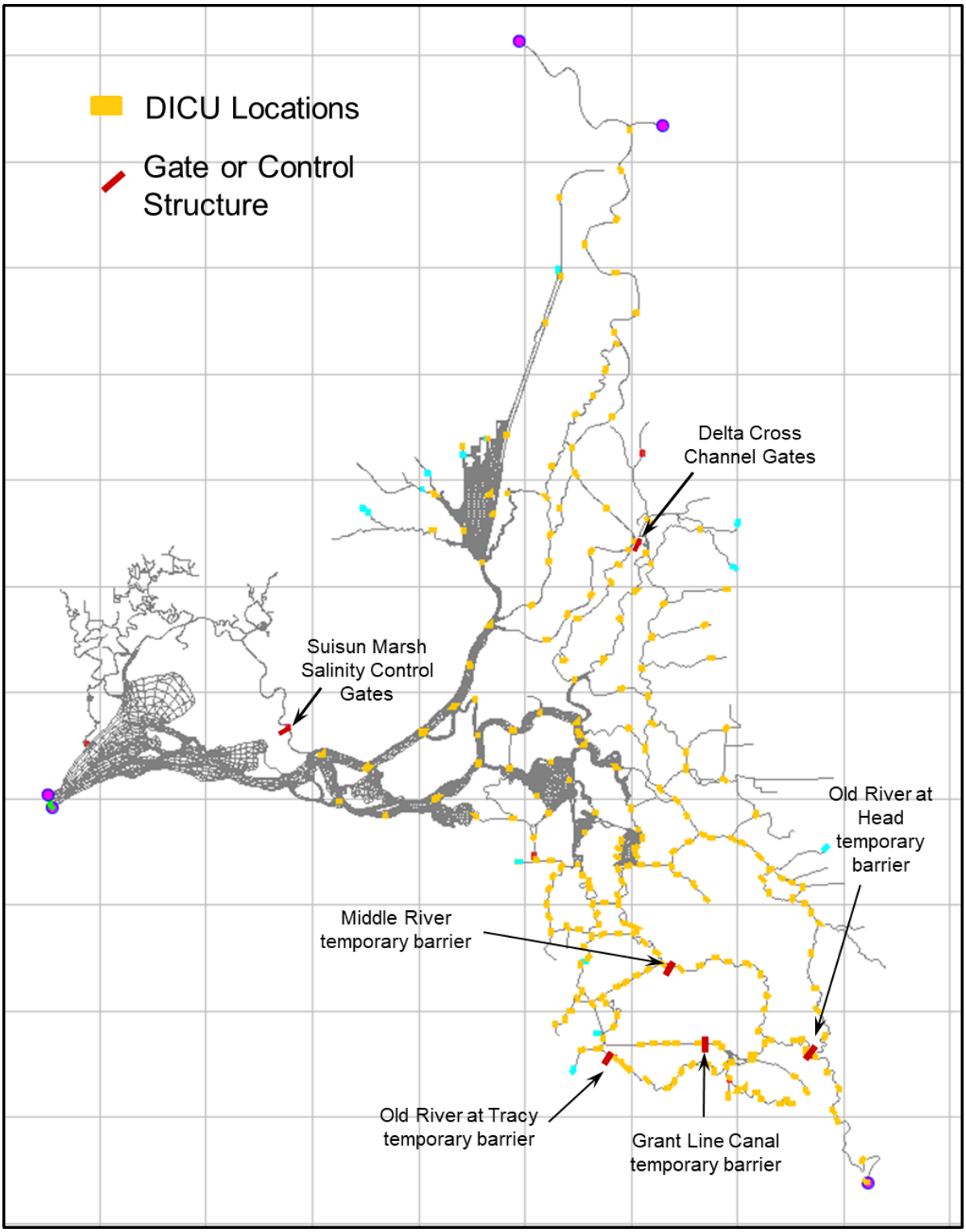

Figure 5 Locations of RMA Bay-Delta Model Delta Island Consumptive Use withdrawals and returns and operational hydraulic structures.

Particle Tracking

The RMA particle tracking model is driven by hydrodynamic output files calculated by the RMA2 model. Velocities and water levels at model node locations are interpolated to obtain conditions at a given particle's location and time. These local conditions are used to calculate the particle's trajectory along a streamline. Dispersion coefficients are used to estimate the stochastic aspect of particle transport and represent processes not resolved by the depth-averaged (in 2D elements) or depth- and laterally-averaged (in 1D elements) flow fields. The dispersion coefficients have been calibrated and assigned based on comparisons to modeled tracer release results. The full set of differential equations describing particle transport is given in Heemink (1990).

The RMA particle tracking model has the ability to incorporate modeled scalar fields (e.g., salinity or water temperature) and assign behavioral rules allowing particles to respond to thresholds or gradients in the fields. For simulations in this study, however, no behavior rules were assigned to the particles, and their behavior is termed *passive*.

In the RMA particle tracking user interface, virtual particles are released from user-defined release locations at set times or at set intervals. After release, certain attributes of each particle are tracked, including particle age (time from release) and total distance traveled. The particle tracking model allows the user to set virtual monitoring stations throughout the model domain, each of which output a record of particle attributes at the time when an individual particle passes. By placing monitoring stations at the upstream and downstream ends of reaches in the North Delta, differences between particle attributes can be calculated to determine the time spent and distance traveled within each reach.

The locations of particle monitoring stations were set up to correspond to the locations of the USGS acoustic telemetry stations, and are shown in Figure 6. All particles were released along a transect in the Sacramento River near the I Street bridge, corresponding with the actual release location of tagged salmon. Fifteen particles were released at 15-minute intervals throughout the simulations, in order to obtain an approximately continuous release record.

Because of the tidal nature of the system, particles may pass the same station multiple times; this is particularly true at downstream stations during low flow periods. To calculate the travel time and time spent within a given reach, the first time a particle passes the upstream station and the first time it passes the downstream station were used. This is consistent with how fish are treated in the multi-state statistical model of Perry et al. (2018a).

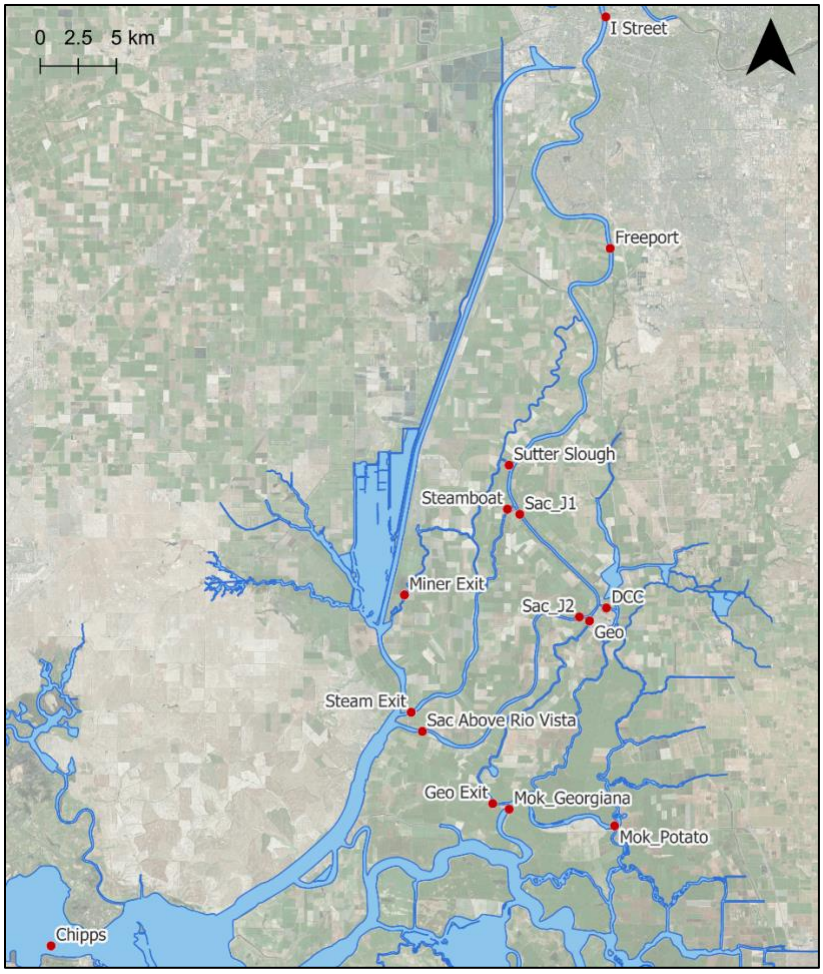

Figure 6 Particle tracking model monitoring locations. Particles were releases were made from the I Street Station.

Historical Simulations

Historical hydrodynamic and particle tracking simulations were performed to correspond with acoustically tagged juvenile salmon release periods used in the salmon survival model. These periods corresponded to outmigrating late-fall run Chinook salmon and spanned the November to May period of water years 2007–2011. River inflow boundary conditions for this period are shown in Figure 7 and exports are shown in Figure 8. DWR has classified the water years according to the Sacramento Valley unimpaired flows as Dry (2007), Critical (2008), Dry (2009), Below Normal (2010), and Wet (2011). During each year, the Delta Cross-Channel was typically closed in December and opened again in May.

The results of the model simulations were compared against flow measured at USGS and DWR monitoring stations throughout the North Delta (Appendix A). Results are shown for water year 2009; plots showing he accuracy of the hydrodynamic model in reproducing observed flows in the other water years are roughly similar and are not shown.

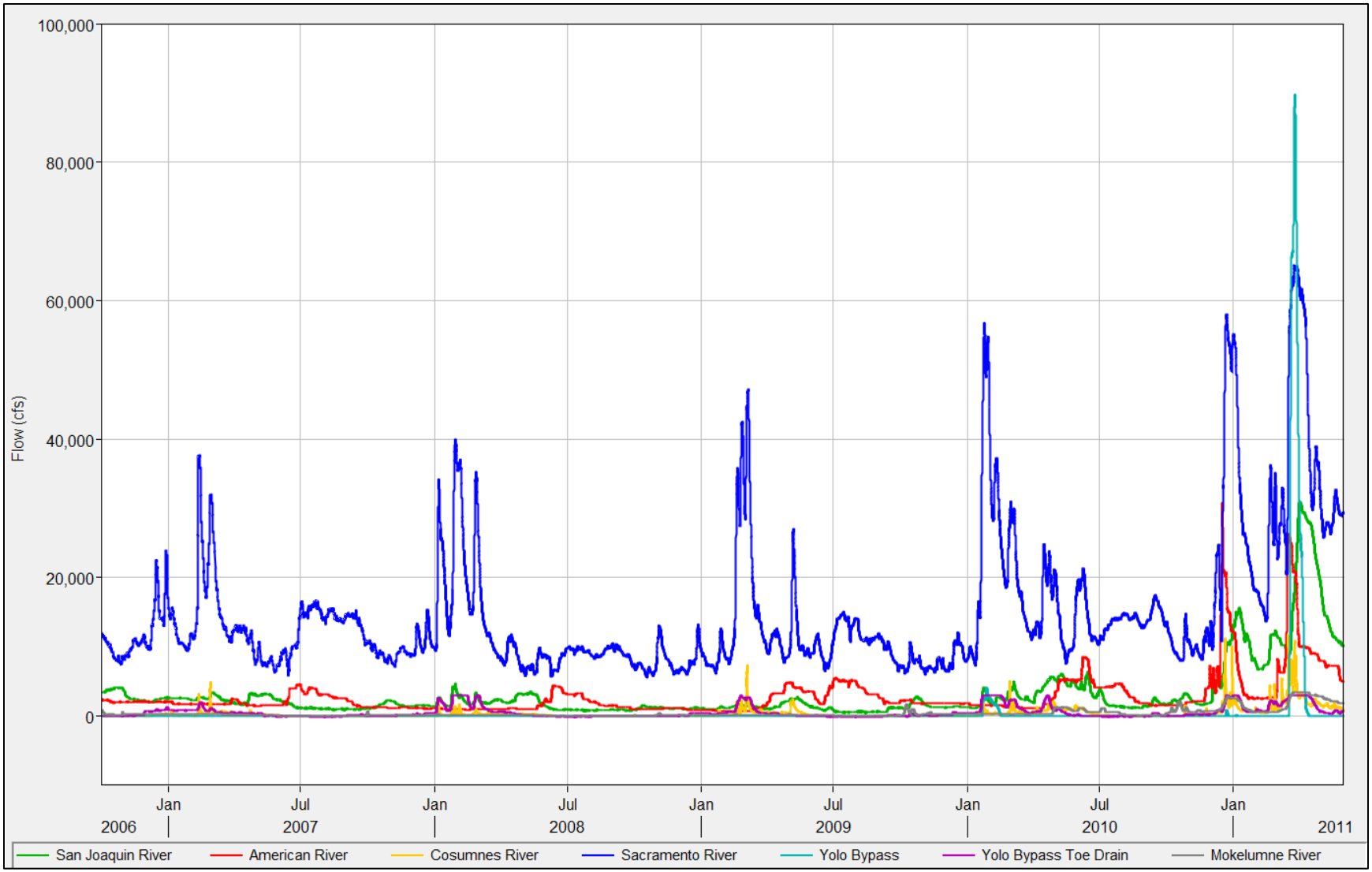

Figure 7 Historical simulation river inflows

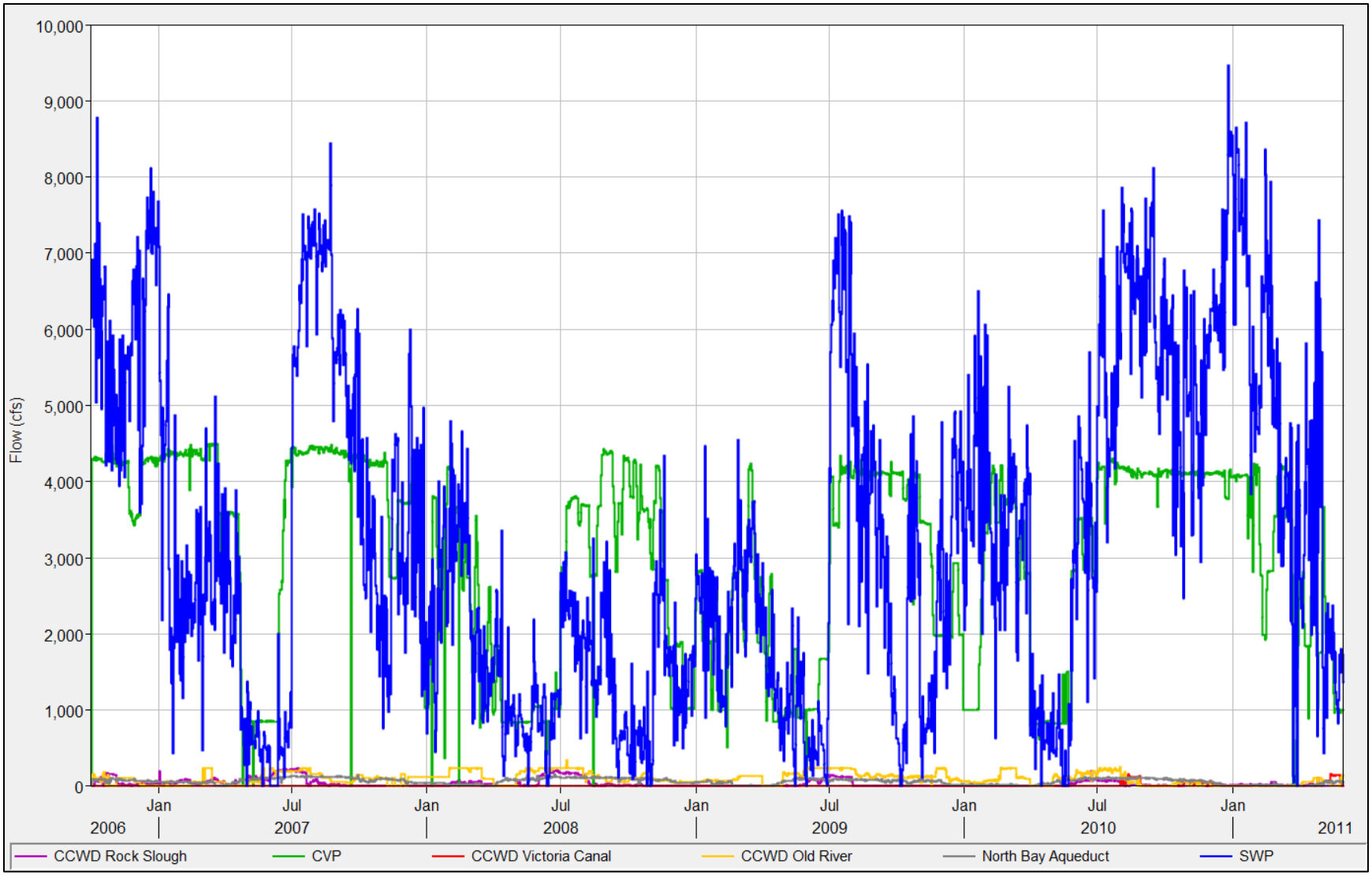

Figure 8 Historical simulation diversions

Constant Sacramento River Inflow Simulations

Simulations with a constant Sacramento River inflow were performed in order to assess the impact of Freeport flow magnitude on a hydrodynamic environment that is also impacted by tidal conditions. The San Francisco Estuary has mixed, semi-diurnal tides. Interactions between the O1 and K1, and S2 and M2 tidal frequencies create spring-neap cycling, with a period of approximately 14.8 days. Other tidal constituents and overtides resulting from tidal interaction with bottom friction contribute additional periodic variation. By holding flow constant, the impact of the tides—and an examination of the effects of spring-neap cycling—can be analyzed without having to filter out the complicating effects of unsteady flow.

Steady flow simulations were performed for Sacramento River flows between 4,000 and 30,000 cfs in increments of 2,000 cfs; between 35,000 and 50,000 cfs in increments of 5,000 cfs; and for flows of 60,000 and 70,000 cfs. A total of 20 steady flow runs were performed.

Increased resolution at the lower flow magnitudes was designed to capture the range of flows most frequently encountered in the North Delta (Figure 9) with sufficient resolution to capture changes occurring in the transitional reaches.

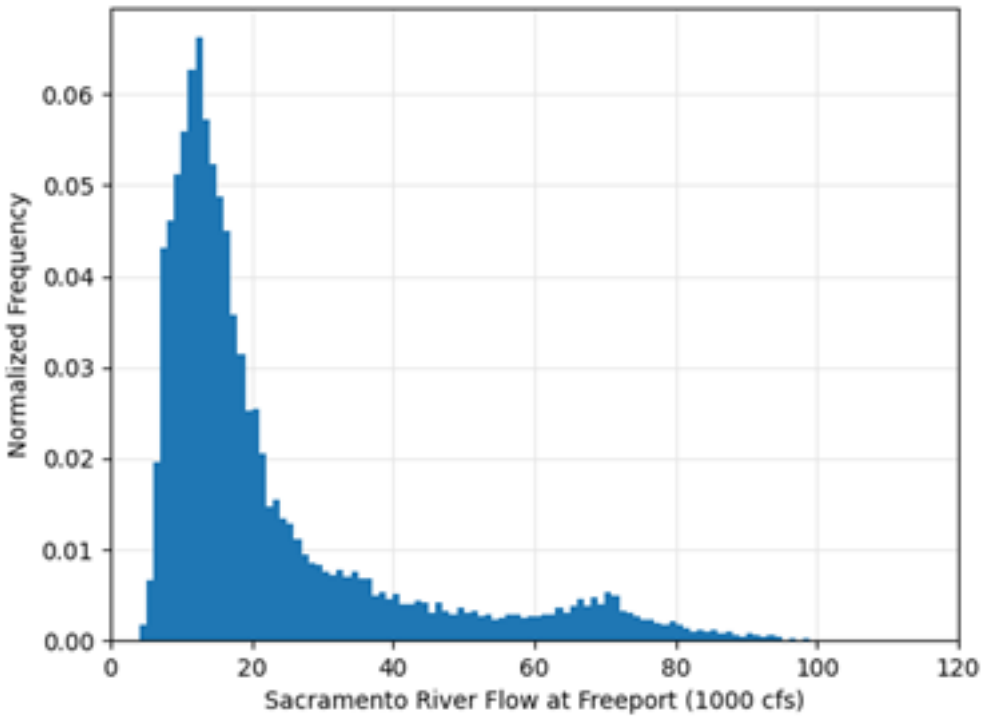

Figure 9 Histogram of daily Sacramento River flows at Freeport for USGS monitoring station period of record.

The seasonal period of interest for this study is December through March, generally corresponding to peak late-fall run Chinook salmon outmigration and the timing of USGS field

studies. (Historical simulations were run for a longer time period, November through May, in order encompass early and late-season migrants.) Boundary conditions for Delta inflows, exports, gate operations, and other simulation inputs were chosen to be consistent with conditions in the Delta during these months.

All Delta inflows, exports, and gate operations were held constant through the duration of each steady flow simulation. Because of the importance of the Delta Cross Channel (DCC) operation to conditions in the North Delta, two steady flow runs were performed for each target Sacramento River flow magnitude: one with the DCC open and one with the DCC closed.

Tidal Water Level Boundary Condition

The steady flow simulations were forced with an observed tidal stage record near Martinez. A three-year simulation period during a set of dry to critical water years—from 2013 through 2015—was chosen in order to minimize the impact of high flows on the downstream boundary.

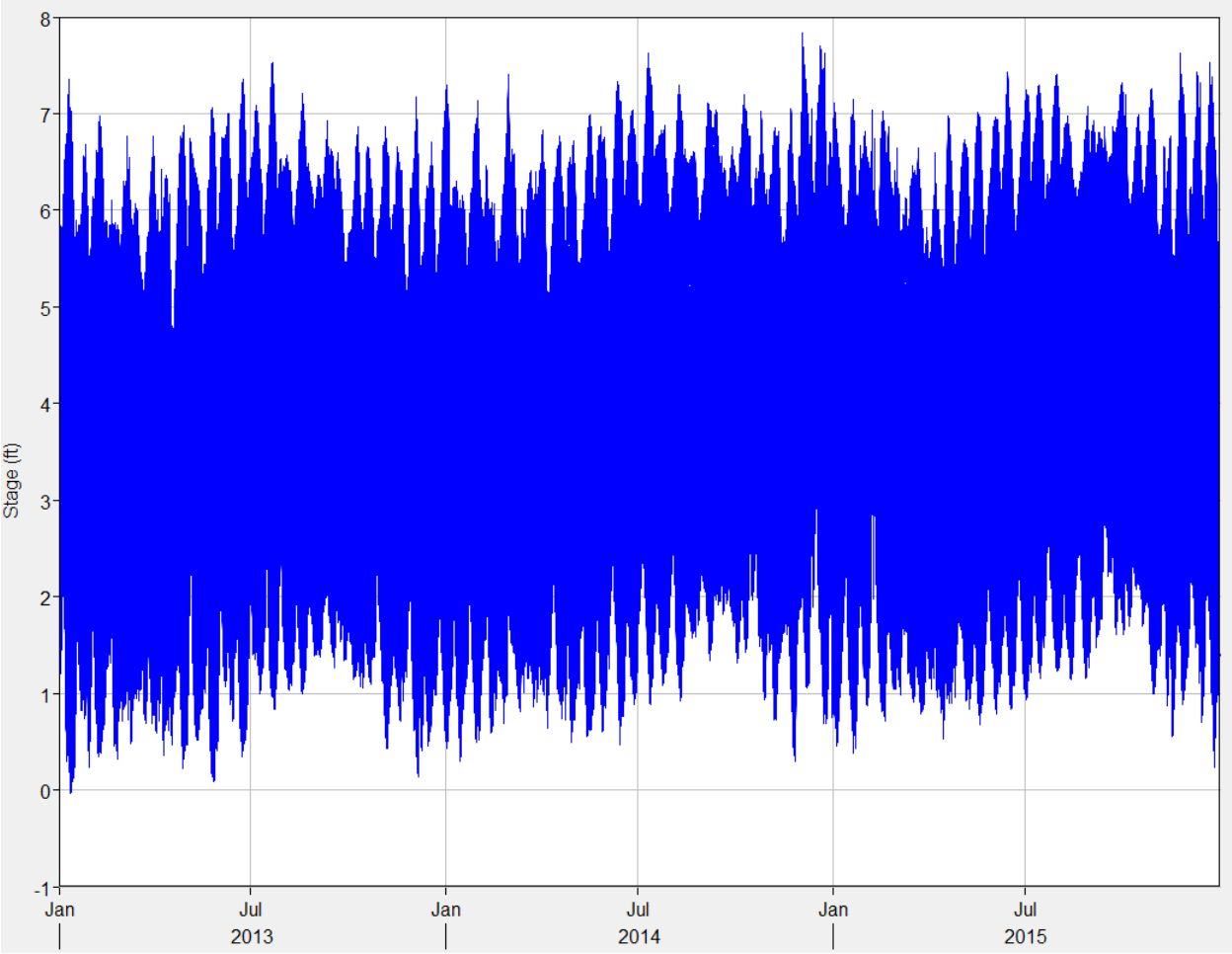

Figure 10 Steady flow run downstream stage record near Martinez

Flow Boundary Conditions

In order to perform *representative* simulations of Delta flow conditions for each of the Sacramento River target flows, an analysis of historical December–March conditions from Dayflow[3] daily flow data (WY 1997–2018) was performed. Delta boundary inflows and exports were binned to find daily flow values corresponding to each Sacramento River flow condition. An example of this binning procedure is shown for San Joaquin River flows in Figure 11.

Exports showed little correlation with Sacramento River flows. North Bay Aqueduct and CCWD withdrawals were set at historical December–March median values for all simulations. SWP and CVP withdrawals were set at historical median values for all simulations above Sacramento River flows of 15,000 cfs. At lower flows, water project exports are reduced and the median of the binned export flows corresponding to each target Sacramento River flow was used (see Table 1).

At low to moderate Sacramento River flows, Delta inflows from the Mokelumne River are regulated by releases from Camanche Reservoir and are relatively constant. These were set at historical December–March median values. The median of the binned Mokelumne flows corresponding to each target Sacramento River flow was used for the higher flow simulations. A similar procedure was applied to combined flows coming from the Yolo Bypass and Toe Drain. The Toe Drain was apportioned flows up to 3,000 cfs (its approximate capacity). Additional flow above 3,000 cfs is allocated to the model boundary at the Yolo Bypass locations (in Prospect Slough and Shag Slough).

Flows for the San Joaquin River, Cosumnes River, and Calaveras River were set using the median of the binned flows corresponding to each target Sacramento River flow (see Figure 11 example). Some smoothing was applied to the binned values to ensure monotonically increasing flows with increasing Sacramento River flow. Table 1 lists flow boundary conditions for each steady flow simulation.

Hydraulic Structure Operations

Hydraulic structure operations were determined using the prevailing operating condition during the December–March study period. Because of the importance of the Cross Channel operation, two steady flow runs will be performed for each target Sacramento River flow—one with the gates open and one with the gates closed. The Suisun Marsh Salinity Control Gates are typically operating during times of low Delta outflow and open during higher Delta outflows. The flow

[3] https://data.ca.gov/dataset/dayflow

cutoff used to determine which operation to use was set at a Sacramento River flow of 15,000 cfs, based on an analysis by Chris Enright[4].

Operating conditions are summarized in Table 2.

DICU

The locations of small-scale water withdrawals and return flows throughout the Delta are shown in Figure 5. The net removal of water from these locations was determined from the long-term median value of net channel depletions for the December–March time period. This value was derived from the Dayflow record and is 671 cfs (roughly 15% of peak summer net withdrawals). This net withdrawal was applied to the DICU locations using a spatial pattern typical of winter conditions.

[4] http://www.cwemf.org/Asilomar/ChrisEnright.pdf

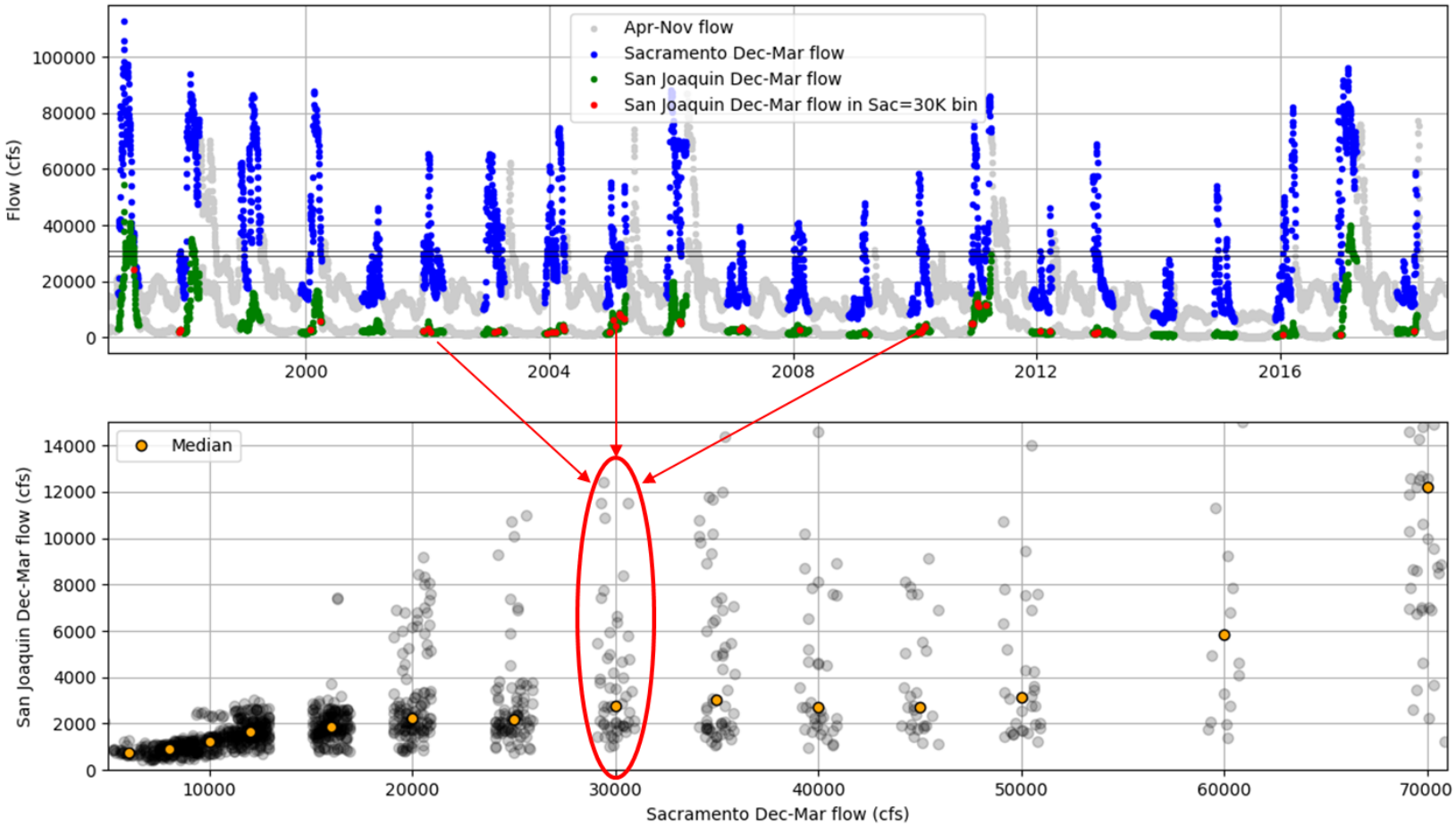

Figure 11 Example of binning procedure used to determine steady San Joaquin River inflow magnitude corresponding to a Sacramento River inflow magnitude of 30,000 cfs. Top plot shows Dayflow timeseries of Sacramento River and San Joaquin River flows, WY1997–2018. Flows within the months of December through March (study period) are highlighted in blue (Sacramento) and green (San Joaquin). San Joaquin River flows on days when Sacramento River flow is 30,000 cfs ± 1,000 cfs are plotted in red. These values are collected, and the median is used for the steady San Joaquin River flow corresponding to Sacramento 30,000 cfs. Bottom plot shows binned values and medians for additional Sacramento River inflow magnitudes.

Table 1 Steady flow run boundary conditions

Sacramento River	San Joaquin River	Toe Drain	Yolo Bypass	Cosumnes River	Mokelumne River	Calaveras River	CCWD Export	SWP Export	CVP Export	North Bay Aqueduct Export
4000	679	94	0	6	277	30	88	689	403	24
6000	881	94	0	43	277	32	88	689	403	24
8000	1059	94	0	79	277	35	88	1485	996	24
10000	1222	94	0	115	277	37	88	2399	1729	24
12000	1373	94	0	151	277	39	88	2933	2646	24
14000	1516	94	0	187	277	41	88	3478	3512	24
16000	1651	94	0	223	277	43	88	3478	3569	24
18000	1780	94	0	259	277	46	88	3478	3569	24
20000	1905	94	0	295	277	48	88	3478	3569	24
22000	2025	94	0	332	277	50	88	3478	3569	24
24000	2141	94	0	368	277	52	88	3478	3569	24
26000	2253	94	0	404	277	54	88	3478	3569	24
28000	2363	94	0	440	277	57	88	3478	3569	24
30000	2470	1848	0	476	277	59	88	3478	3569	24
35000	2726	2269	0	566	277	64	88	3478	3569	24
40000	2969	2690	0	657	277	70	88	3478	3569	24
45000	3202	3000	111	747	277	76	88	3478	3569	24
50000	3426	3000	532	837	277	81	88	3478	3569	24
60000	5860	3000	1374	1060	552	226	88	3478	3569	24
70000	12200	3000	23701	1610	1380	1638	88	3478	3569	24

Table 2 Steady flow simulation hydraulic structure operations

Hydraulic Structure Location	Hydraulic Structure Type	Steady Flow Simulation Operating Condition
Fall Head of Old River	Partial Temporary Rock Barrier with Culverts	Not Installed
Spring Head of Old River	Temporary Rock Barrier with Culverts	Not Installed
Old River Barrier near Tracy	Temporary Rock Barrier with Flap Gate Culverts	Not Installed
Middle River Barrier	Temporary Rock Barrier with Flap Gate Culverts	Not Installed
Grant Line Canal Barrier	Temporary Rock Barrier with Flap Gate Culverts	Not Installed
Delta Cross Channel	Gate	Two Simulations to Cover Both Open and Closed Conditions
Suisun Marsh Salinity Control Gate	Tidal Gates and Stop Logs	Gates Open, Stop Logs Out for Sacramento Flows > 15,000 cfs; Gates Operating, Stop Logs In for Sacramento Flows < 15,000 cfs

Management Alternatives

Three alternative model grids were constructed in order to investigate the impacts of large-scale tidal marsh restoration and an operable gate at the head of Georgiana Slough. By opening up large areas to restoration, tidal ranges in the Delta are dampened, travel times and distances through transitional reaches in the North Delta may be reduced, and consequently, juvenile salmon survival may be increased. Examples of these grids are shown in Figure 12 for a large-scale Suisun Marsh restoration and Figure 13 for a restoration scenario involving the Cache Slough Complex and areas in the eastern Delta. Both restorations were chosen for this analysis because they were predicted to dampen tides in the North Delta without impacting net flow through the Delta Cross Channel (and thus affecting salinity intrusion).

A final alternative grid was constructed with an operable gate at the head of Georgiana Slough. With the gate closed, salmon can be physically prevented from traveling into the Central and South Delta. Closure may also lead to changes in travel time and distance traveled in the rest of the North Delta. By operating both the Georgiana and DCC gates, the other pathways in the North Delta become more riverine and travel times and distances are reduced. Consequently, juvenile salmon survival may be increased.

Following grid development, the alternatives were run using steady Sacramento River flows of 10, 16, and 24 thousand cfs. These flows were chosen to span a range of relevant flow

conditions without running the full set of 20 steady Freeport flows. The tidal marsh restoration alternatives were run with the DCC open and compared against base (no restoration) steady flow results with the DCC open. The Georgiana gate alternative was run with the DCC closed and compared against base (no gate) steady flow results with the DCC closed.

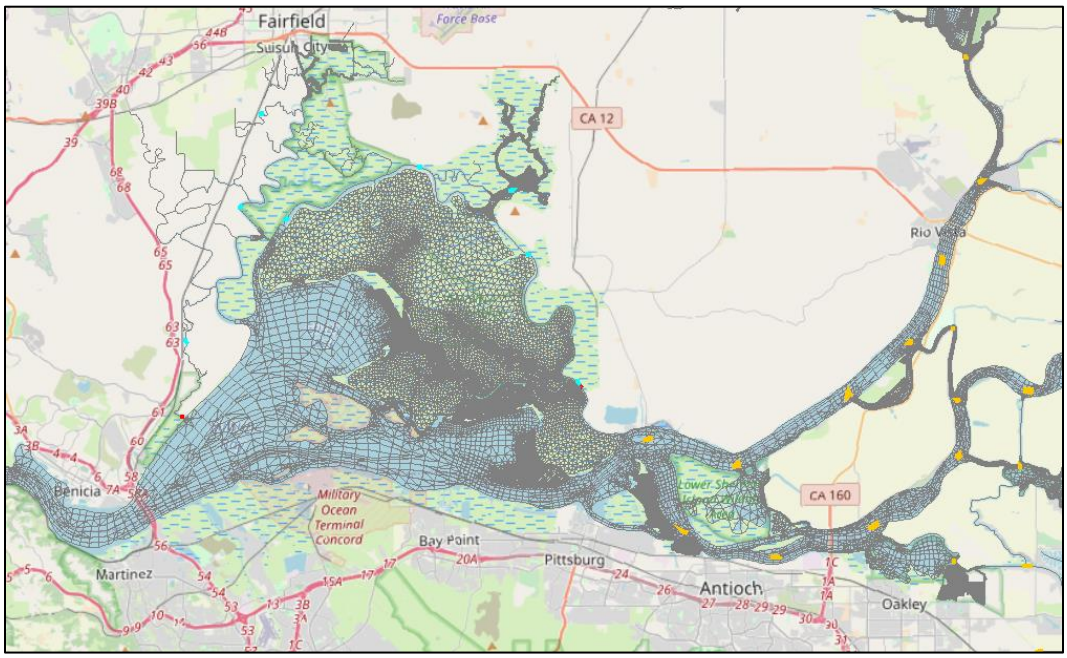

Figure 12 RMA Bay-Delta model alternative grid with large tidal marsh restoration on Grizzly Island

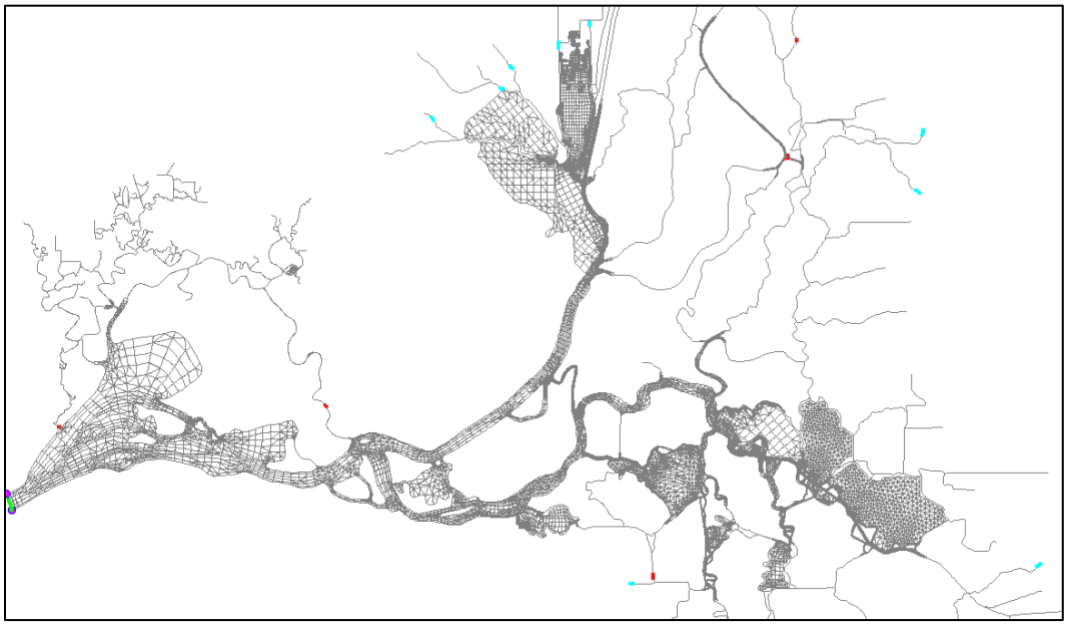

Figure 13 RMA Bay-Delta model alternative grid with large tidal marsh restorations in the Cache Slough Complex and the eastern Delta

Results

Particle Travel Time and Distance Traveled Within a Transitional Reach

A time series of particle travel times and distance traveled is given in Figure 14 for a representative transitional reach in the North Delta. The reach shown is Steamboat Slough, and travel times and distances were calculated from post-processing model results using first arrivals at the upstream and downstream monitoring locations ("Steamboat" and "Steam exit", see Figure 6). Results are plotted for the water year 2009 simulation. The patterns shown are typical of those in other transitional reaches and in other water years. They will be described qualitatively in this section to aid understanding of particle transport in the system before more advanced metrics and graphics are presented.

In Figure 14, every particle that passes through Steamboat Slough is plotted using a black marker at the time of its first passage by the upstream station. The dependence of time and distance within the reach on Freeport flow is apparent, with travel times and distances doubling or tripling between periods of low and high flow. While travel times continue to decrease incrementally with higher and higher flows, a limit is reached in the distance traveled plot in late February to early March. At these flows, velocities in the entirety of Steamboat Slough are unidirectional, and the distance traveled approaches its lower limit of the reach length (approximately 18 km).

At lower Freeport flows, a multi-modal distribution of travel times and distances is seen. This presents as horizontal bands of points in the travel time plot for the first half of the simulation in Figure 14. Figure 15 shows the January to February time period to highlight the details of this pattern. It is a consequence of the tidal excursion length being a large percentage of the length of the reach. Particles can only experience an integer number of tidal reversals during their journey downstream through the reach. Particles that enter the reach at the start of a strong ebb tide may only experience two flood tides (where the current direction reverses to upstream) before they exit the reach. But particles entering in the middle of ebb may experience three upstream reversals, and those entering at the end of ebb may experience four. This leads to the behavior whereby particles that enter a reach within a span of a few hours may differ in their time spent in the reach by 12 or 25 hours. An illustration of this behavior is shown in Figure 16.

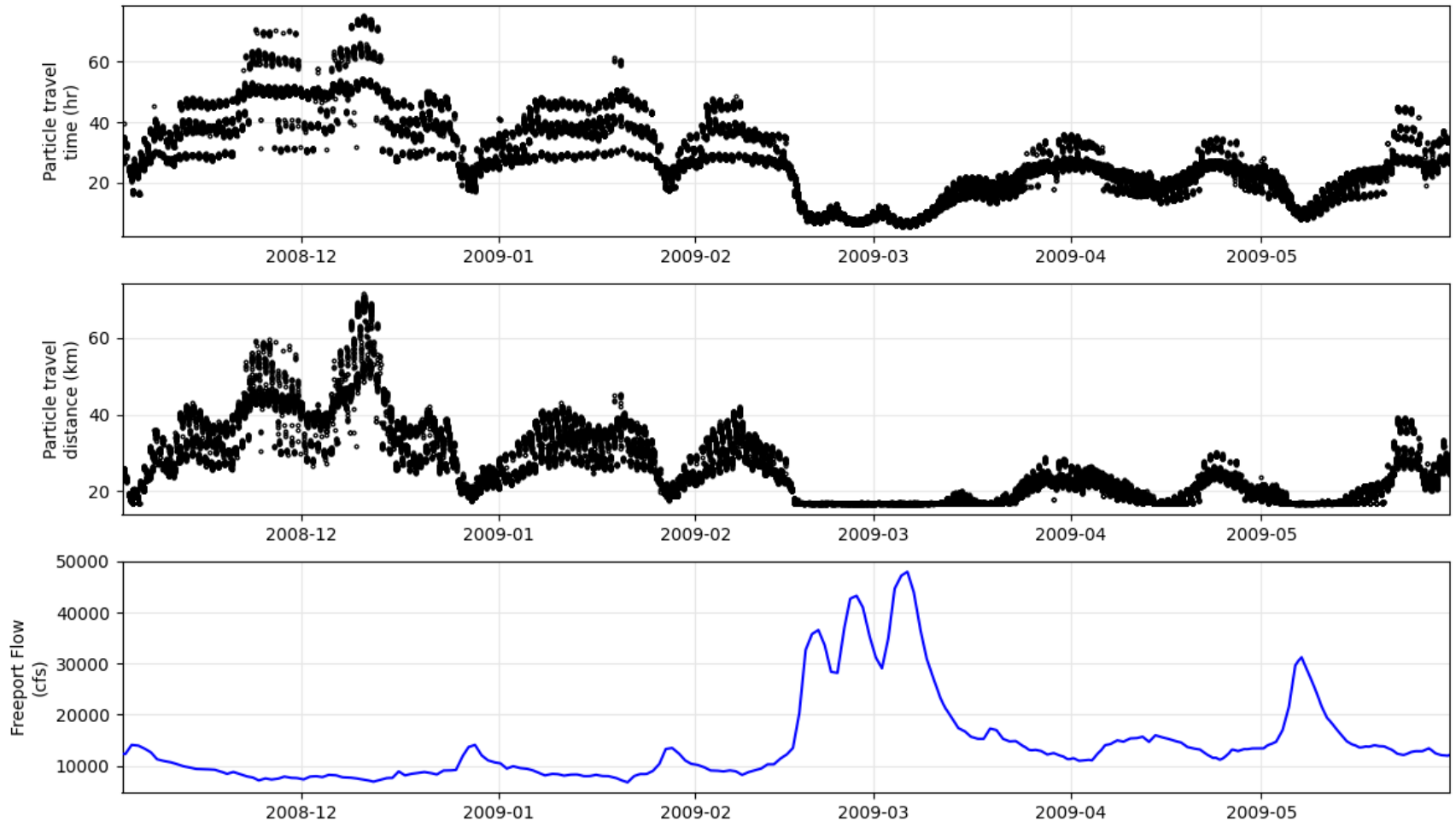

Figure 14 Particle travel time (top panel) and distance traveled (middle panel) in a transitional North Delta reach (Steamboat Slough) for November–May of water year 2009. Black circles represent results from individual particles and are plotted using the first time they pass the upstream station. Bottom panel shows daily averaged Sacramento River flow at the Freeport station.

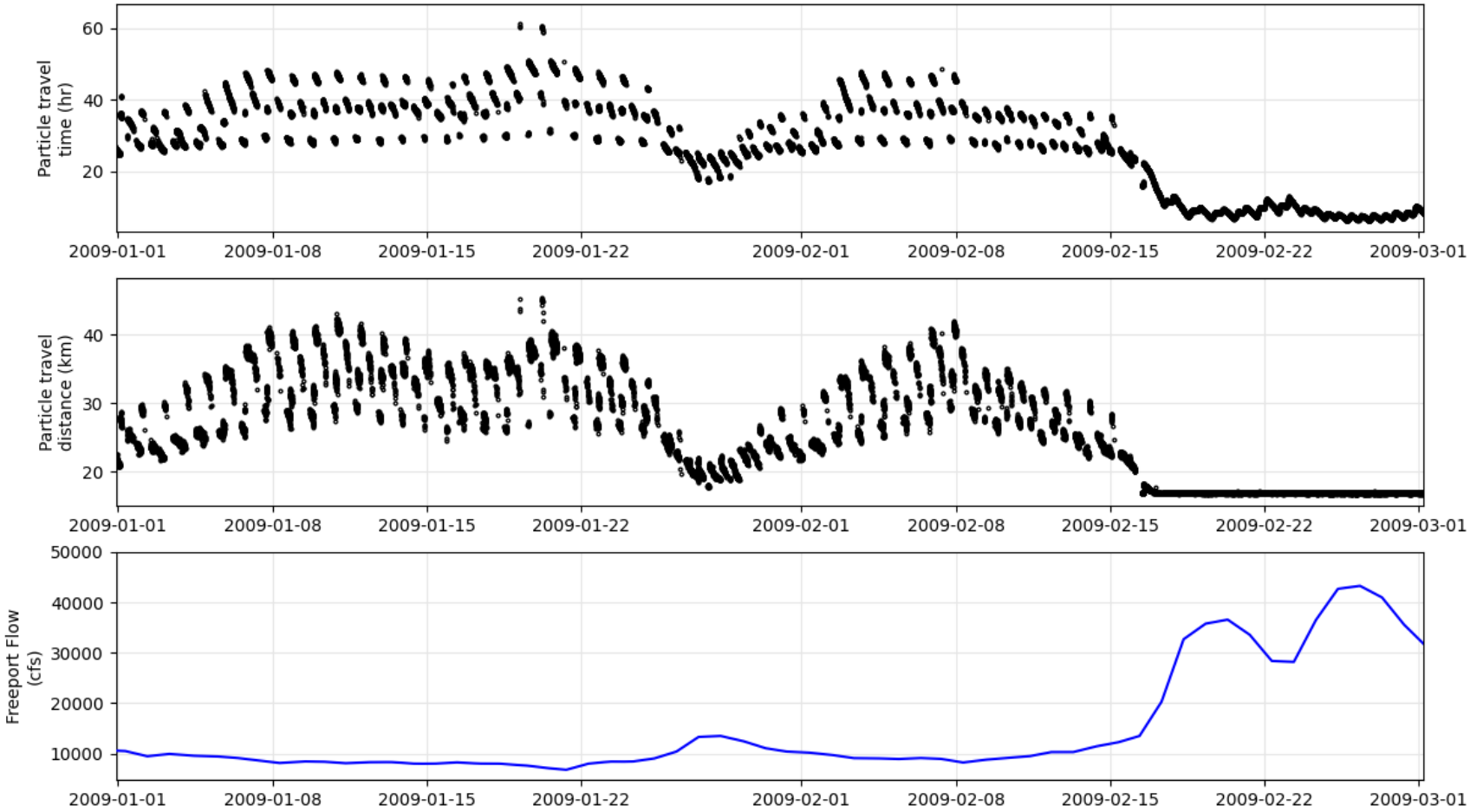

Figure 15 Same as Figure 14, but for the January–February 2009 time period.

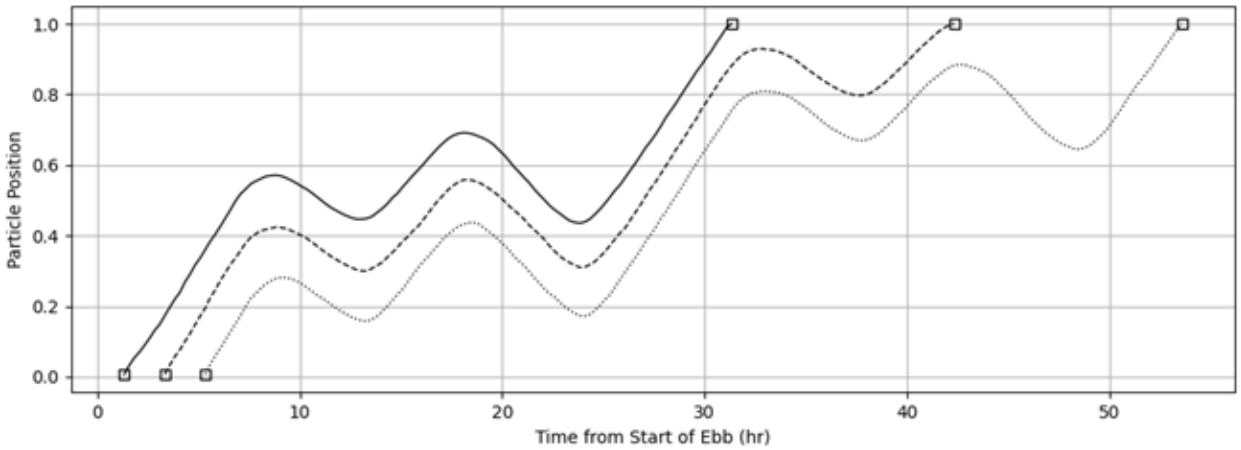

Figure 16 Relative position of three particles entering Steamboat Slough near the beginning, middle, and end of ebb tide, during a spring tidal cycle. A particle position of 0 represents the upstream end of the reach and 1 represents the downstream end.

Figure 14 and Figure 15 show particle results from a historical simulation with unsteady flow and are useful in understanding the impact of net flow on particle metrics. Figure 17 shows the results from three months of a steady flow simulation, where Freeport flow was held constant at 10,000 cfs. The banding in this figure is again due to particles entering at the start, middle, and end of ebb tide. The bottom panel of Figure 17 shows a running root mean square (RMS) of the tidal velocity in the reach and is a proxy for tidal strength (and spring-neap variation). The dependence of travel distances on tidal strength is evident. During strong spring tides, higher tidal velocities move the particles back and forth greater distances. Conversely during strong neap tides, weaker tidal velocities cause shorter tidal oscillations and result in lower distances traveled. Although a spring-neap signal can be seen in the travel time metric time series as well, the net impact is less. Changes in the tidal excursion do not appear to impact the average time spent within the reach. Average particle travel times during spring tides differ from neap tide averages by only fractions of an hour, and are very small compared variations resulting from changes in net flow or entry time relative to the start of ebb.

For the purposes of creating covariate time series of travel time and distance traveled within each reach, an hourly median of all particles entering within a given hour was used. Figure 18 shows how the median values compare to the individual particle results on a daily time scale. The hourly time series is discontinuous because passive particles cannot enter a reach during flood tide. However, juvenile salmon do not always behave like passive particles and there are records of fish entering reaches on flood tides, especially the weaker flood tide from each tidal day. For that reason, the salmon survival model requires a continuous covariate time series; this was developed from the median timeseries (such as the one shown in Figure 18), by

linearly interpolating through flood tide gaps. Larger gaps occurring between water year simulations—no particles were simulated between June 1st and October 31st of each year—were filled using constant values. These constant values were derived by calculating the average travel time and distance traveled for all particles entering a given reach over all of the historical simulations.

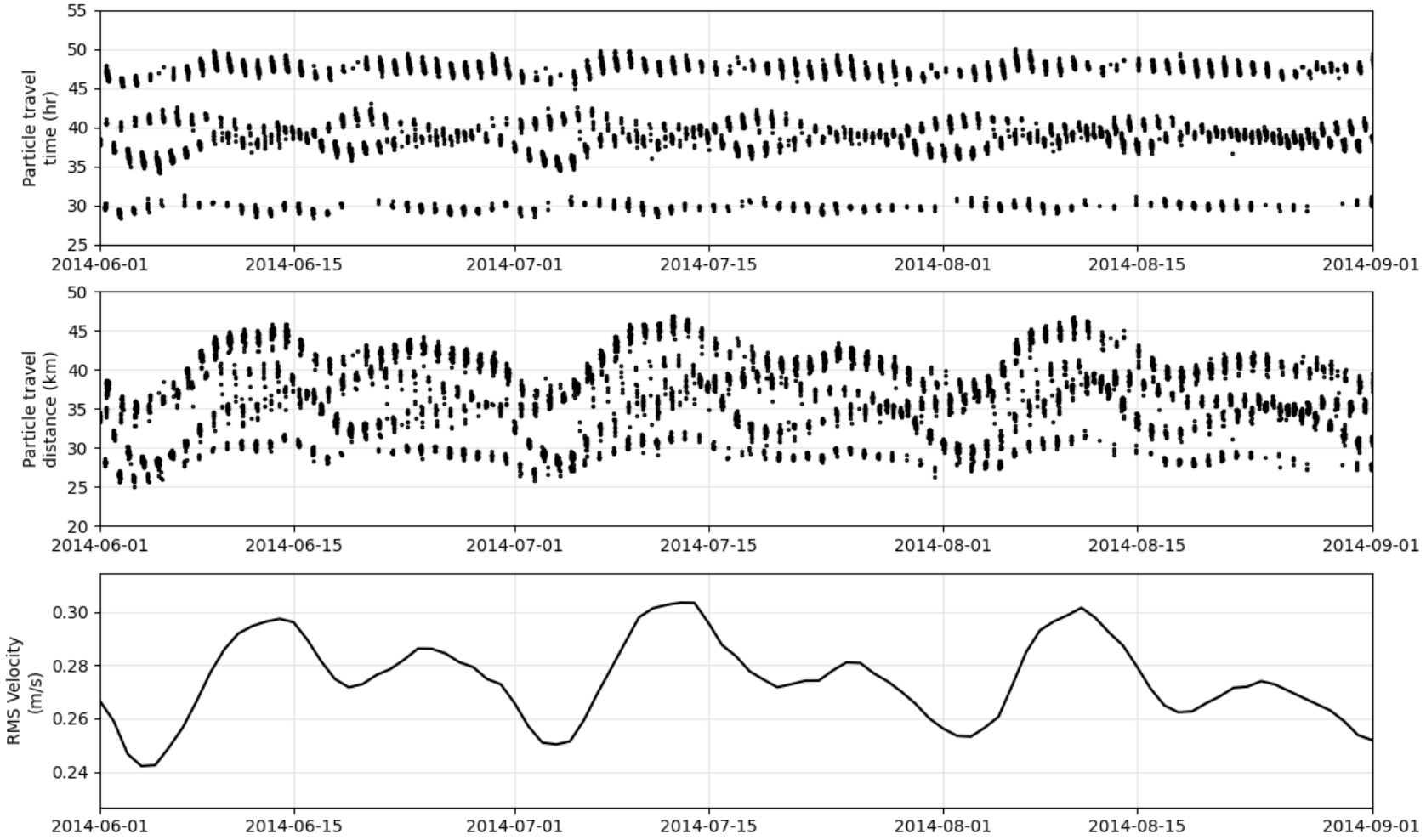

Figure 17 Particle travel time (top panel) and distance traveled (middle panel) in Steamboat Slough for a three-month period during a steady flow simulation. Sacramento River flow was held constant at 10,000 cfs and the DCC is open. Black circles represent results from individual particles and are plotted using the first time they pass the upstream station. Bottom panel shows root mean square velocity (a proxy for tidal strength) at the upstream end of Steamboat Slough.

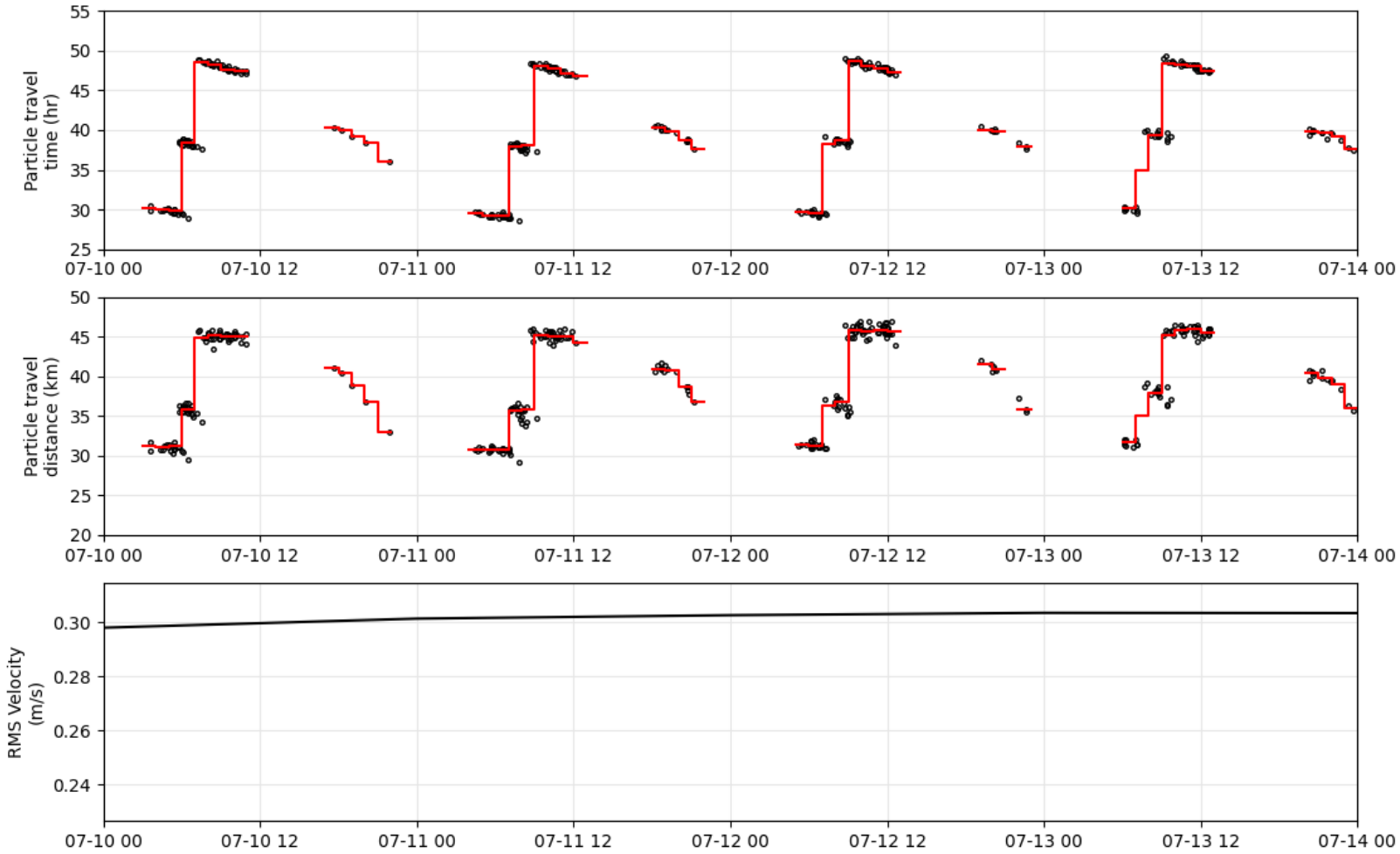

Figure 18 Same as Figure 17, but for a four-day time period. Red lines show the median values of all particles entering a reach within a given hour (e.g., 1:00–2:00).

Travel Time and Distance Traveled Covariate Timeseries for Survival Model

Timeseries of travel time and distance traveled were calculated for 18 reaches throughout the North Delta for input to the juvenile salmon survival model of USGS WFRC. Each reach is defined using bounding upstream and downstream stations and is denoted by a black arrow in the schematic shown in Figure 19. The locations of the stations (denoted with red text in Figure 19) are shown in Figure 6.

Figure 20 shows timeseries of the travel times and travel distances for eight of the reaches for the water year 2009 simulation. All reaches shown become unidirectional during the high flows of late February and early March. Reaches at the upstream end of the system (FPT-J1, J1-J2) have unidirectional flow for much of the simulation period, as does Georgiana Slough. During lower Freeport flows, entry time relative to the start of ebb causes large variations on a daily time scale. Two reaches—Sutter-Miner and the Mokelumne forks—show very large increases in travel time and distance traveled at low flows. This is due to the presence of blind sloughs intersecting these reaches and causing tidal trapping of particles. Elk Slough at the north end of the Sutter-Miner pathway is an example. Particles which get tidally dispersed up into Elk Slough are colored red in Figure 21; those that do not are colored black. Particles that enter Elk Slough may oscillate in the dead-end channel for several tidal cycles before exiting, greatly increasing their travel time and distance traveled in the reach. The lower panel in Figure 21 shows the proportion of particles traveling down the Sutter-Miner pathway that enter Elk Slough. It varies within 0% and 30% of the total particles. Figure 22 compares this proportion with Freeport flow and tidal strength. Particles are more likely to enter Elk Slough at low Freeport flows and during spring tide conditions.

A similar tidal trapping mechanism impacts particles traveling through the Delta Cross Channel (DCC) and south through the Mokelumne River forks. Particles may get tidally dispersed northward and caught in the dead-end channel of Snodgrass Slough. Particles that travel down the south fork of the Mokelumne also may get entrained into any of three terminal sloughs branching off to the east: Beaver Slough, Hog Slough, or Sycamore Slough. A final mechanism acting to increase travel times in this reach may occur when the DCC is closed. Closure substantially decreases net flows in the Mokelumne and leads to high travel times and distances for any particles that were in the reach when the gates were closed.

Pathways from Freeport to the junction of Sutter-Slough and Freeport to Steamboat Slough are not shown in Figure 20 because of their similarity to the Freeport-J1 path. The J1-Georgiana Slough and J1-DCC are not shown for similar reasons. The five reaches ending at Chipps Island are shown in a separate figure (Figure 23) because of the much longer travel times and distances traveled associated with these downstream, tidally dominated reaches. The Miner-

Chipps, Steamboat-Chipps, and Sacramento-Chipps pathways have similar properties. Particles take significantly longer to travel from the downstream ends of Georgiana Slough and the Mokelumne forks to Chipps Island. This is because they must exit the Delta by traveling through the more tidally dominated lower San Joaquin River. Net southward flows along the Old and Middle River corridor may advect particles south into the Central and South Delta, where they may stay for long periods of time. There, the combination of low net flows, entrapment zones such as Franks Tract and the interconnectedness of channels causes many of the particles exiting Georgiana and the Mokelumne to not reach Chipps Island within the time frame of the simulation. The percentage of passively transported particles exiting each of the five downstream reaches that are ultimately record at the Chipps Island station is given in Table 3 for each of the water year simulations. While approximately 80% of particles exiting Miner, Steamboat and the Sacramento River reach Chipps, an average of only 42% from Georgiana and 14% from the Mokelumne River do.

Table 3 Percent of simulated particles that traverse each reach and are detected at the Chipps Island monitoring station.

Water Year	Reach				
	Sutter-Miner Slough	Steamboat Slough	Lower Sacramento	Georgiana Slough	DCC-Mokelumne
2007	73.6	75.1	72.8	12.5	2.2
2008	73.0	76.5	76.4	31.5	13.0
2009	79.3	81.8	81.8	35.5	26.1
2010	84.1	86.7	87.1	52.5	15.8
2011	88.6	92.3	92.7	79.9	14.2
Average	79.7	82.5	82.2	42.4	14.3

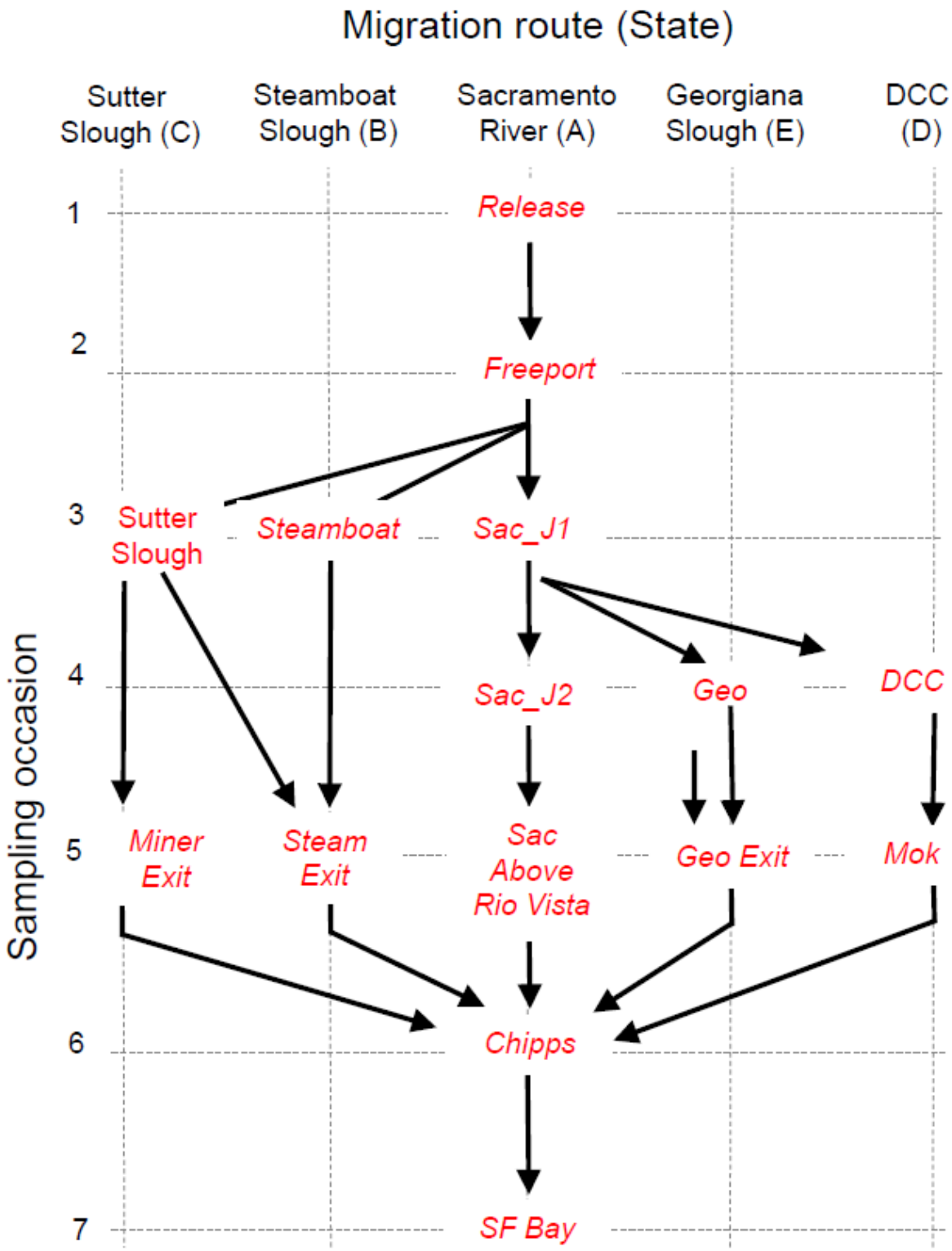

Figure 19 Spatial schematic for juvenile salmon survival model (figure from USGS WFRC). Sampling stations (e.g., Sac_J1) are shown in Figure 6. Black arrows represent reaches for which travel time and distance traveled covariate timeseries were calculated.

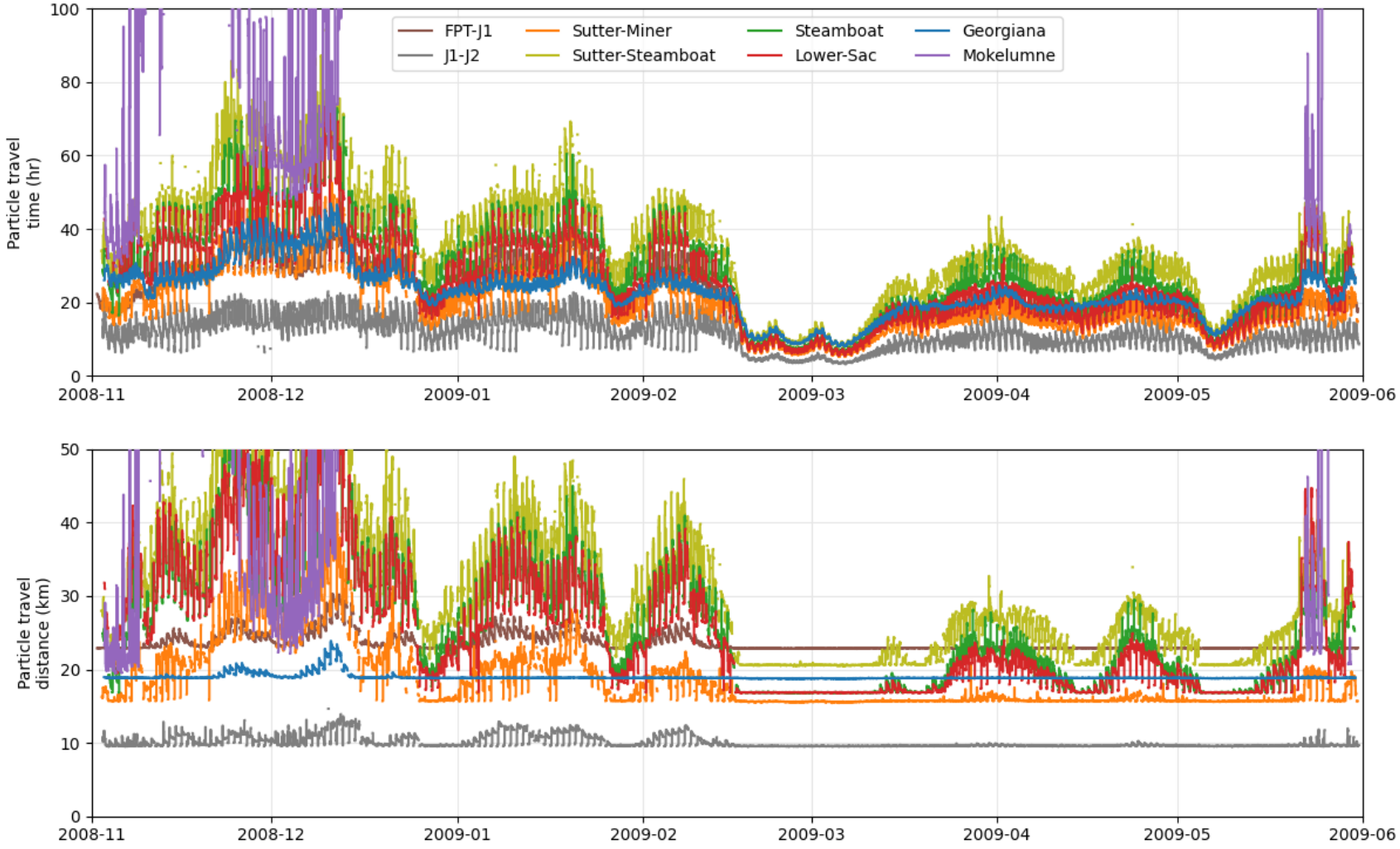

Figure 20 Timeseries of median hourly particle travel times (top panel) and distance traveled (bottom) for upstream North Delta reaches for the water year 2009 simulation.

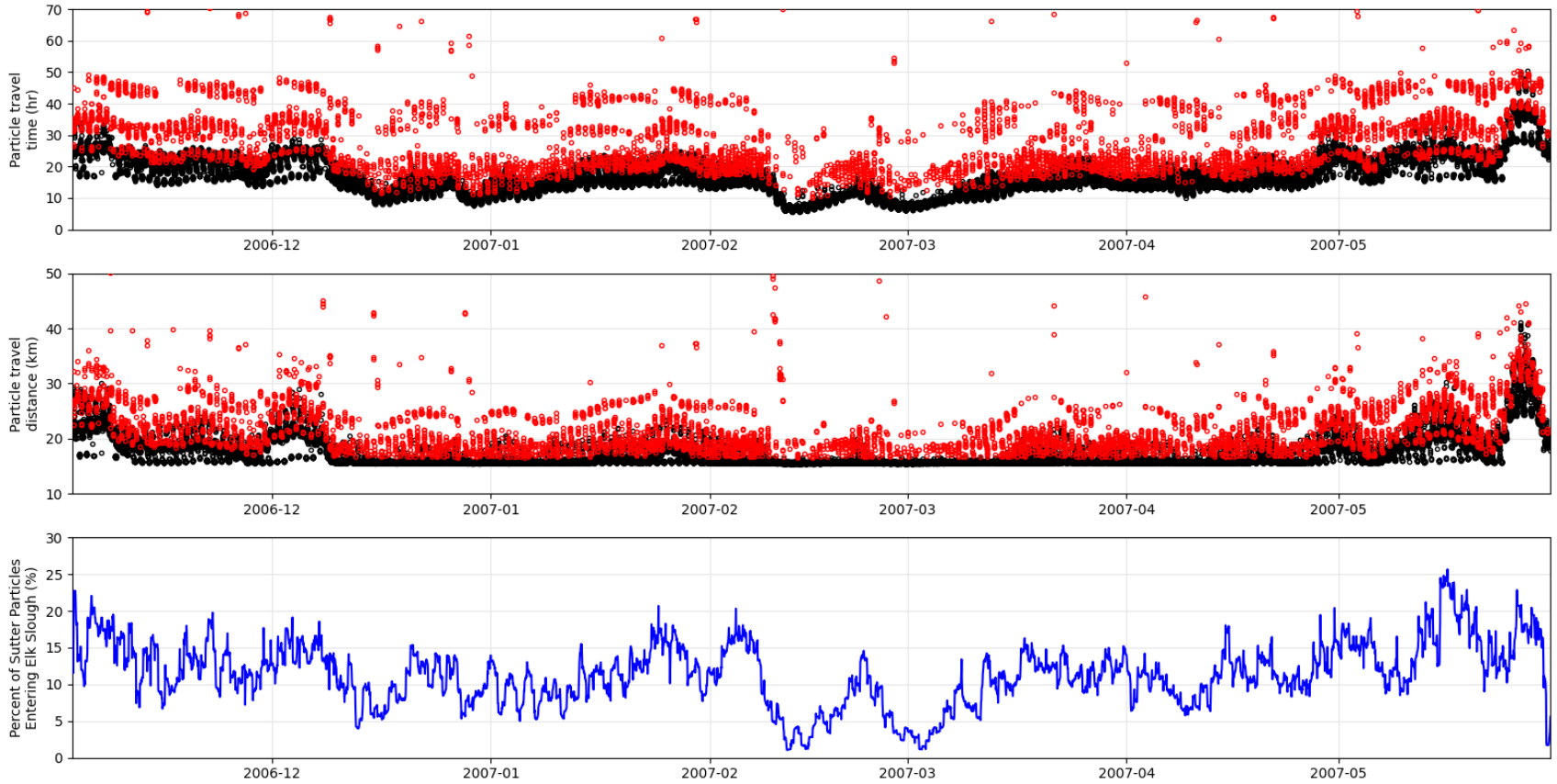

Figure 21 Particle metrics for water year 2007 in the Sutter Slough-Miner Slough reach. Particle travel time and distance traveled are given in the upper two panels. Black circles represent travel times and distances for particles that do not enter Elk Slough. Red circles represent particles that enter Elk Slough. Bottom panel shows percent of particles that enter Sutter Slough that also enter Elk Slough.

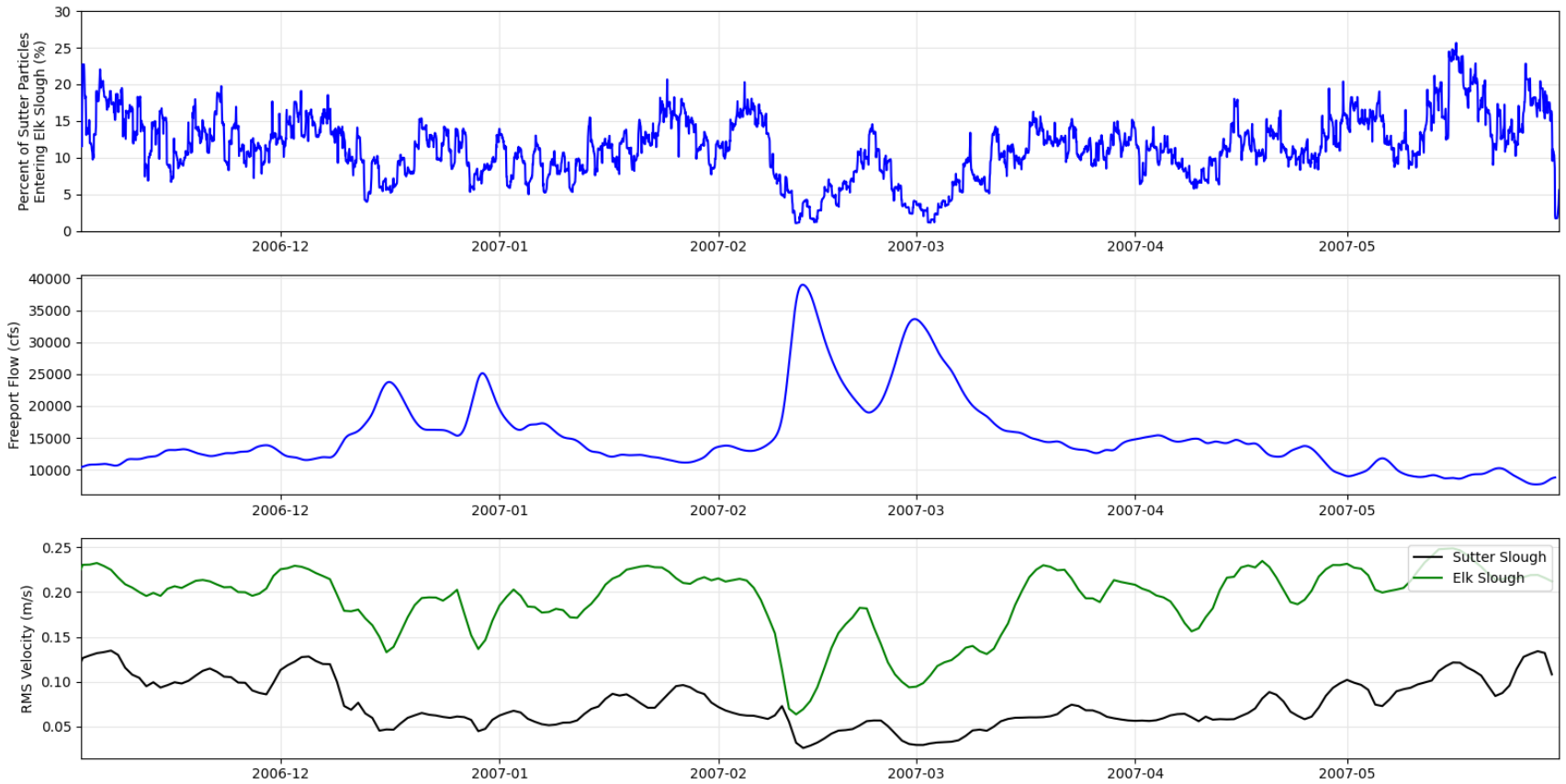

Figure 22 Correlation of percent of particles that enter Sutter Slough and also enter Elk Slough (top panel) with Sacramento River flow at Freeport (middle) and the root mean square of tidal velocity, a measure of tidal strength (bottom).

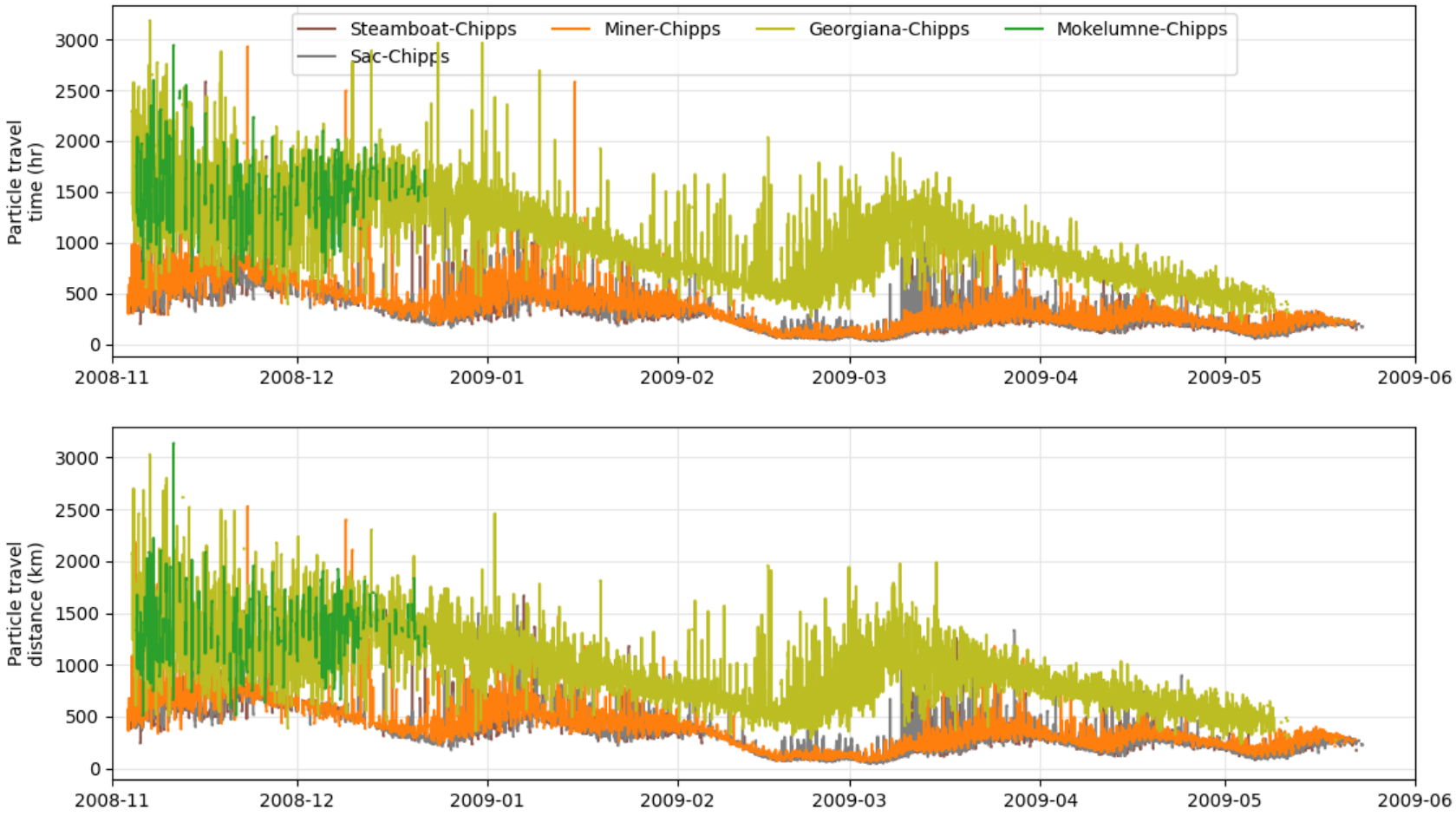

Figure 23 Timeseries of median hourly particle travel times (top panel) and distance traveled (bottom) for downstream North Delta reaches for the water year 2009 simulation.

Observed travel times for tagged juvenile salmon were available for several reaches and were provided by USGS WFRC. Result of the Bayesian survival model with and without the travel time and distance covariates are intended to ultimately determine the utility of these metrics in predicting salmon survival. Here, we qualitatively compare observed salmon travel times to modeled particle times in order to understand how representative particle results may be of fish behavior. Figure 24 shows fish travel times compared to particle tracking result for the Lower Sacramento River reach (between stations Sac_J2 and Sac Above Rio Vista) during the winter of 2009–2010. Patterns in this reach are typical of the other reaches and time periods. Fish results are clustered in time compared to the particle results because of discrete tagging and release events at the Sacramento River at I Street. The majority of the fish travel times lie on or just above the calculated particle values. Some fish, however, have very long travel times that are not well predicted by passive particle simulations. This results in a fish travel time distribution curve with a "long tail", which is commonly observed (USGS WFRC). Figure 26 and Figure 27 show the correlation between observed and calculated travel times, broken down by reach. Particle results generally underpredict tagged juvenile salmon travel times.

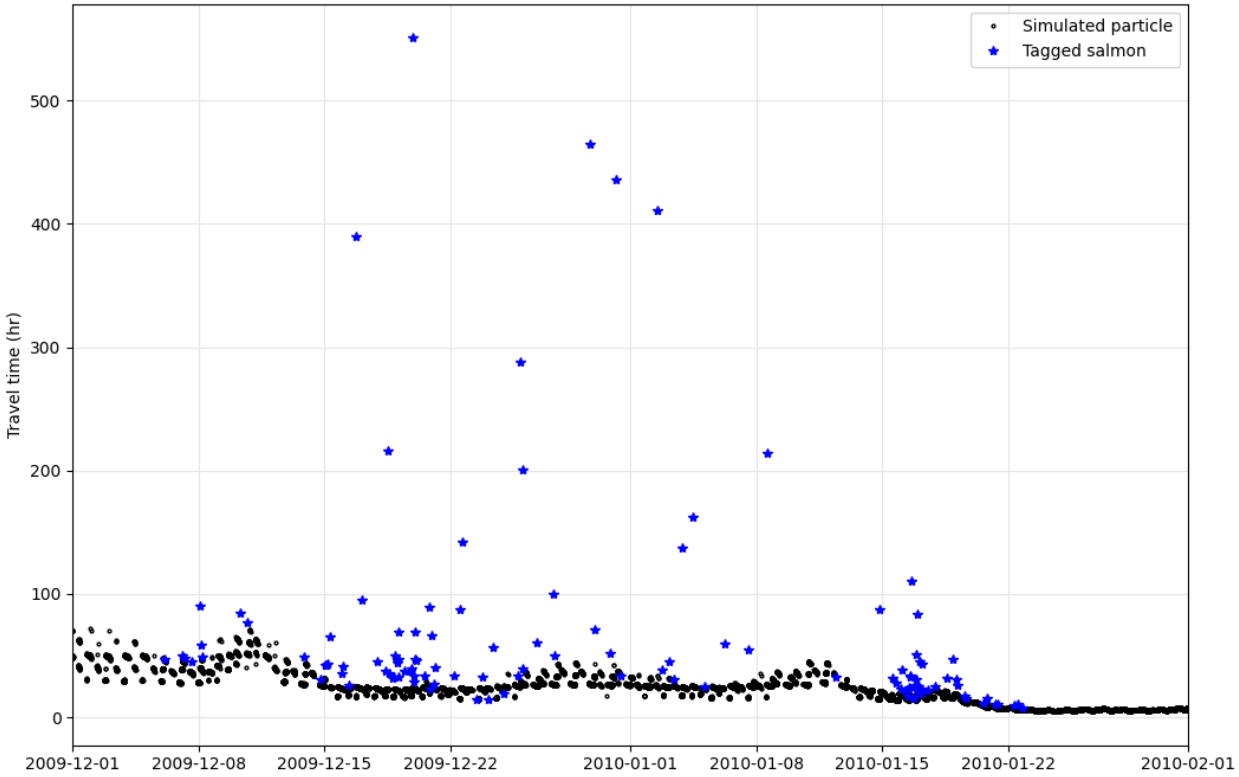

Figure 24 Simulated particle travel times and observed fish travel times for the Lower Sacramento reach for the winter of 2009–2010.

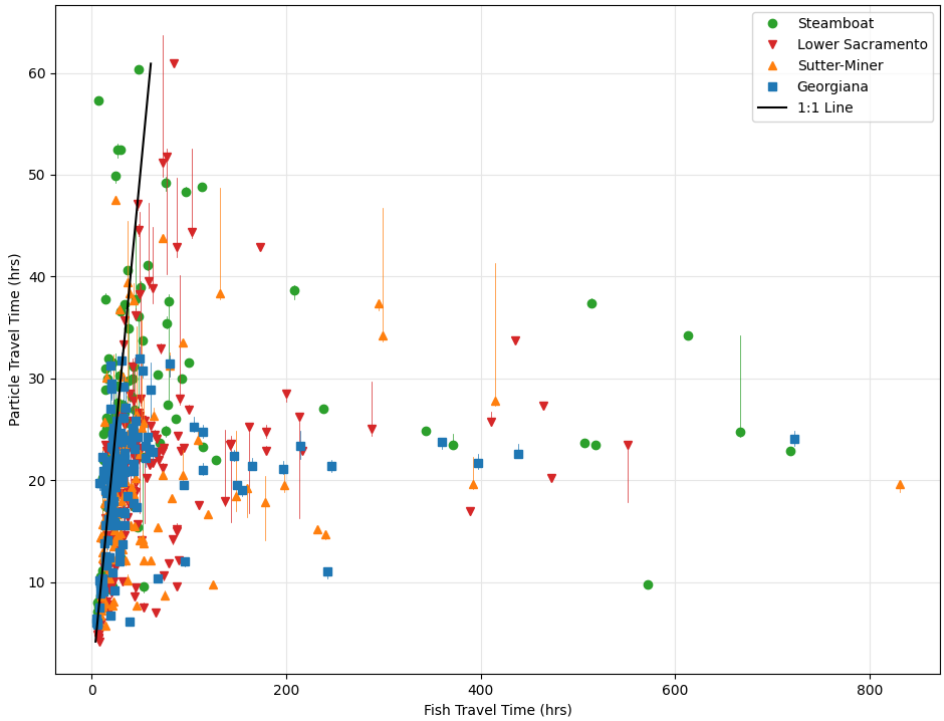

Figure 25 Correlation between simulated particle travel times and observed tagged juvenile salmon travel times, 2007-2011. Markers denote the median hourly particle travel time derived from the simulation. Vertical error bars show the range of travel times calculated for individual particles within that hour.

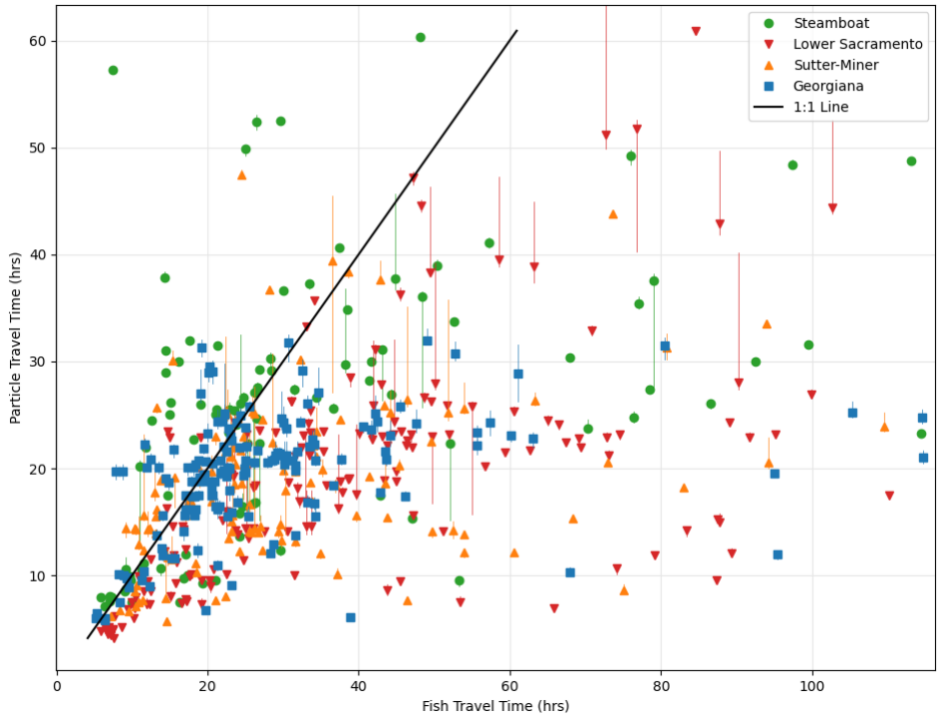

Figure 26 Same as Figure 25, but detail given for travel times less than 100 hours.

Sacramento River Flow and Cross-Channel Gate Operation Impacts on Travel Time and Distance

The Sacramento River steady flow runs were post-processed to determine average travel times and distance traveled as a function of Freeport flow and DCC operation (open/closed). Summary results are shown in Figure 27 and Figure 28. As flows increase, travel time decreases rapidly for all reaches up to about 12,000 cfs and then decreases more gradually with increasing flows after that. All reaches asymptote toward 10–15 hours travel time. The shape of the curve is similar to the function $y = \frac{1}{x}$. This functional relationship makes sense, because, on average, reach travel time = reach distance / average reach velocity.

Closing the DCC pushes most of the north Delta reaches toward being more riverine in character (with the exception of the Mokelumne River forks). At lower Sacramento flows (below about 10,000 cfs), gate closure causes Sutter and Steamboat Slough travel times to decease about 15%, Lower Sacramento times to decrease 25%, and Georgiana times to decrease 30%. The South Fork Mokelumne River reach includes a downstream section which connects to several dead-end sloughs and has a large tidal prism. This results in significantly higher travel times than other transitional reaches (Figure 27A).

Decreases in travel distances as a result of the DCC closure (Figure 28) are broadly similar (Sutter and Steamboat 20% lower, Lower Sacramento 30% lower, Georgiana Slough 15% lower). However, the travel distance metric reaches a floor at the total reach length when velocities are fully unidirectional. (The total reach length is remarkably uniform at about 20 km for all of the transitional reaches shown, Figure 28B.) Increases in Sacramento River flow beyond that unidirectional limit do not lead to decreases in total particle distance traveled.

A procedure was developed to assess the deviation in the average travel times and distances resulting from changes in spring-neap tidal conditions. (This procedure is explained in detail in one of the following sections.) This variation is shown in Figure 27 and Figure 28 as shading around the line for each reach. Spring-neap variations are larger for the distance traveled metric than the travel time metric (see Figure 17), but are still small compared to variations resulting from different Freeport flows. The tidal variations decrease at higher Freeport flows as the effects of the tides become dampened.

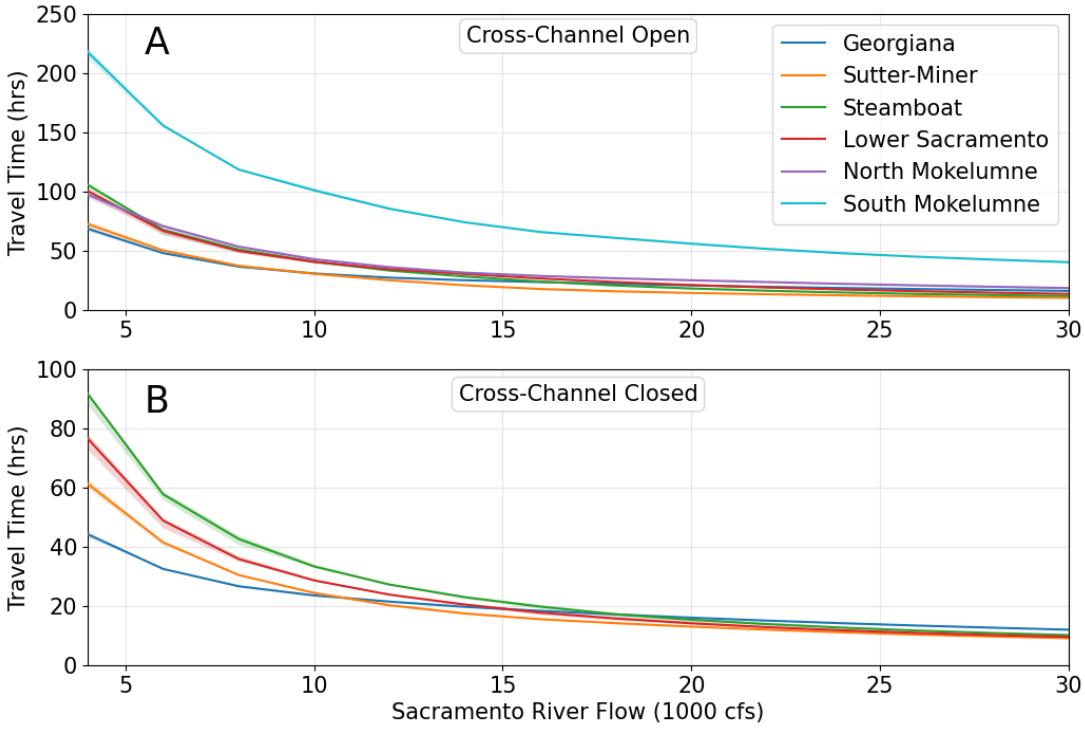

Figure 27 Particle travel time as a function of Freeport flow and Cross-Channel operation (A) open and (B) closed. Shaded regions show spring-neap variation.

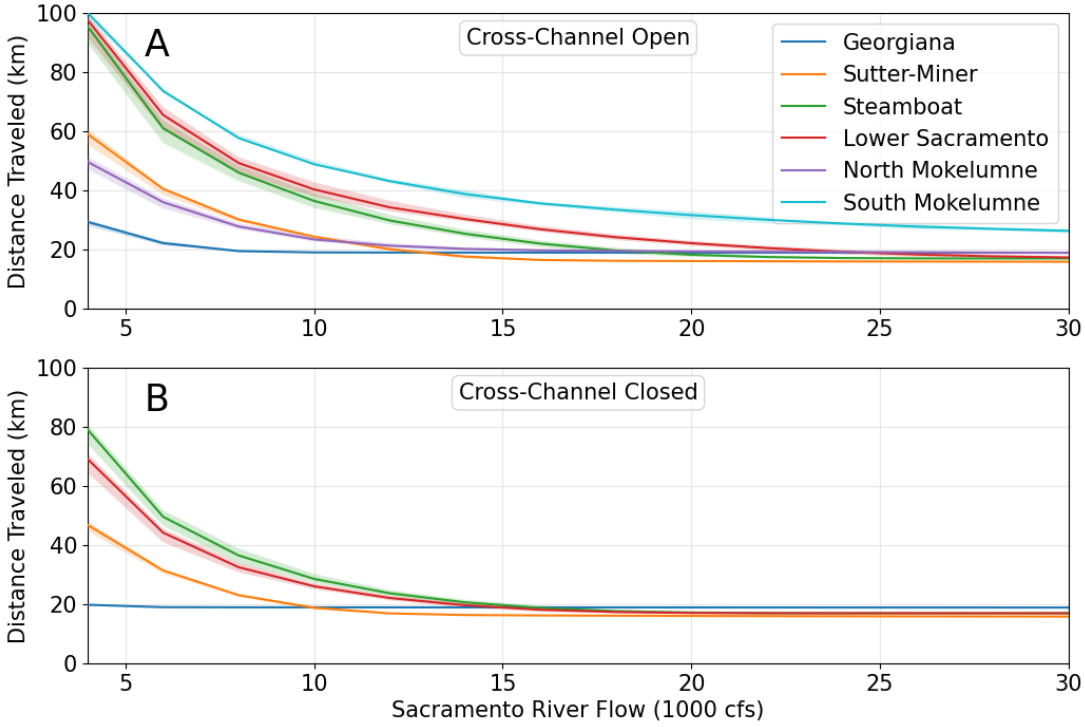

Figure 28 Particle distance traveled as a function of Freeport flow and Cross-Channel operation (A) open and (B) closed. Shaded regions show spring-neap variation.

Restoration and Operational Scenarios

Two large-scale tidal marsh restoration scenarios and one operational gate scenario were performed to assess the impacts of management actions on the particle travel time and distance traveled metrics. The first restoration scenario involved opening a large area in Suisun Marsh (Grizzly Island) to tidal action from breaches to Grizzly and Honker Bays (see Figure 12). By increasing shallow flooded area in the western estuary, it was believed that tides would be dampened through the Delta, decreasing tidal excursions and travel distances. The second large-scale marsh restoration scenario was chosen based on the result of modeling scenarios performed by RMA (2020). Simulations in this report showed that broad decreases in tidal excursion throughout the North Delta could be achieved by a combination of restorations in the Cache Slough Complex and the East Delta (Figure 29). Critically, this scenario did not change net flows through the DCC. Changes in flow through the Cross Channel can have large impacts on salinity intrusion and municipal and agricultural water supply systems, and should be avoided. Because of the effort involved in simulating hydrodynamics and particle tracking with substantially different computational grids, results were only evaluated for three steady flow runs (10,000; 16,000; and 24,000 cfs) with the DCC open.

Changes in the average particle travel times and distances relative to the base (no restoration) results are presented in Table 4 and Table 5. The Suisun Marsh restoration showed only small impacts on the metrics. Particle travel times and distances generally decreased between 0 and 2% in the 10,000 cfs Freeport flow simulation and were even less effective at higher flows. The Cache and East Delta restoration scenario, however, showed significant changes from the base results. Travel distances decreased for all reaches for all Freeport flows, consistent with the changes in tidal excursion from previous modeling results (Figure 29, left). Average travel times were not expected to decrease with decreases in tidal excursion (see Figure 17). Instead, the changes reflected differences in net flows in the system (Figure 29, right). Restoration changed flow splits in the North Delta, leading to more flow and higher net velocities down the Sutter-Miner pathway and the Mokelumne River forks. This additional flow decreased travel times on these reaches significantly (by 5–15%), but occurred at the expense of decreased flow and increased travel times in other North Delta reaches (Steamboat Slough, the Lower Sacramento River, and Georgiana Slough).

The operational scenario with the added (and closed) gate at the head of Georgian Slough primarily acted to alter net flows in the North Delta, decreasing travel times and distances (Figure 30). The average decreases are shown across a range of Freeport flows for four major transitional reaches resulting from closure of the DCC gates and additional closure of the Georgiana gate. At lower (10,000 cfs and below) flows, average travel times and distances decreased 50% in the Lower Sacramento reach compared to 30% with just the DCC closed.

Times and distances in Steamboat Slough decreased 40% compared to 20% with just the DCC closed, and Sutter-Miner decreased 35% compared to 20% with just the DCC closed.

Table 4 Percent change in average particle travel time and distance relative to the base (no restoration) for the Grizzly Island restoration alternative.

Reach	Sacramento River Flow					
	10,000		16,000		24,000	
	Travel Time Change (%)	Distance Change (%)	Travel Time Change (%)	Distance Change (%)	Travel Time Change (%)	Distance Change (%)
Sutter-Miner	0.1	-1.4	0.4	-0.2	0.7	0.1
Steamboat	-0.4	-2.2	-0.7	-2.2	-0.4	-0.3
Georgiana	0.5	0.0	0.8	0.0	0.6	0.0
Lower Sac	-0.2	-1.8	0.0	-1.7	-0.6	-1.5
N Mokelumne	-1.0	-0.8	0.7	-0.1	1.1	0.3
S Mokelumne	-1.7	-1.3	1.2	-0.1	1.7	0.3

Table 5 Percent change in average particle travel time and distance relative to the base (no restoration) for the Cache Slough + East Delta restoration alternative.

Reach	Sacramento River Flow					
	10,000		16,000		24,000	
	Travel Time Change (%)	Distance Change (%)	Travel Time Change (%)	Distance Change (%)	Travel Time Change (%)	Distance Change (%)
Sutter-Miner	-10.5	-24.0	-4.7	-1.6	-0.1	-0.1
Steamboat	7.4	-3.2	0.0	-7.4	-0.3	-0.7
Georgiana	5.2	-0.2	3.3	0.0	2.5	0.0
Lower Sac	9.4	-0.5	3.6	-5.6	-0.8	-5.1
N Mokelumne	-5.6	-12.5	-0.1	-2.4	0.2	-1.2
S Mokelumne	-15.0	-29.3	-7.2	-20.0	-3.9	-14.0

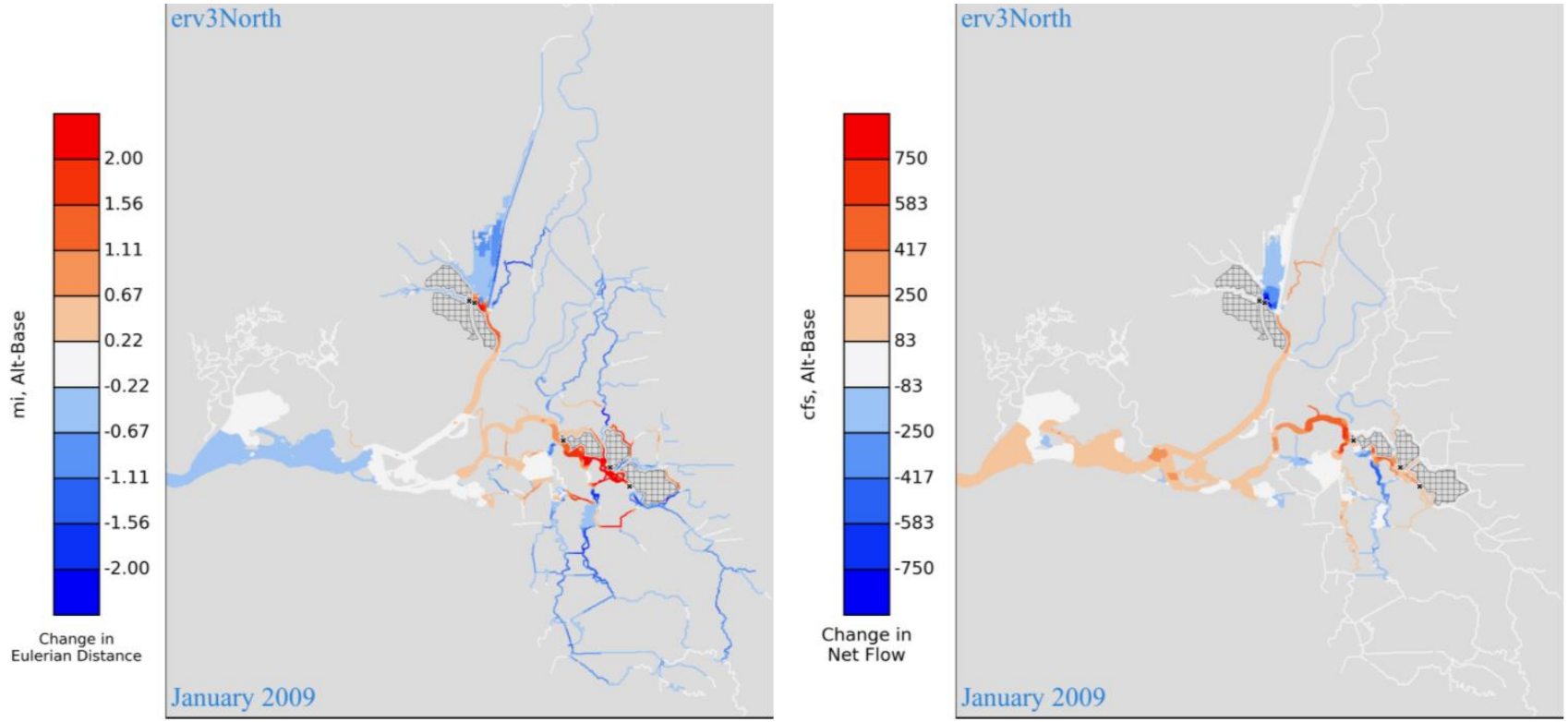

Figure 29 Heatmap plots highlighting changes in tidal excursion (left plot) and net flow (right) for a combination of restorations in the Cache Slough Complex and the East Delta relative to a base (no restoration) simulation for a January 2009 historical period. Simulations and analyses were performed by RMA (2020) and were used to guide selection of a restoration alternative for this project.

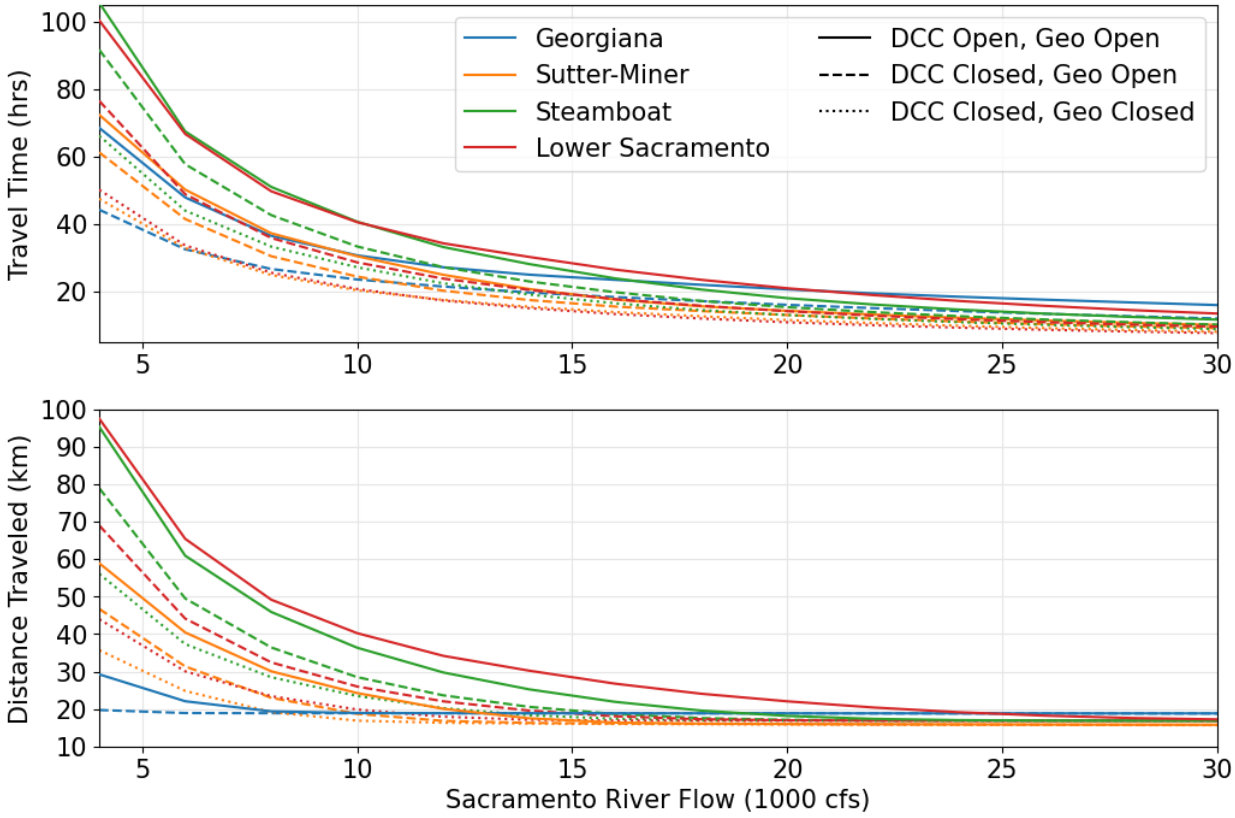

Figure 30 Particle travel times (top panel) and distance traveled (bottom) as a function of Freeport flow, Cross-Channel operation, and the closure of a gate at the head of Georgiana Slough.

Hydrodynamic Character of the North Delta

In collaboration with USGS CA WSC, a set of hydrodynamic metrics was developed to describe conditions in the North Delta and how they respond to changes in net flow and tidal strength. The primary metric used is the ratio of the tidal to net current, and is denoted $u'/\langle u \rangle$. Its derivation is shown in Figure 31, which is described in detail here. The bottom panel shows a timeseries of cross-sectionally averaged channel velocity, u, measured on the Sacramento River above Walnut Grove. This velocity is first decomposed into net and tidal components by applying a tidal filter (e.g., the Godin filter). The net current timeseries is shown in the second panel from the top. The tidal current timeseries is shown in the third panel from the top. The outer envelope of the flood tide time series is then calculated (the bottom red line in the third panel from the bottom). This represents the maximum flood tide velocity during each tidal day. The ratio of this time series to the net velocity time series is the $u'/\langle u \rangle$ metric and is shown in the top panel.

The utility of this metric is its ability to quickly differentiate between tidally dominant, reversing current environments and riverine-like, unidirectional environments. When the metric is greater than one, tidal velocities outweigh net velocities, and water in a channel reverses direction on flood tides. This allows non- and poor-swimming organisms that have the ability to ride tidal currents the chance to migrate upstream. When $u'/\langle u \rangle$ is less than one, net flows dominate and velocities in the channel are unidirectional. While velocities slow on flood tides, they never reverse direction, and non-swimming organisms are not able to travel upstream.

The effect of spring-neap variations can be seen in the tidal velocities (Figure 31, third panel from the top). To assess these variations, a spring-neap filter is applied to the maximum flood tide velocity (resulting in the cyan line) and the residual (denoted in light green) used to calculate spring-neap fluctuations in $u'/\langle u \rangle$.

Heatmaps were developed to examine spatial variations in the $u'/\langle u \rangle$ metric over the North Delta. An example of two such heatmaps is shown in Figure 32: one for a constant Freeport flow of 12,000 cfs with the DCC open, and another for 16,000 cfs with the DCC closed. At 12,000 cfs, the Sacramento River is unidirectional down to the DCC junction and Georgiana Slough and the North Fork Mokelumne are unidirectional; the rest of the North Delta is tidal. At 16,000 cfs, Sutter and Miner Sloughs have transitioned to unidirectional, as has part of Steamboat Slough and the Sacramento River between Walnut Grove and Isleton. Closing the DCC causes the Mokelumne system to become highly tidal.

The results of the two extremes of the constant flow simulations are shown in Figure 33. At a Sacramento River flow of 4,000 cfs, the entire system is tidal to north of Freeport. At 70,000 cfs, flows are unidirectional on the Sacramento and tributaries downstream until the confluence with Cache Slough is reached. Even at these extreme Sacramento River flows, this area remains tidal. Similarly, Elk Slough, the San Joaquin River, and parts of the lower south fork of the Mokelumne River remain tidal because of large tidal prism and/or little net flows.

Many transitional reaches transform from fully tidal to fully unidirectional over a relatively narrow range of flows. Because of the oscillating strength of the tides with spring-neap cycling, this can cause the entirety of the channel to transition between unidirectional and tidal on a spring versus neap tide, with no changes in net flow. An example is shown for the Sutter-Miner pathway in Figure 34, where the reach transitions from fully tidal during spring tides to fully unidirectional during neap tides.

A summary plot of these transitions is given in Figure 35. The transition between unidirectional and bidirectional flow (the *reversing current limit*) is given as a relative distance along each reach. At very low Freeport flows with the DCC open, all reaches are fully tidal and the reversing current limit is located at the downstream end (relative location = 0). As Freeport flows

increase, the reversing current limit moves upstream and the reach transitions to be more riverine. At high Freeport flows, the reversing current limit is located at the upstream end of the reach (relative location = 1) and the reach is fully unidirectional.

Figure 35 shows at what Freeport flows each reach transitions from riverine to tidal environments. The Georgiana reach transition occurs over a narrow range of very low Freeport flows. Sutter-Miner, the North Fork Mokelumne, and Steamboat Slough transition at higher Freeport flows and over a wider range of flows. Because of highly tidal southern end, the South Fork Mokelumne becomes fully unidirectional only at the highest simulated Freeport flows with the DCC open, a situation that would be unlikely to occur in reality.

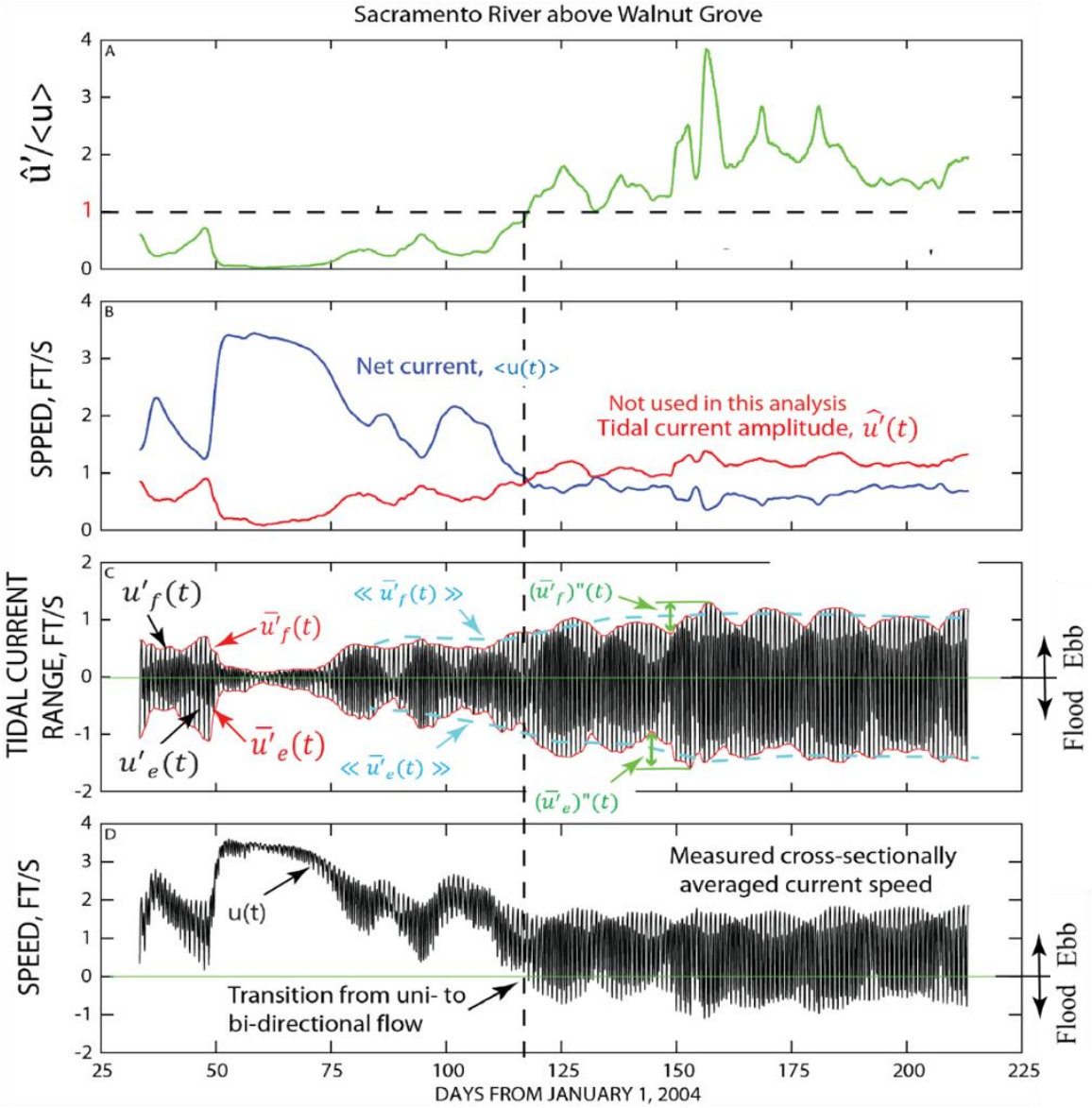

Figure 31 Derivation of the tidal to net current ratio metric and associated spring-neap variability. See text for details. Figure from USGS CA WSC with modifications.

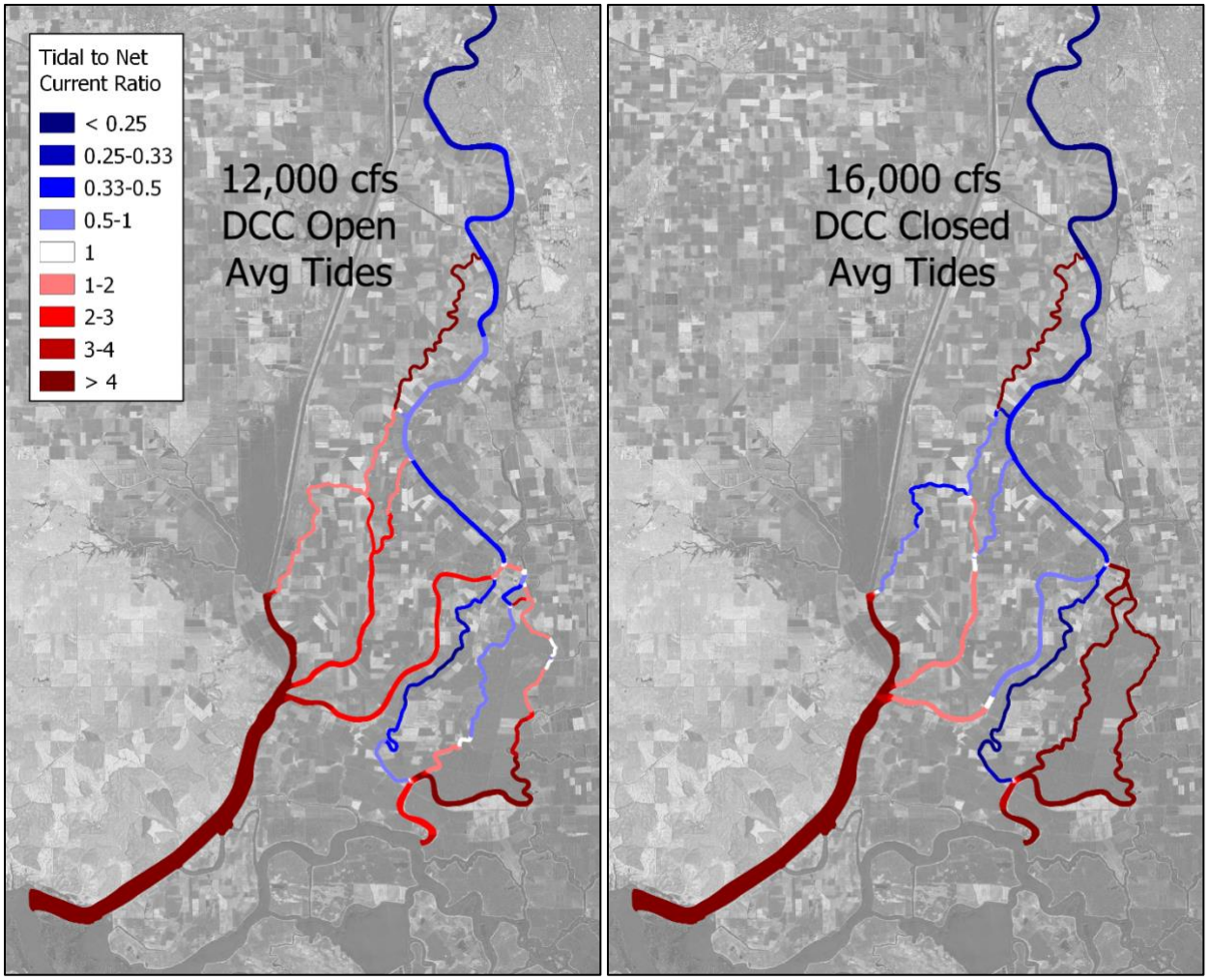

Figure 32 Tidal to net current ratio (u' / <u>) for (left) a Freeport flow of 12,000 cfs with the Cross-Channel open, and (right) a Freeport flow of 16,000 cfs with the Cross-Channel closed. Blue contours indicate a more riverine environment and red contours indicate a more tidal environment.

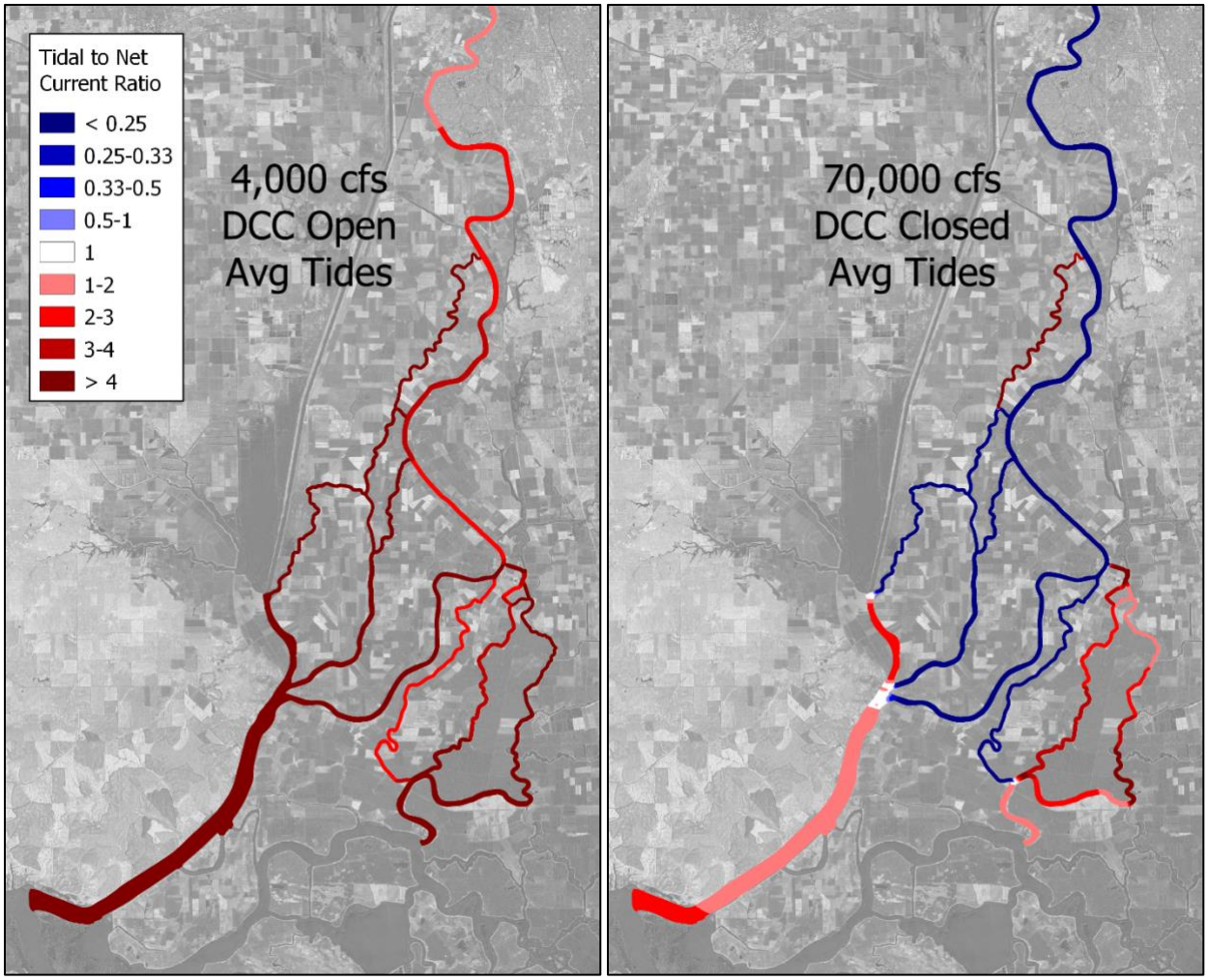

Figure 33 Tidal to net current ratio (u' / <u>) for (left) a Freeport flow of 4,000 cfs with the Cross-Channel open, and (right) a Freeport flow of 70,000 cfs with the Cross-Channel closed.

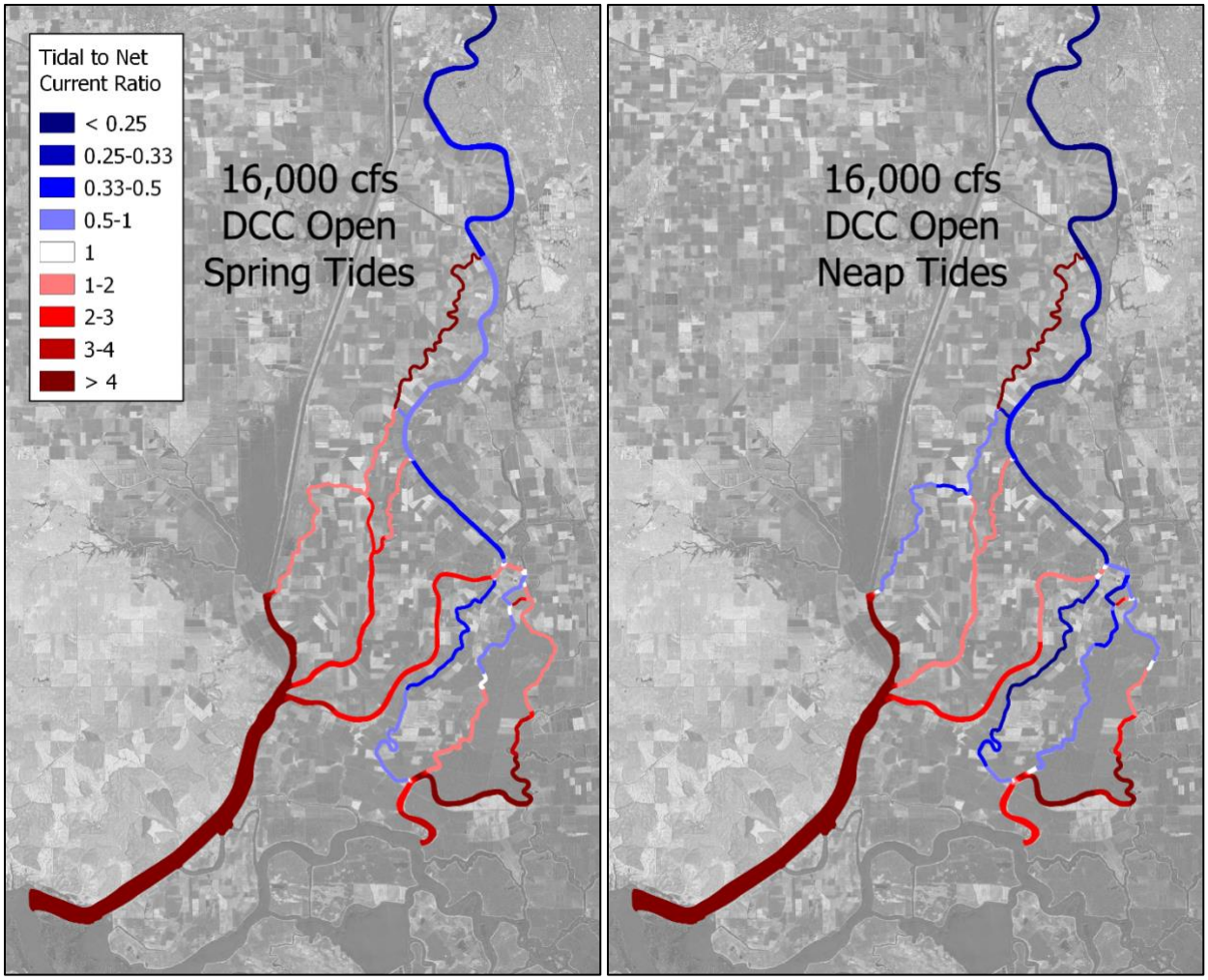

Figure 34 Tidal to net current ratio (u' / <u>) for (left) a Freeport flow of 16,000 cfs with the Cross-Channel open and spring tide conditions, and (right) the same but under neap tide conditions.

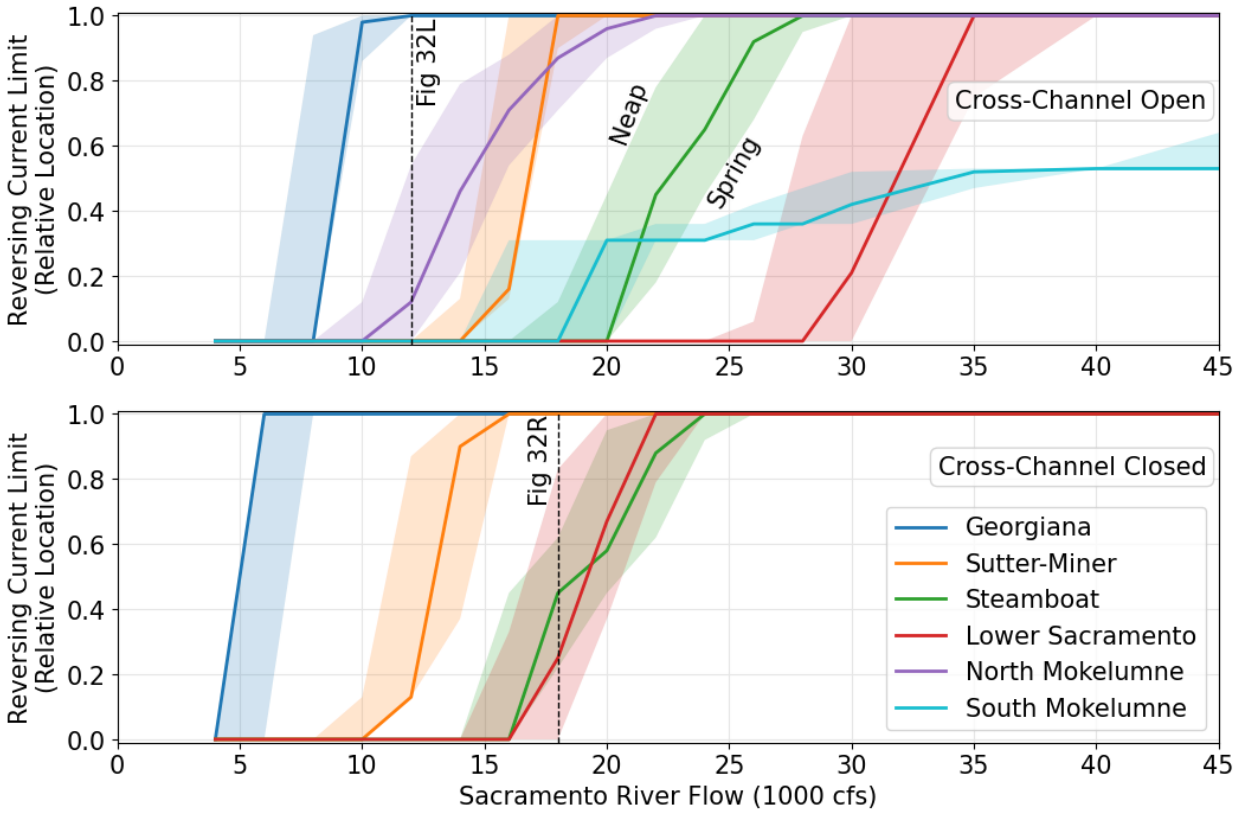

Figure 35 Location of reversing current limit (u'/<u>=1) for North Delta reaches as a function of Freeport flow and Cross-Channel operation (top) open and (bottom) closed. A value of 0 denotes the upstream end of the reach and 1 denotes the downstream end. Shaded areas show spring-neap variation in the position. Vertical dashed lines correspond to the heatmaps shown in Figure 32.

Entrainment Ratios at Junctions in the North Delta

A final analysis was performed in collaboration with the USGS CA WSC to examine the ratio of Sacramento River water entrained at each of the North Delta junctions (Sutter, Steamboat, the DCC, and Georgiana Slough) and how they are affected by net flows and local tidal hydrodynamics. To accomplish this, modeled flows were extracted at locations just upstream and downstream of each junction and the ratio of flow in the tributary to upstream flow was calculated to obtain an entrainment ratio.

Entrainment ratios were first calculated using tidally-averaged flow time series, and these are shown in Figure 36. This plot shows the proportion of water volume coming from the upper Sacramento that travels down each tributary. If juvenile salmon are uniformly distributed in the water column, this plot also represents the proportion of fish which take each path through the North Delta. When the DCC is open, there are only small changes in the flow splits with changes in Freeport flow. When the DCC is closed, however, there is more variation. As Freeport flows

increase, proportionally more water travels down Sutter and Steamboat Sloughs (a combined increase of about 10% of Sacramento flows). Significantly less water travels through Georgiana Slough, with approximately 35% of the Freeport flow being entrained at 4,000 cfs but only 17% at 45,000 cfs.

Outmigrating juvenile salmon are not typically uniformly distributed with the flow. Although their maximum swimming speeds are low compared to tidal velocities, they may explore and redistribute themselves across a channel during slack water. Bends in channels and surface seeking behavior may act to concentrate them on one side of the channel. Another method of calculating the average entrainment through each junction is to calculate the entrainment ratio at 15-minute intervals using tidal velocities and then take the long-term average of that time series. For these entrainment ratios to apply to outmigrating juvenile salmon, it must be assumed that fish arrive at a junction at a constant rate in time, and that they are evenly distributed across the channel when they do so.

Discharge ratios calculated in this manner are shown in Figure 37. At high Freeport flows, the effects of tidal hydrodynamics at the junctions are dampened and the ratios converge to those calculated in Figure 36. At lower flows, there are differences. When the DCC gates are closed, there is a maximum in the Georgiana Slough entrainment ratios around 10,000 cfs. At that flow, the reversing current limit on the Sacramento is located close to the DCC junction. On ebb tides, approximately 15% of the flow goes down Georgiana Slough. But on many flood tides, water enters Georgiana from both the upstream and downstream sides of the Sacramento, leading to entrainment ratios at or near 1.0. A schematic of these flow patterns is illustrated in Figure 38. This junction is particularly important to juvenile salmon survival because of the low probably of fish entering Georgina Slough that are also detected at the Chipps Island station (Perry et al. 2018b; this report Table 3). Other North Delta junctions display similar tidal dynamics as shown in Figure 38, but these occur at different Freeport flows and have slightly different tidal reversal timings.

Actual fish behavior occurring at junctions is complicated and the subject of ongoing research (Romine et al. 2021). Neither the assumption made to calculate the entrainment ratios shown in Figure 36 nor those shown in Figure 37 is completely correct.

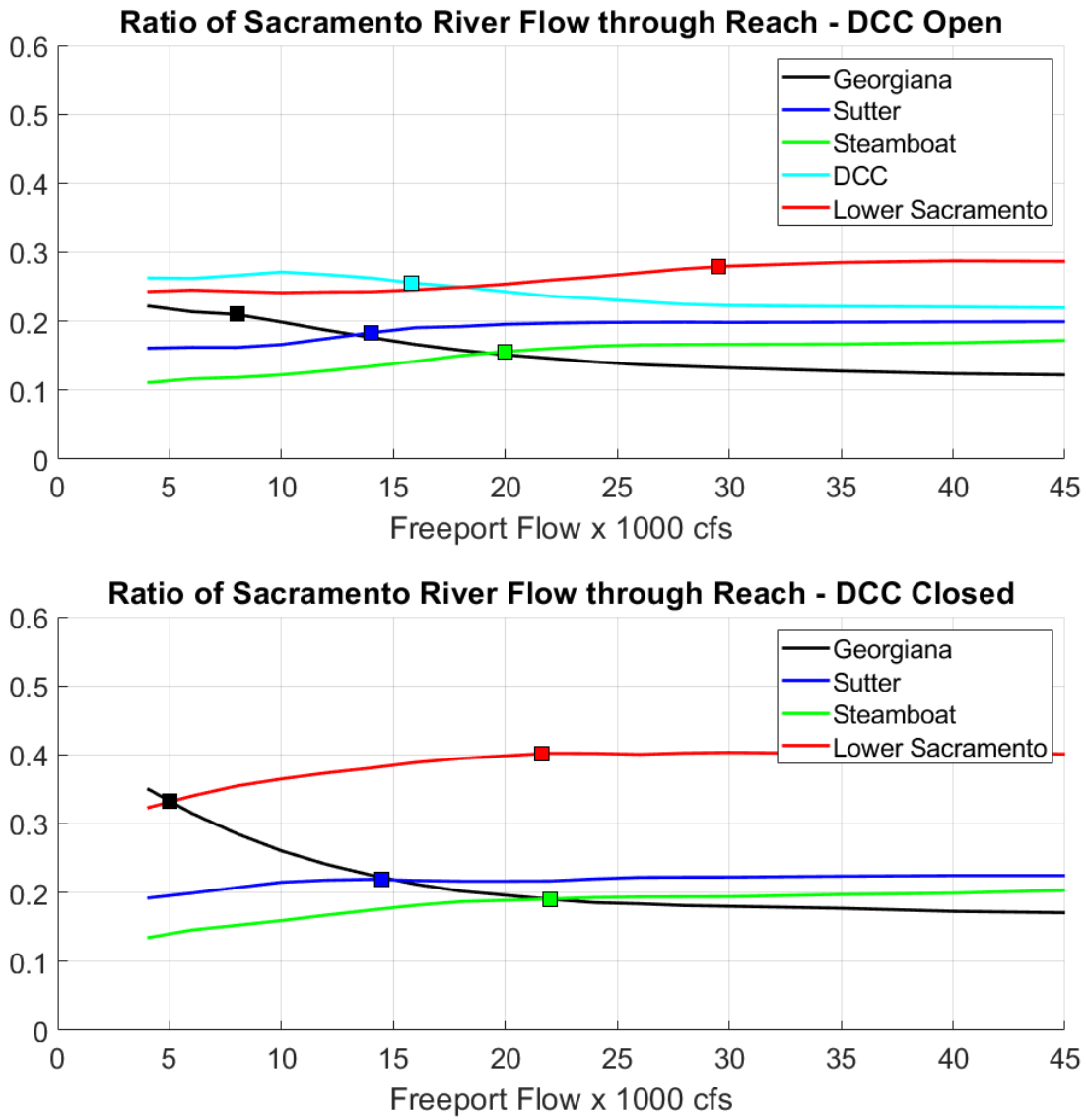

Figure 36 Entrainment ratios at north Delta junctions, calculated using tidally averaged flows. Squares show the flows at which the upstream end of the tributary transitions between unidirectional and bidirectional flow. Figure from USGS CA WSC.

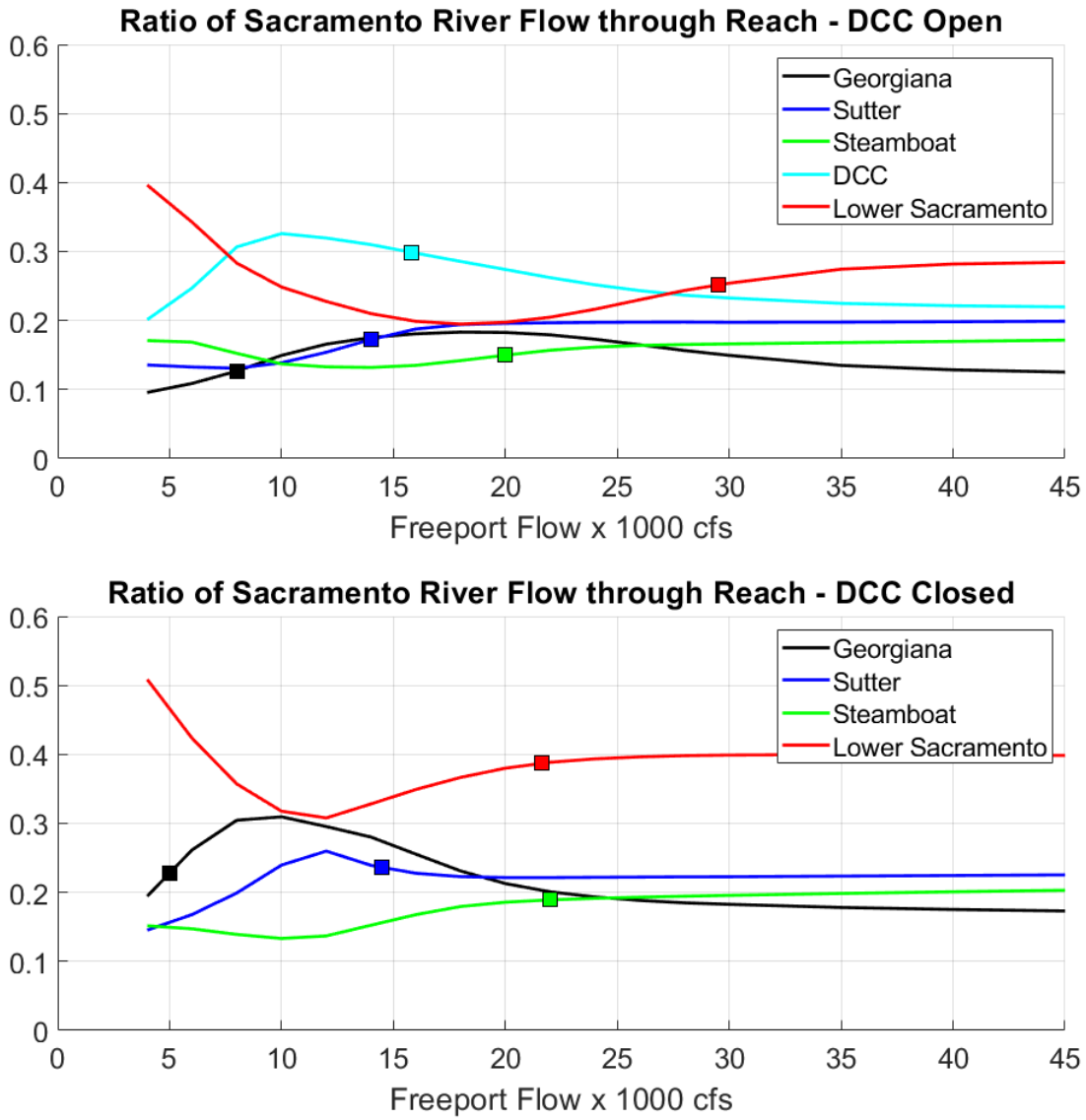

Figure 37 Entrainment ratios at north Delta junctions, calculated using tidal flows and then tidally averaging the ratio time series. Squares show the flows at which the upstream end of the tributary transitions between unidirectional and bidirectional flow. Figure from USGS CA WSC.

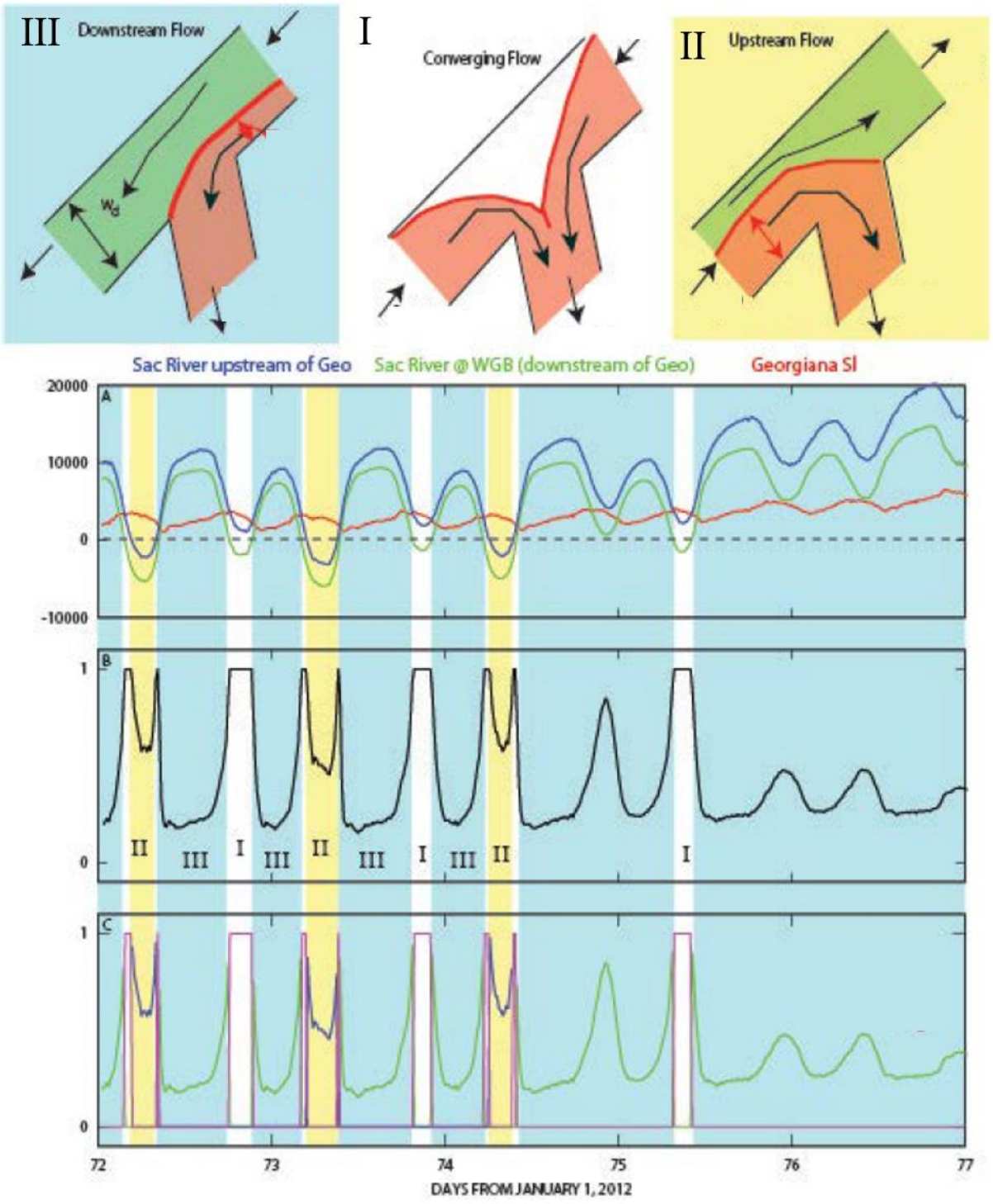

Figure 38 Illustration of generalized tidal flow dynamics (top figures), velocity time series (top panel) and entrainment ratios (bottom two panels) at the junction of Georgiana Slough and the Sacramento River. Converging and upstream (flood tide) flow at the junction leads to higher entrainment ratios than downstream (ebb tide) flows. Figure from USGS (2015).

Summary and Conclusions

A set of 2D hydrodynamic model simulations were performed in order to examine the experience of passive material transported through the North Delta from a Lagrangian point of view. The North Delta was broken up into a series of reaches (or pathways), and particle tracking model results were processed to calculate the time spent and distance traveled within each reach and relate it to net flow and tidal conditions (spring-neap phase).

Time and distance metrics were calculated for historical simulations and input into a Bayesian juvenile salmon survival model to test the hypothesis that reach-specific survival is dependent on time spent and/or distance traveled within that reach. Salmon survival was previously found to be dependent on the magnitude of Sacramento River flow at Freeport (Freeport flow). If survival model results confirm additional dependence on travel times or distances, some proposed physical mechanism for salmon survival can be confirmed or ruled out. And management actions that influence tidal dynamics or redistribute flows through the North Delta can be better evaluated for their impacts on salmon survival. The results of testing with the Bayesian model remain in progress, but are expected in the summer of 2022.

Simulated particle travel times and distances within a reach fell into two main regimes. When net flows were relatively high, reaches became unidirectional (no current reversals on flood tide) and changes in tidal strength or net flow had no impact on travel distance and little impact on travel times. At lower flows when the reach is tidal (having current reversals on flood tide), travel times and distances became highly variable and dependent on the time each particle entered a reach, relative to the start of ebb tide. Particles entering at the start of ebb could expect three (for example) tidal reversals before exiting the reach, whereas particles entering at the end of ebb might experience five tidal reversals before exiting. This led to high variation, and the behavior where two particles entering a reach within a few hours of one another may differ in their times spent within the reach by a total of 25 hours (a full tidal day). This variation became more pronounced with decreases in net flow.

In the tidal flow regime when net flow was held constant, tidal conditions were found to impact the average particle distance traveled but did not have much of an effect on the travel times. Spring tides caused higher tidal excursions and higher distances traveled, but resulted in similar times spent in the reach as occurred during neap tides. This leads to a management implication for large-scale tidal marsh restoration. If a new restoration dampens tides in the North Delta, it can reduce travel distances. But unless that restoration redistributes net flows, it won't impact travel times. If net flows are redistributed, travel times will be reduced in some reaches, but at the expense of increases in other pathways. This was demonstrated with modeling results in the Cache Slough and East Delta restoration scenario.

It is also important to remember that these impacts are flow dependent, and decreases in travel time and distances only apply when the reach is in the tidal flow regime (and not unidirectional). This transition between tidal and unidirectional happens at different Freeport flows for different reaches (e.g., Georgiana Slough around 8,0000 cfs, but the Lower Sacramento not until 25 to 30,000 cfs). It may happen over a narrow range of flows, and near the transition point, may alternate back and forth with spring-neap cycling. Net flows during a typical salmon outmigration season may be in the unidirectional range for at least some of the transitional reaches.

An operable gate at the head of Georgina Slough was modeled. Closure of this gate along with the Delta Cross Channel gates showed significant decreases in travel time and distance traveled (35–50%) versus the open gates condition by increasing net flows through the Sutter, Steamboat, and Sacramento pathways. The gate additionally prevented particles from traveling down Georgian Slough, where modeled results suggested they were half as likely to be transported out of the Delta than particles traveling down other North Delta pathways.

References

Heemink, A.W. 1990. Stochastic modelling of dispersion in shallow water. *Stochastic Hydrology and Hydraulics* 4, 161–174.

Perry, R.W., Pope, A.C., Romine, J.G., Brandes, P.L., Burau, Blake, A.R., Ammann, A.J., Michel, C.J. 2018a. Flow-mediated effects on travel time, routing, and survival of juvenile Chinook salmon in a spatially complex, tidally forced river delta. *Canadian Journal of Fish and Aquatic Sciences* 73, 1886–1901. dx.doi.org/10.1139/cjfas-2017-0310

Perry, R.W., Romine, J.G., Pope, A.C., Evans, S.C. 2018b. *Effects of the Proposed California WaterFix North Delta Diversion on Flow Reversals and Entrainment of Juvenile Chinook Salmon (Oncorhynchus tshawytscha) into Georgiana Slough and the Delta Cross Channel, Northern California.* USGS Open-File Report 2018-1028.

Resource Management Associates (RMA). 2003. *RMASIM Users Guide*. April 2003.

RMA. 2020. *Pilot Modeling to Examine Regional Effects of Delta Geometry Changes – Phase 1 and 2 Summary Report*. Prepared for the Delta Science Program, Delta Stewardship Council. April 2020.

Romine, J.G., Perry, R.W., Stumpner, P.R., Blake, A.R., Burau, J.R. 2021. Effects of tidally varying river flow on entrainment of juvenile salmon into Sutter and Steamboat Sloughs. San Francisco Estuary and Watershed Science 19(2). https://doi.org/10.15447/sfews.2021v19iss2art4

USGS. 2015. Ch. 3 Analysis Methods, Results and Discussion in: *2012 Georgiana Slough Non-Physical Barrier Performance Evaluation Project Report*. Prepared for California Department of Water Resources. December, 2015.

Appendix A: Water Year 2009 Simulation Results

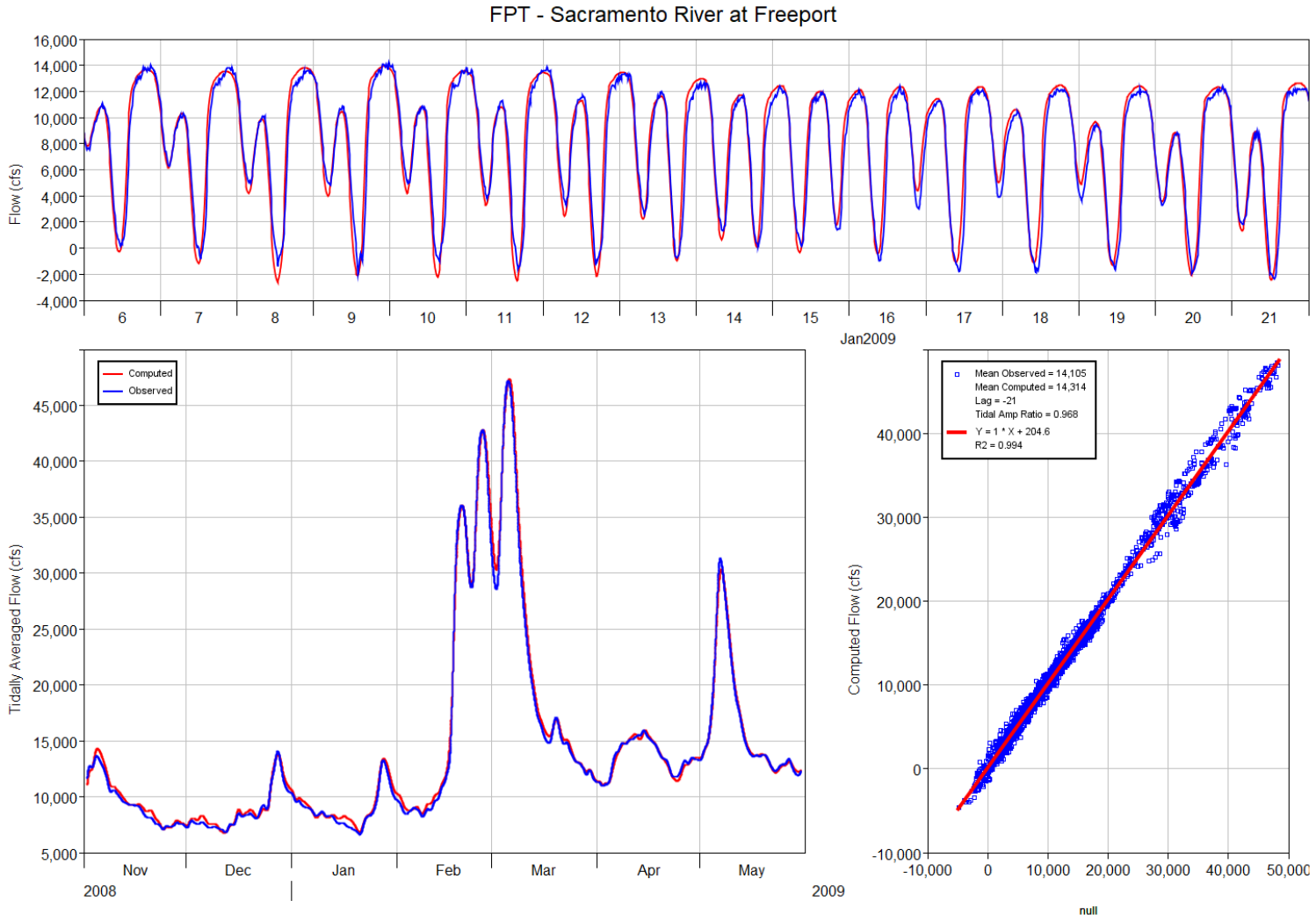

Figure 39 Modeled and observed flow on the Sacramento River at Freeport for the WY 2009 simulation period

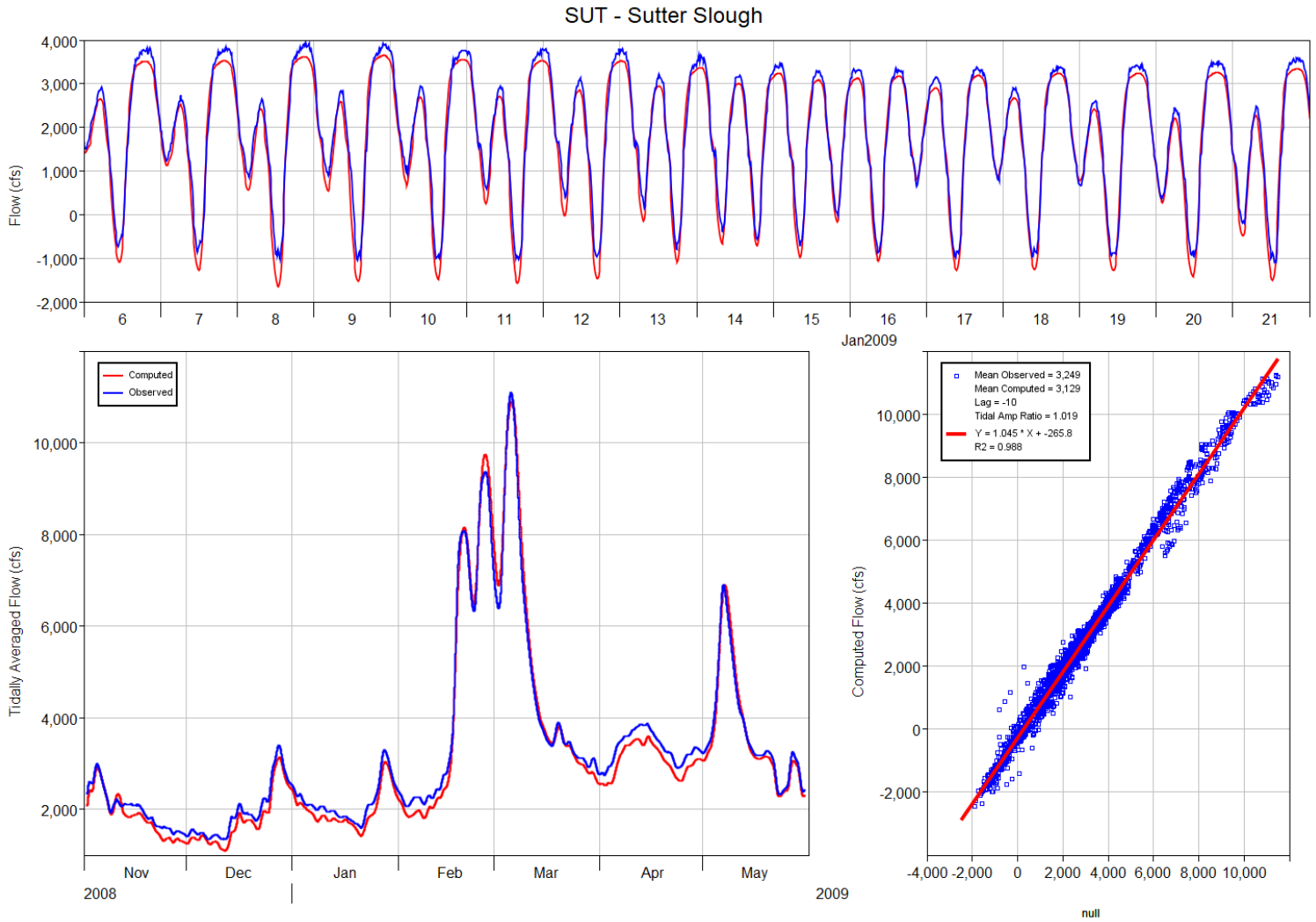

Figure 40 Modeled and observed flow on Sutter Slough for the WY 2009 simulation period

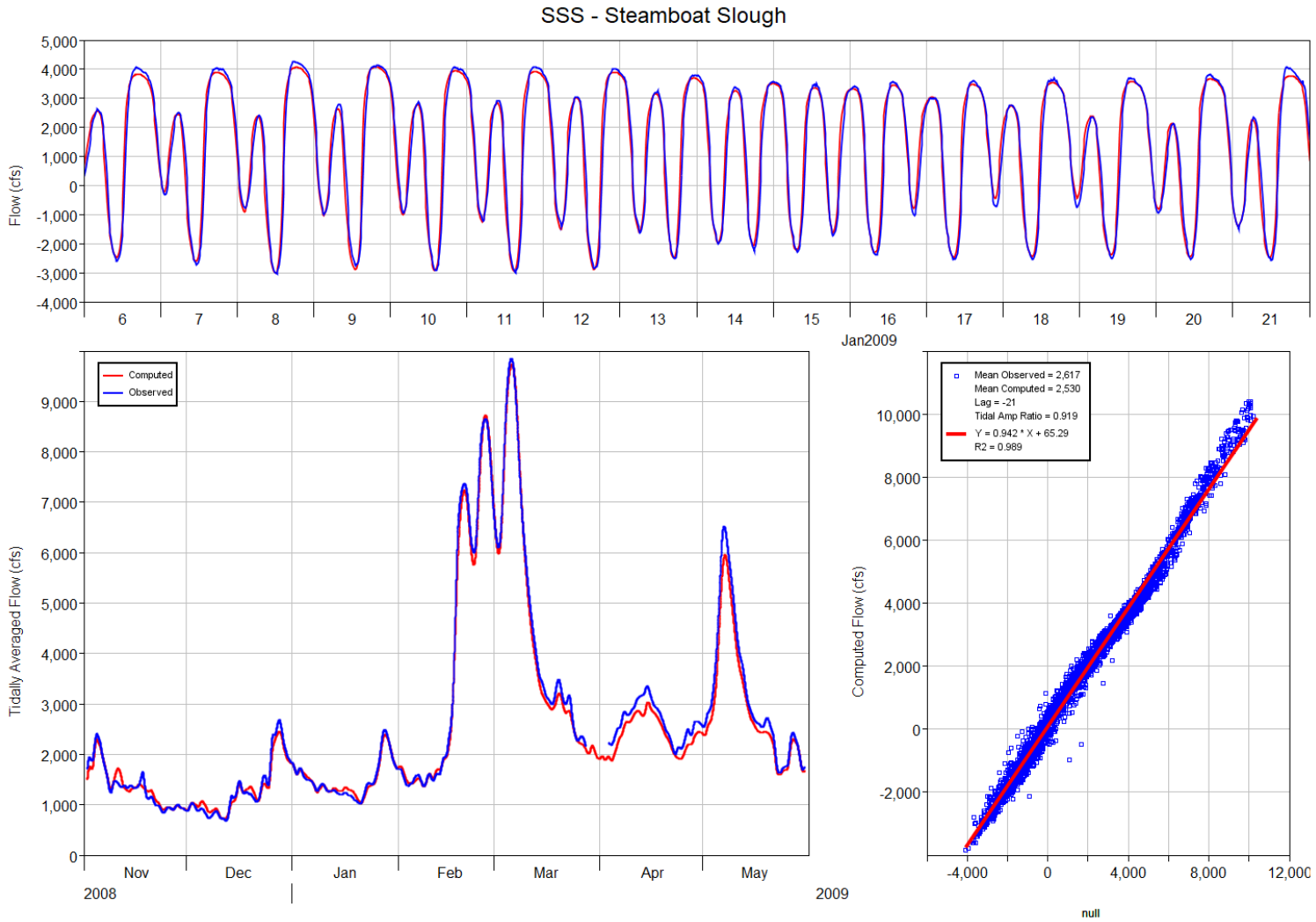

Figure 41 Modeled and observed flow on Steamboat Slough for the WY 2009 simulation period

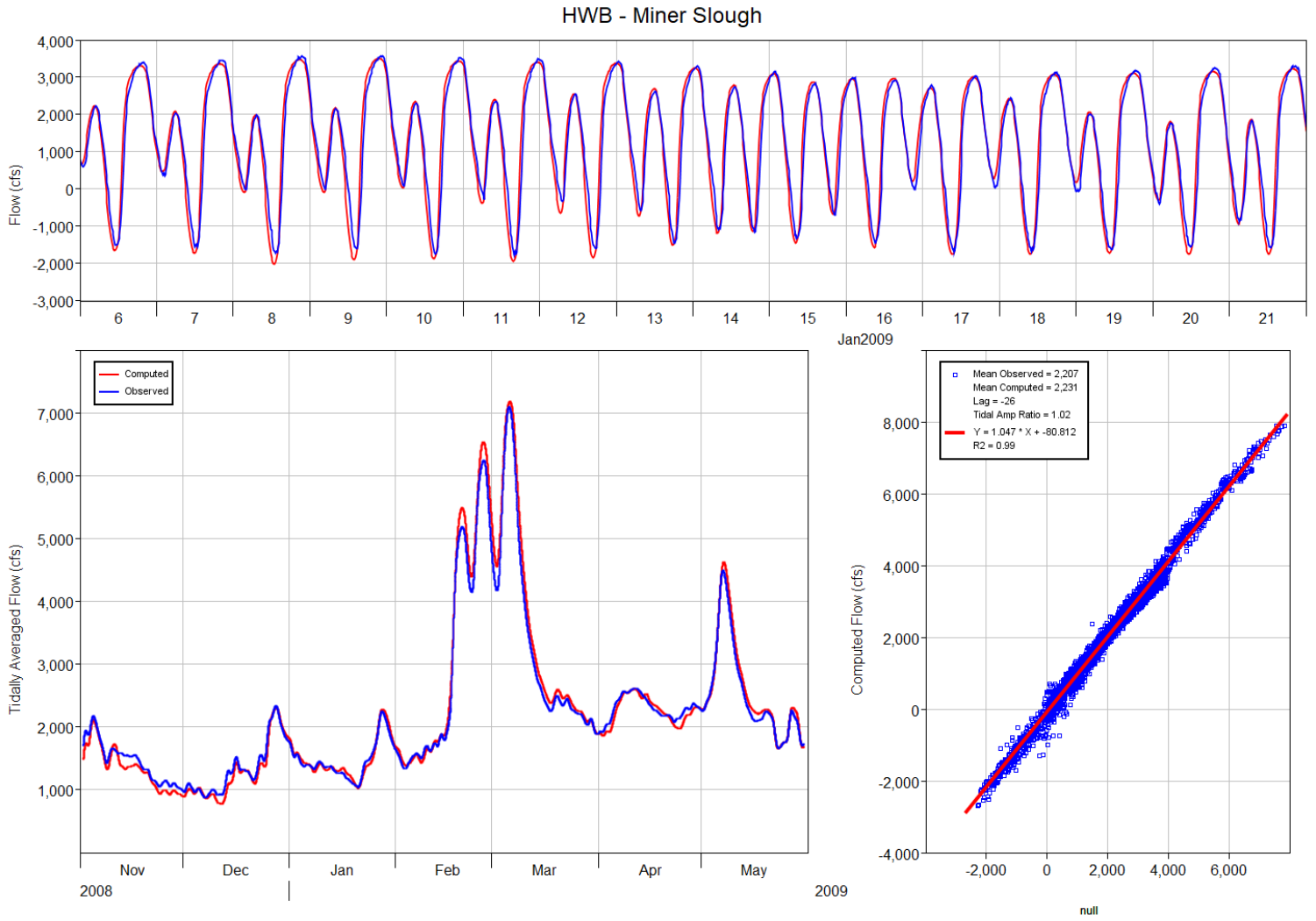

Figure 42 Modeled and observed flow on Miner Slough for the WY 2009 simulation period

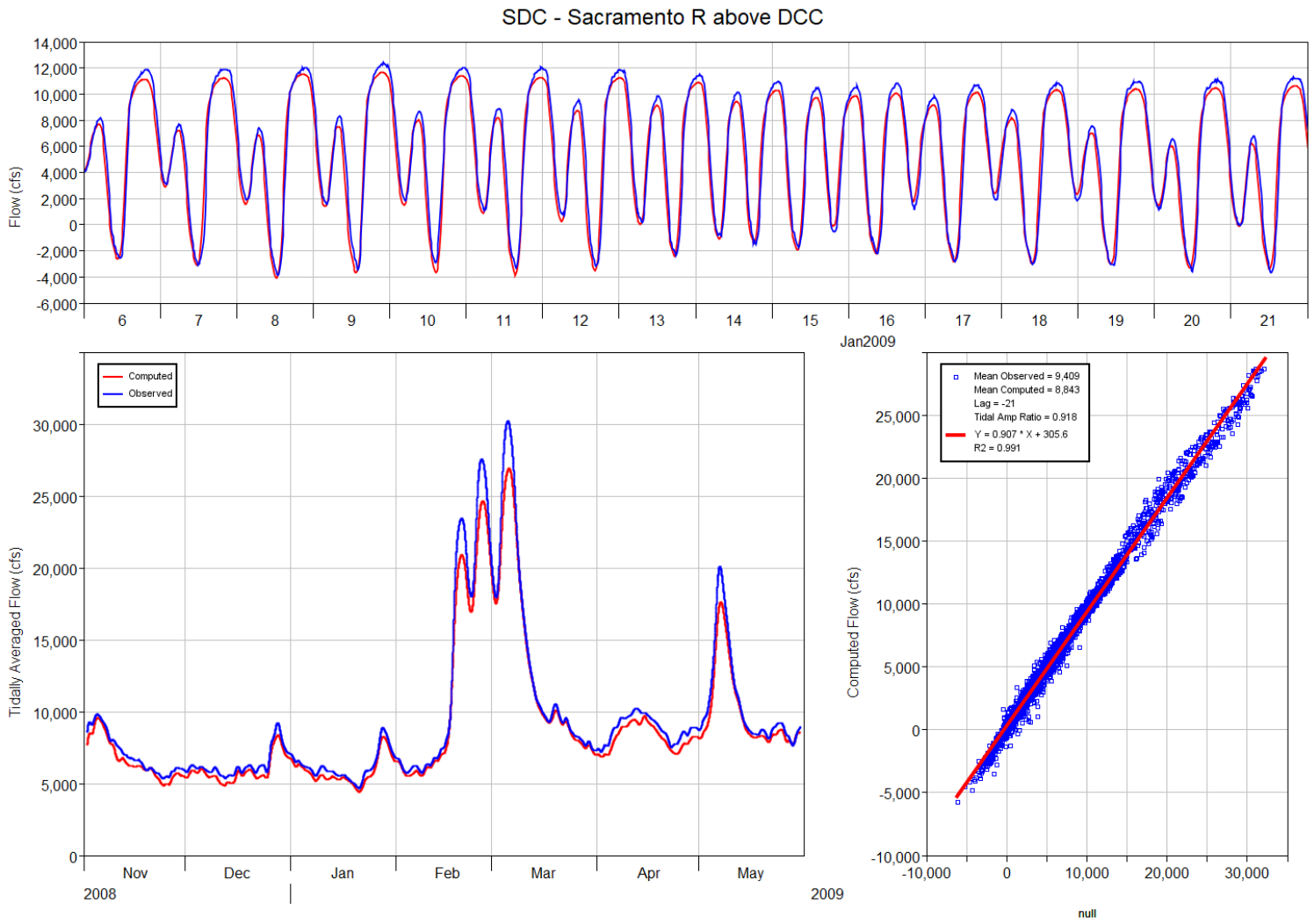

Figure 43 Modeled and observed flow on the Sacramento River above the Cross-Channel for the WY 2009 simulation period

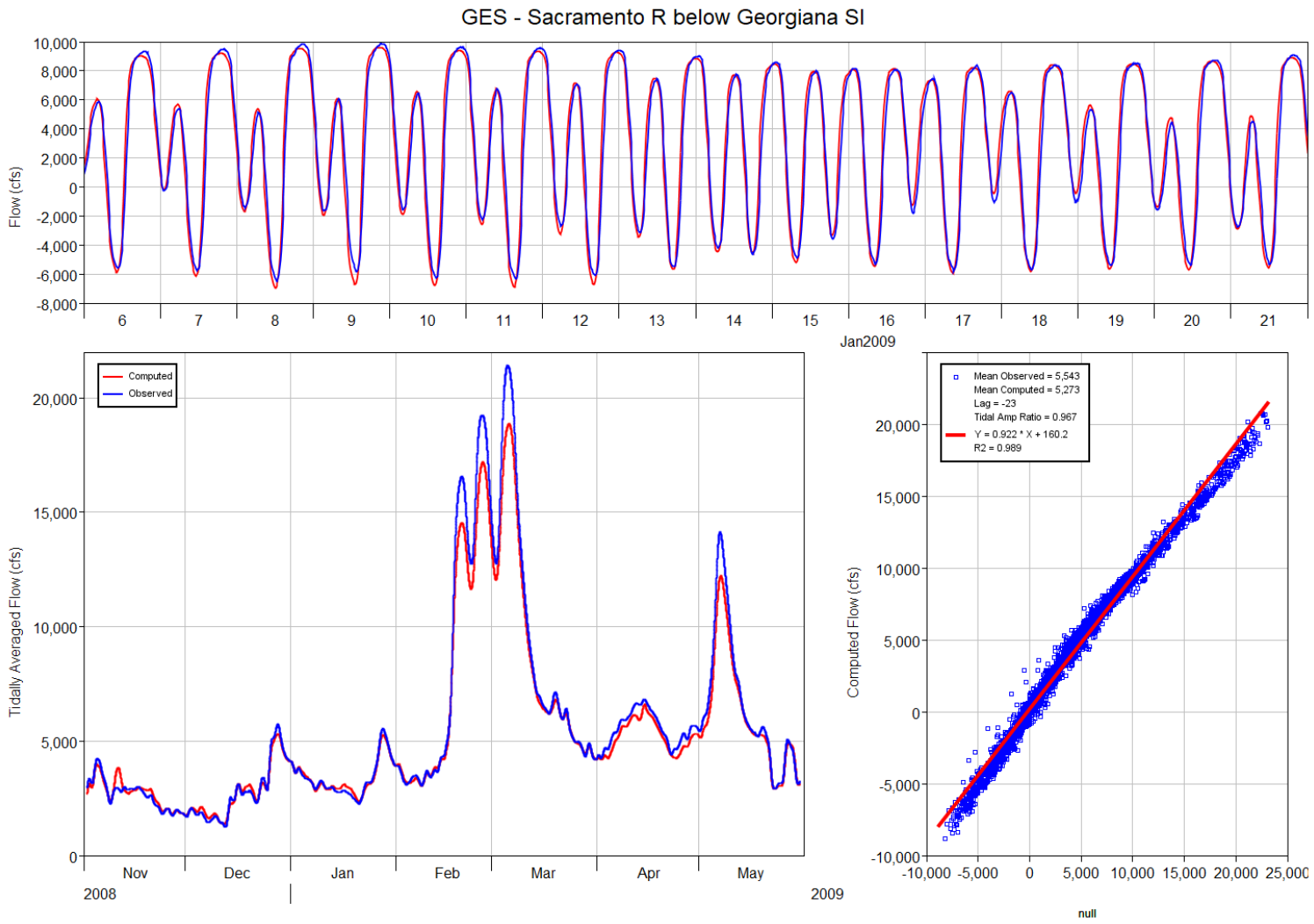

Figure 44 Modeled and observed flow on the Sacramento River below Georgiana Slough for the WY 2009 simulation period

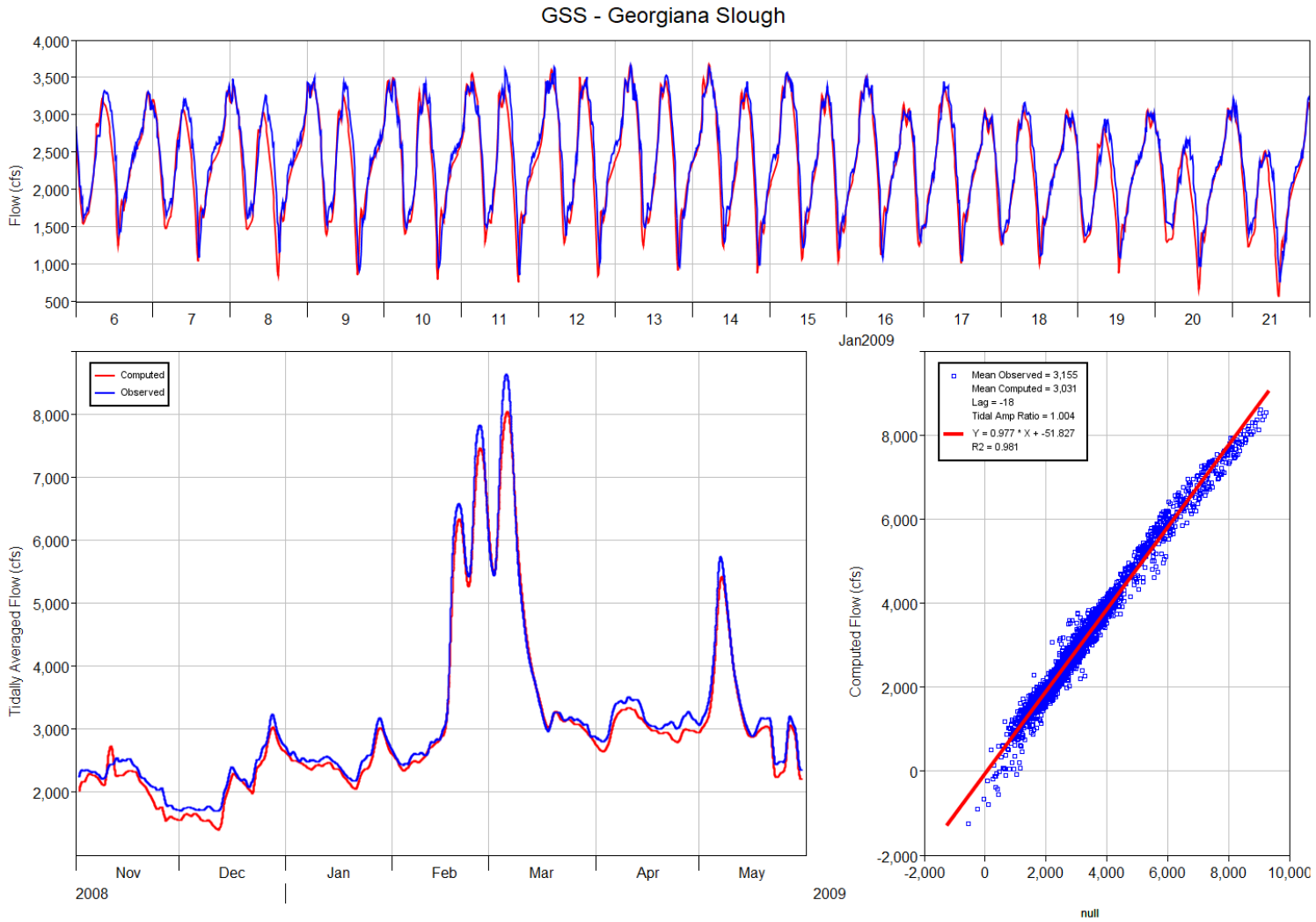

Figure 45 Modeled and observed flow on Georgiana Slough for the WY 2009 simulation period

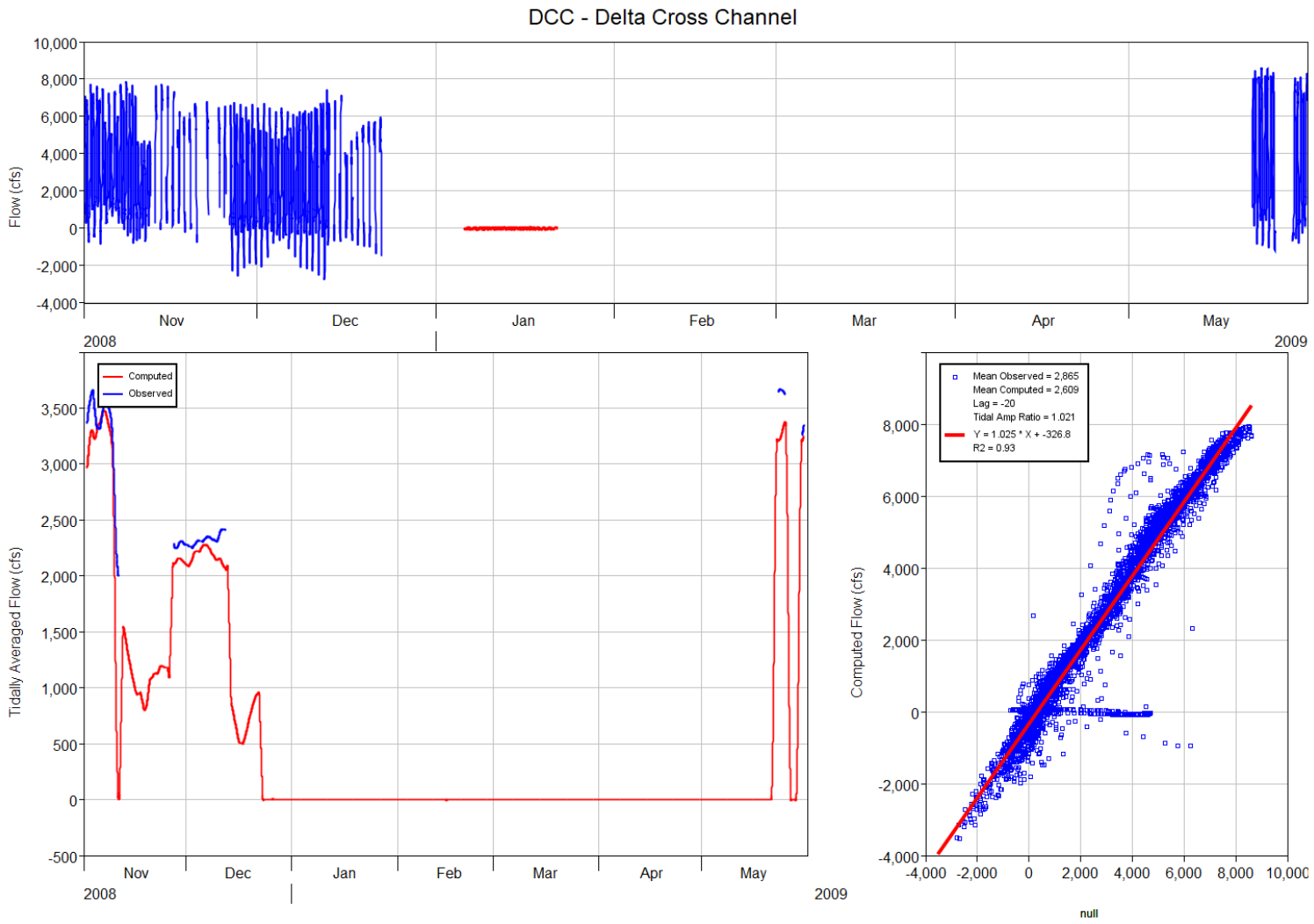

Figure 46 Modeled and observed flow through the Delta Cross Channel for the WY 2009 simulation period

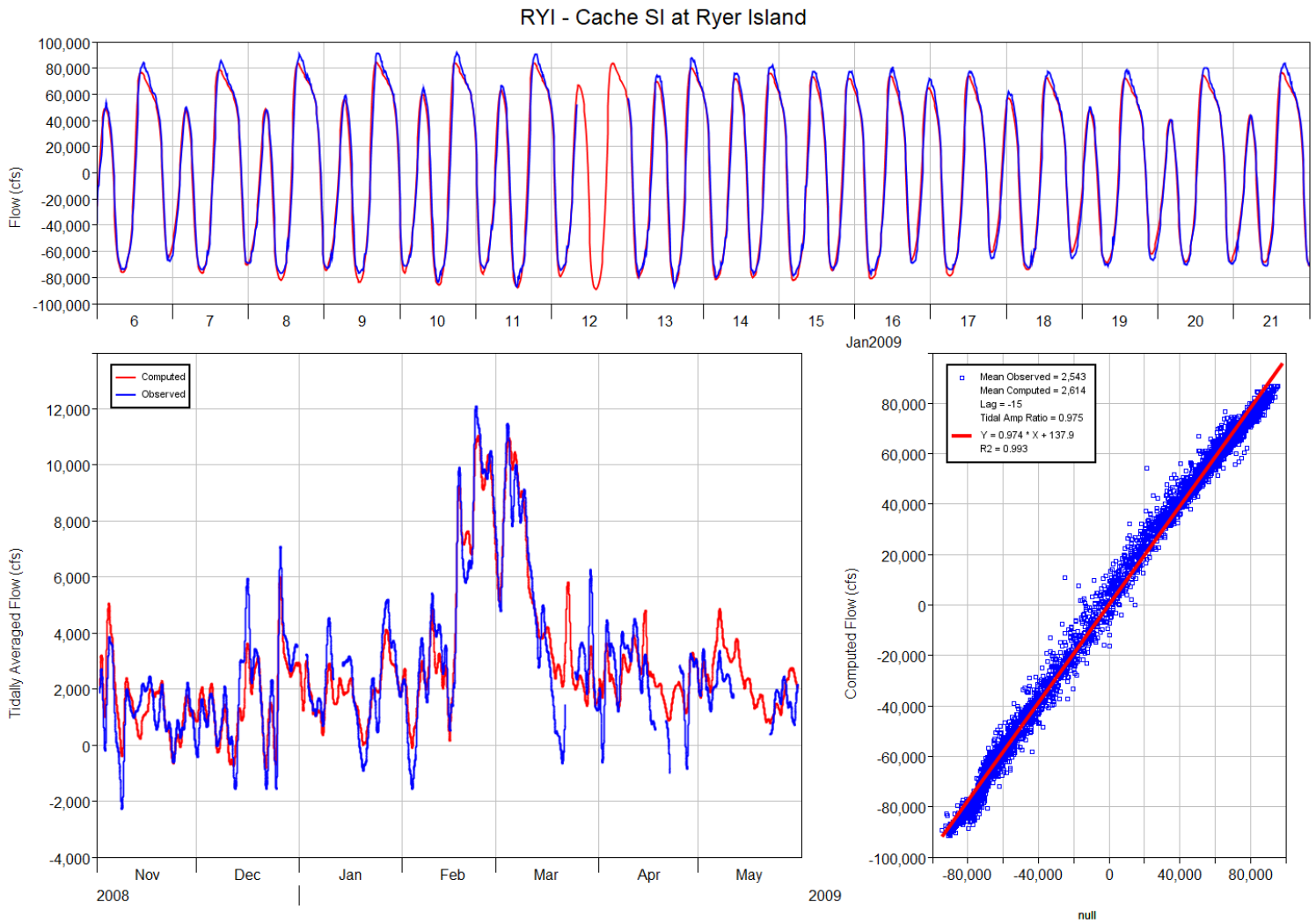

Figure 47 Modeled and observed flow on Cache Slough at Ryer Island for the WY 2009 simulation period

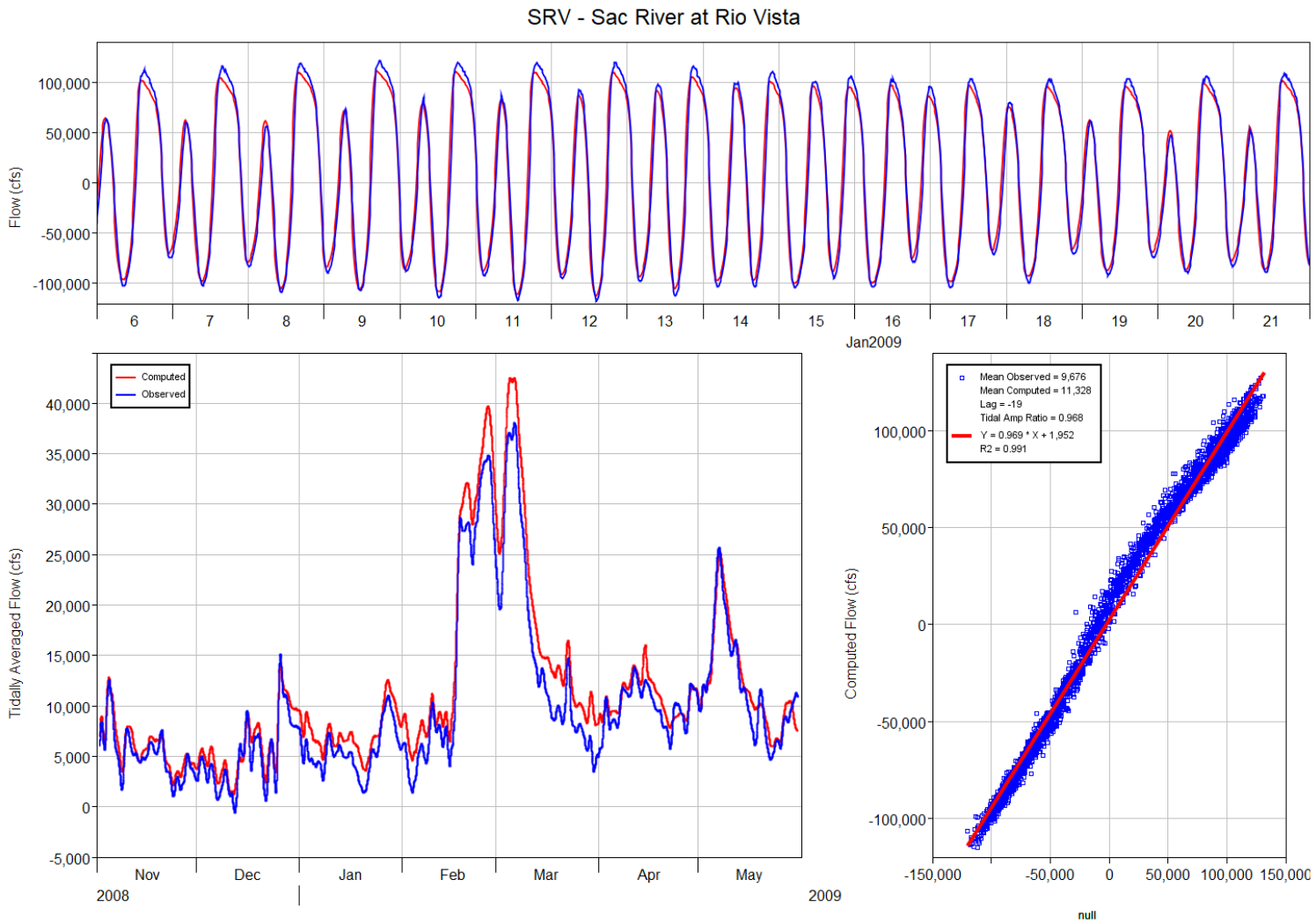

Figure 48 Modeled and observed flow on the Sacramento River at Rio Vista for the WY 2009 simulation period

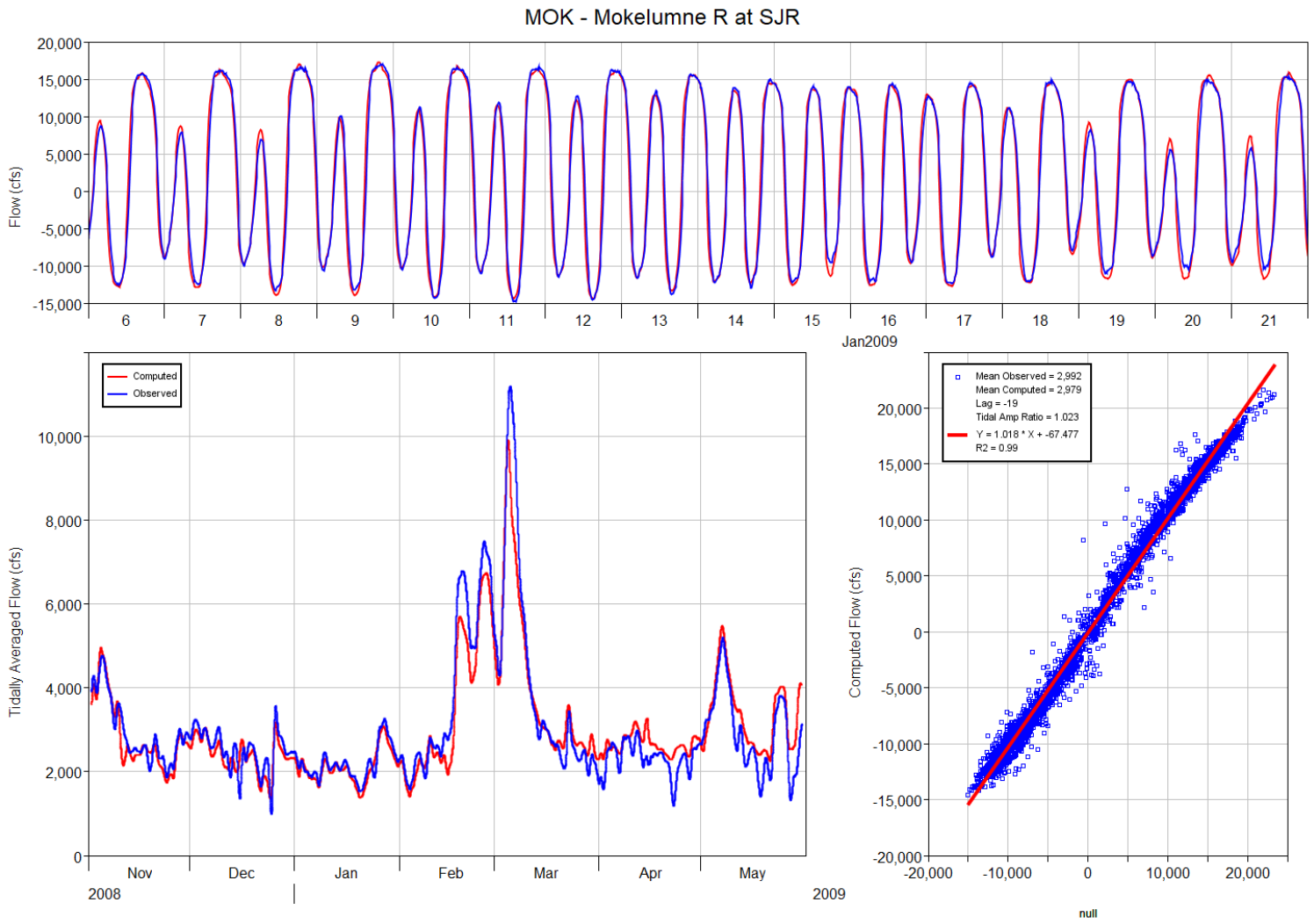

Figure 49 Modeled and observed flow on the Mokelumne River near the San Joaquin River for the WY 2009 simulation period

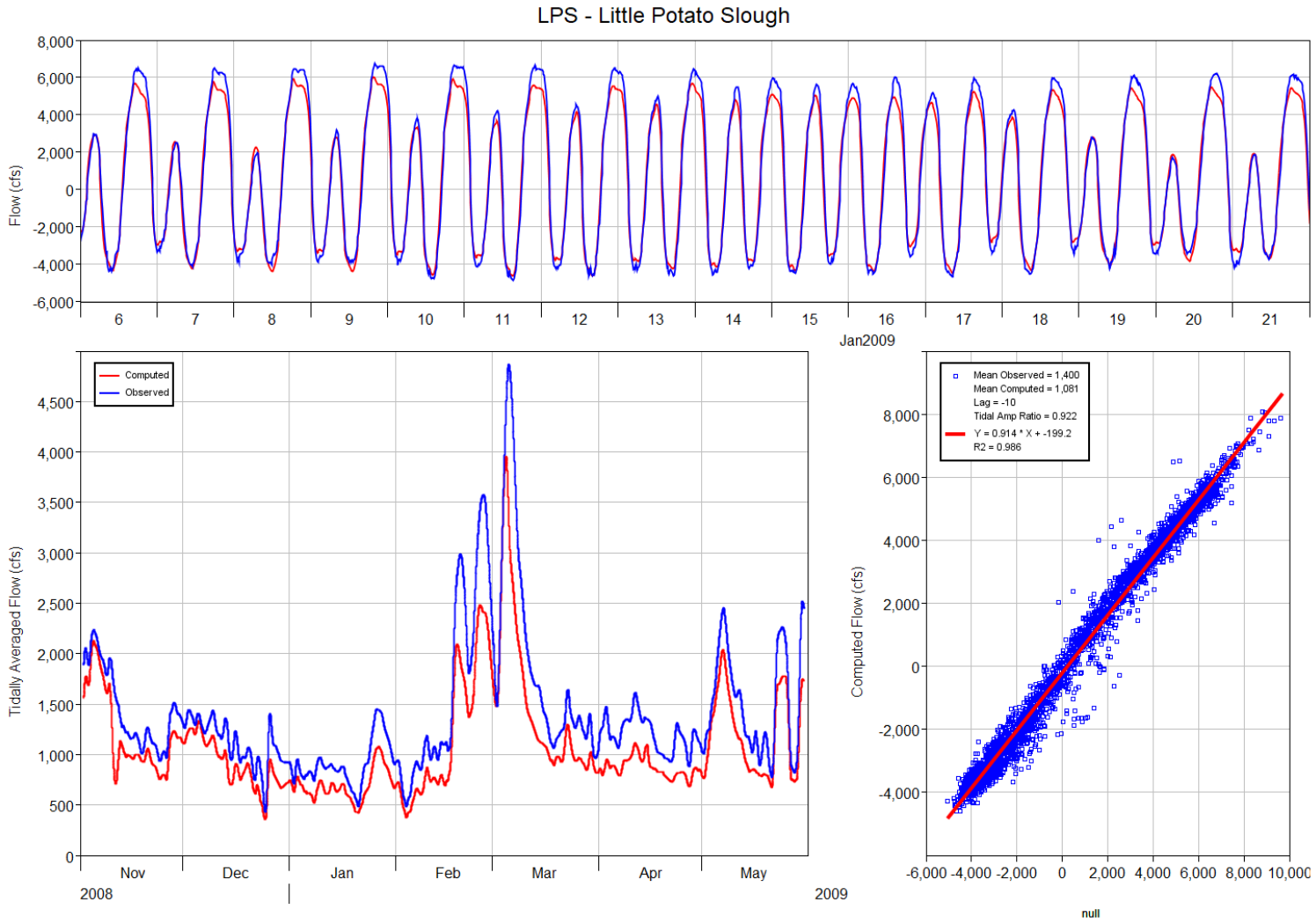

Figure 50 Modeled and observed flow on Little Potato Slough for the WY 2009 simulation period